Fuel Management Study for a Pebble Bed Modular Reactor Core

by

Raisibe Shirley Movalo

Thesis presented in partial fulfilment of the requirements for the degree of Master of Science (Nuclear Physics)

at

Stellenbosch University

Department of Physics

Faculty of Science

Supervisor: Dr JA Stander
Technical Editor: Dr V Naicker
Date: March 2010

Declaration

By submitting this thesis electronically, I declare that the entirety of the work contained therein is my own, original work, that I am the owner of the copyright thereof (unless to the extent explicitly otherwise stated) and that I have not previously in its entirety or in part submitted it for obtaining any qualification.

Date:

Abstract

This dissertation reports on the impact of a set of selected nuclear fuel management parameters on reactor operations of the PBMR core. This is achieved by performing an assessment of the impact of nuclear fuel management parameter variations on the most important safety and economics issues for the PBMR core. These include the maximum fuel temperature at steady state and during **D**epressurized **L**oss of **F**orced **C**ooling (DLOFC) accident conditions. The reactivity worth of the **R**eactor **C**ontrol **S**ystem (RCS which determines the shutdown capability of the reactor core and the average discharge burn-up of fuel are also established. The fuel management parameters considered in this study include different enrichment levels, heavy metal loadings and fuel sphere circulation regimes. The impact and importance of these parameters on plant safety and economics is assessed. The dissertation will report the effects on the standard core physics parameters such as power peaking, multiplication factor, burn-up (safety and economics) and derive the benefits and drawbacks from the results. Based upon the findings from this study, and also experimental data, an optimum fuel management scheme is proposed for the PBMR core.

Opsomming

Hierdie verhandeling beskryf die uitwerking van ‘n gekose stel kernbrandstofparameters op die bedryf van die PBMR reaktor. Die impak wat variasies in kernbrandstofparameters op belangrike veiligheids- en ekonomiese oorwegings het, is tydens hierdie studie ondersoek. Van die belangrikste oorwegings is die maksimum brandstoftemperatuur tydens normale, konstante bedryf, asook gedurende ‘n “**D**epressurized **L**oss of **F**orced **C**ooling (DLOFC)” insident waar alle verkoeling gestaak word. Ander belangrike fasette wat ondersoek is, is die reaktiwiteitwaarde van die beheerstelsel (RCS), wat die aanleg se vermoë om veilig af te sluit bepaal, asook die totale kernverbruik van die brandstof. Die kernbrandstofparameters wat in ag geneem is, sluit die brandstofverryking, swaarmetaalinhoud en die aantal brandstofsirkulasies deur die reaktorhart in. Die belangrikheid en impak van elk van hierdie parameters is ondersoek en word in die verhandeling beskryf . Daar word verslag gelewer oor die voor- en nadele, asook die uitwerking van hierdie variasies op standaard reaktorfisika-parameters soos drywingspieke in die brandstof, neutronvermenigvuldigingsfaktore en kernverbuik van die brandstof, vanaf ‘n veiligheids- en ekonomiese oogpunt. Gebaseer op die gevolgtrekkings van hierdie studie, tesame met eksperimentele data, word ‘n optimale kernbrandstofbestuurprogram voorgestel.

Acknowledgements

I would like to thank GOD and the ZCC church for guidance and my Mother and my sons for their support and understanding. I want to thank Dr Anton Stander for supervising this work and his constructive comments and advice. I would like to express my gratitude to thank Klaus Kassel and Peter Scott for performing the screening review of this dissertation.

TABLE OF CONTENTS

Declaration 2
Abstract 3
Opsomming 4
Acknowledgements 5
List of Figures 9
List of Tables 11
List of Addendums 12
Chapter 1 13
Introduction 13
1.1 Background on the High Temperature Gas Cooled Reactor (HTGR) 13
1.2. The inherent safety of the High Temperature Gas Cooled Modular Reactor (HTGR) 20
1.3 Why A High Temperature Reactor? 22
1.4 The PBMR layout and description 23
1.5 Motivation and Study definition 26
Chapter 2 30
Theoretical Background 30
2. Neutron life cycle 30
2.1 Description of the neutron life cycle 32
2.2 Neutron Transport 37
2.3 Evaluation of multi group constants 45
2.4 Reactivity effects 59
2.5 Determination of power distribution and criticality 62
2.6 Evaluation of core capability and changes 63
2.7 Fission product poisoning and its effects on reactor operation 64
2.8 Reactor Core Thermal Hydraulics 69
2.9 Reactivity control 69
2.10 Computational methods for solving the diffusion equation 70
Chapter 3 72
Code Description 72
3.1 Background on computer codes (V.S.O.P) 72
3.2 V.S.O.P capabilities 73
3.3 V.S.O.P code layout 75

3.3.1 Nuclear Data 76
3.3.2 ZUT-DGL 77
3.3.3 BIRGIT/TRIGIT 78
3.3.4 DATA-2 code 80
3.3.5 GAM code 80
3.3.6 THERMOS code 81
3.3.7 ADAGE (Actinide Depletion and Generation) and FEVER codes 81
3.3.8 CITATION code 82
3.3.9 THERMIX/KONVEK 82
3.3.10 FUMAN, KUGELN and BURNUP 82
3.3.11 LIFE 83
3.3.12 PRIOR 83
Chapter 4 84
Fuel Management Calculation 84
4.1 Description of the fuel and reactor core design model 85
4.2 Model Assumptions 87
4.3 Description of the constraints imposed by investigated fuel management parameters 87
4.3.1 Fuel temperature limitations 87
4.4 Results 94
4.4.1 The impact of the variations of the heavy metal loadings on reactor safety and economics 94
4.4.2 The impact of the variations of the enrichment on reactor safety and economics 99
4.4.3 The impact of the fuel sphere circulations on reactor safety and economics 103
Chapter 5 106
Summary and Conclusion 106
Bibliography 109
APPENDICES 114
Appendix A 114
V.S.O.P Results on Fuel Management Evaluation Study for the PBMR Core. 114
List of Abbreviations and Acronyms 117
Appendix C 118
List of Definitions 118
Appendix D 119

Typical Example of VSOP Input File: **.....119**

List of Figures

Figure 1.1: *The structure of the fuel sphere [7].* 14

Figure 1.2: *The layout of the HTR-10 [8].* 15

Figure 1.3: *The PBMR Plant [9].* 16

Figure 1.4: *Layout of the PBMR [10].* 17

Figure 1.5: *The structure of the HTTR fuel assembly [11].* 18

Figure 1.6: *Layout of HTTR in Japan [11].* 19

Figure 1.7: *VHTR [6].* 20

Figure 1.8: *PBMR passive heat transfer [19].* 22

Figure 1.9: *A cross section of a quarter of PBMR reactor core, where SAS refer to the Small Absorber Spheres [25]* 24

Figure 1.10: *Radial cross section of the PBMR core, where RCS and RSS refer to the Reactivity Control System and Reserve Shutdown System respectively[26].* 25

Figure 2.1: *Neutron life cycle for a critical reactor (K_{eff} = 1).* 32

Figure 2.2: *Fission Spectrum for thermal neutron induced fission in Uranium -235 [27].* 34

Figure 2.3: *Particle located inside an infinitesimal volume dV and moving in the direction of the x-axis, the energy of the particle lies within some space interval [E, E+dE] of the energy space28]* 39

Figure 2.4: *A comparison between the neutron spectrum of the thermal reactor and fast breeder reactor [18].* 47

Figure 2.5: *Doppler Broadening [27].* 49

Figure 2.6: *Space-Energy flux depression in the neighbourhood of resonance [33].* 52

Figure 2.7: *Collapsing of the multi-group to few-group constant [33].* 55

Figure 2.8: *Typical structure for a few group reactor calculations [33].* 56

Figure 2.9: *Flow diagram of a typical reactor model.* 62

Figure 3.1: *Reactor core layout as modelled by V.S.O.P including the flow lines [42].* 74

Figure 3.2: *Axial flux shape for the PBMR core.* 75

Figure 3.3: *V.S.O.P basic programs.* 76

Figure 3.4: *Break down of the neutron escape probability [44.* 78

Figure 3.5: *Radial thermal flux profile for the PBMR.* 79

Figure 4.1: *Thermal conductivity of the graphite as a function of temperature for various neutron fluences [37, 44].* 90

Figure 4.2: *Effective thermal conductivity in a Pebble Bed [37].* 91

Figure 4.3: *The impact of the variations of heavy metal loadings on Burn-up (for 6 passes and 12%wt enrichment).* 95

Figure 4.4: *The impact of the variations of heavy-metal loadings with power in the sphere.* **96**

Figure 4.5: *Results of the fission product release from the matrix during the heat-up experiments in Russian reactor (Koshcheyev KN)* *99*

Figure 4.6: *The impact of variations of enrichment on Burn-up (for 6 passes and 9 grams heavy metal loading).* **100**

Figure 4.7: *The impact of the variation of enrichment on fuel temperature (for 6 passes and 9 grams heavy metal loading).* **100**

Figure 4.8: *The impact of the variation of enrichments on SDM (for 6 grams heavy metal loadings).* **102**

Figure 4.9: *The impact of the variation of enrichments on CRW (for 6 grams heavy metal loadings)*..... ..... *102*

Figure 4.10: *The variations of burn-up with number of passes.* **104**

Figure 4.11: *The variations of burn-up with number of passes at lower burn-up, where "ch" and "p" refers to channel and pass. For example, ch1-p1 refers to channel number one and p1 refers to the initial pass*..... .... *105*

List of Tables

Table 2.1: *Resonance data for several low lying resonance of U-238* ..... ….. **50**

Table 3.1: *Energy grouping within V.S.O.P*…… *77*

Table 4.1: *Main input parameters* **86**

Table 4.2: *Fuel Specification*……..……..*86*

Table 4.3: *Affected parameters and limit*……*94*

Table 4.4: *V.S.O.P. Results on Fuel Management Evaluation Study for the PBMR Core.*……**98**

Table 4.5: *Variations of the number of fuel sphere passes for 9.6% enrichment and 9 grams heavy metal loading*……...…… **103**

Table I: *V.S.O.P Results on Fuel Management Evaluation Study for the PBMR Core (SDM & CRW)*…….. **116**

List of Addendums

Appendix A……..…….. *114*
V.S.O.P Results on Fuel management evaluation for the PBMR……..…….. *114*
Appendix B……..…….. *117*
List of Abbreviations and Acronyms ……..……. *117*
Appendix C……..…….. *118*
List of Definitions.....……..……. *118*
Appendix D……..…….. *119*
Typical Example of V.S.O.P Input File……..…… *119*

Chapter 1

Introduction

The purpose of this thesis is to investigate and make recommendations with respect to the fuel management optimization options for a pebble bed high temperature nuclear reactor. This study will indicate the influence of selected reactor physics parameters on the minimization of electrical generation costs and reactor safety. One of the key parameters is the fuel temperature that must always be maintained below the level where the integrity of fission product retaining barriers may be compromised and reactor control must ensure safe operation. Traditionally, fuel management is considered to consist of three distinct activities. The first one is called front end, which begins with the nuclear fuel processing from mining, conversion, enrichment of the fuel down to fuel fabrication. The second is in-core fuel management. This includes the evaluation and investigation of the reactor physics concepts such as reactivity, power and neutron flux distributions and core power capability evaluations. The third fuel management activity is referred to as the back end which involves fuel storage, shipping, reprocessing of fuel and waste disposal. For this dissertation the main focus will be on the in-core fuel management. In-core fuel management for **H**igh **T**emperature **G**as-cooled **R**eactors (HGTR) is different from the conventional **L**ight **W**ater **R**eactors (LWR) fuel management schemes in a number of respects. For example, the fuel design for HTGR is different from that of the LWR and it allows operation at much higher temperatures. The use of higher uranium enrichment is also allowed. This will result in higher discharge burn-up that can be achieved (> 80 000 MWD/Ton) as compared to the LWR (~50 000 MWD/Ton). Some of the parameters to be investigated and principles important to safety, though, are very similar. A full description of the parameters to be investigated is given in the study definition (section 1.5). This chapter will describe the background of HTGR, the fundamental safety features of the HTGR including reasons why the HTGR is preferred under certain circumstances to the conventional LWR, a description of the selected HTGR reactor design and the study definition.

1.1 Background on the High Temperature Gas Cooled Reactor (HTGR)

The High Temperature Gas-cooled Reactor (HTGR) is not a new concept. It was identified by Keller [1] in the 1940's that the closed cycle gas turbine power plant using helium or mixture (helium, nitrogen, carbon dioxide, argon and neon [1]) of helium appears to be the best system for power generation. Several HTGR's have been built and operated successfully in the USA, Great Britain and Germany since the late fifties and recently in Japan and China [2-4]. In the past years, attention of nuclear power generating plant has shifted from just adding the redundant safety systems or expensive security measures to designing an inherently safe system. Brinkmann [5] has indicated that the HTGR can be designed to be safe, which means that unlike the conventional **P**ressurized **W**ater **R**eactors (PWR), the worst case accident cannot lead to a core melt down or extensive release of radioactivity, even in the complete absence of operator action [5]. There are different types of the HTGR's and the Next Generation Nuclear Power Plant

(NGNP) advisory committee [6] and the Generation IV international forum [6] have grouped the HTGR concept into four categories representing common capability and attributes. These categories are Pebble Bed Modular Reactors, Prismatic Fuel Modular Reactors, Very High Temperature Reactors and Gas Cooled Fast Reactors. The first category is the Pebble Bed Reactor concept and is characterized by the online refuelling of the fuel sphere (sphere circulation) and the use of pebble fuel spheres. These fuel spheres contain ceramic coated particles embedded in the graphite matrix as shown in Figure 1.1.

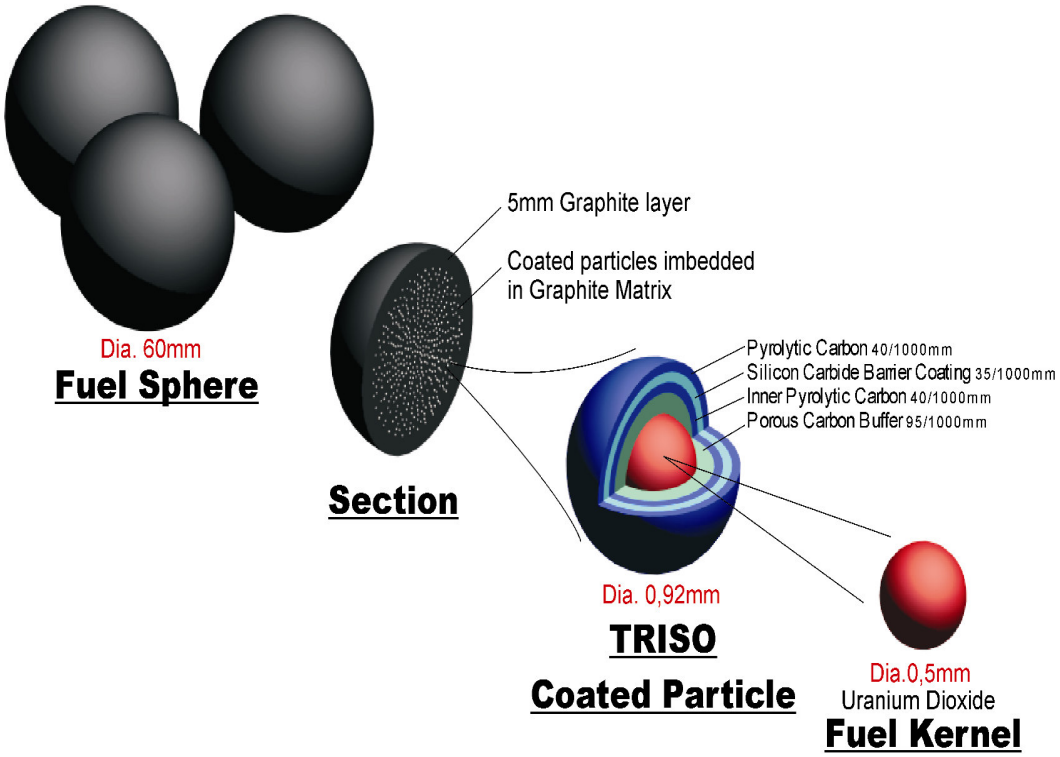

Figure 1.1: The structure of the fuel sphere [7].

The pebble modular reactor uses helium as a coolant and has a reflector graphite core structure for reflection of neutrons and to maintain the core geometry. A coolant exit temperature of above 850ºC can be achieved. Examples of such reactors are the High Temperature reactor (HTR-10) that is currently operating in China (Figure 1.2), the Arbeitsgemeinschaft Versuchs Reaktor (AVR) research reactor and Thorium High Temperature Reactor (THTR) in Germany and the Pebble Bed Modular Reactor (PBMR) that is currently under design in South Africa. The detailed description of the PBMR will be provided later in this chapter (Figures 1.3 and 1.4). The HTR-10, AVR, THTR and PBMR have capacities of about 10, 46, 750 and 400 MW thermal, respectively.

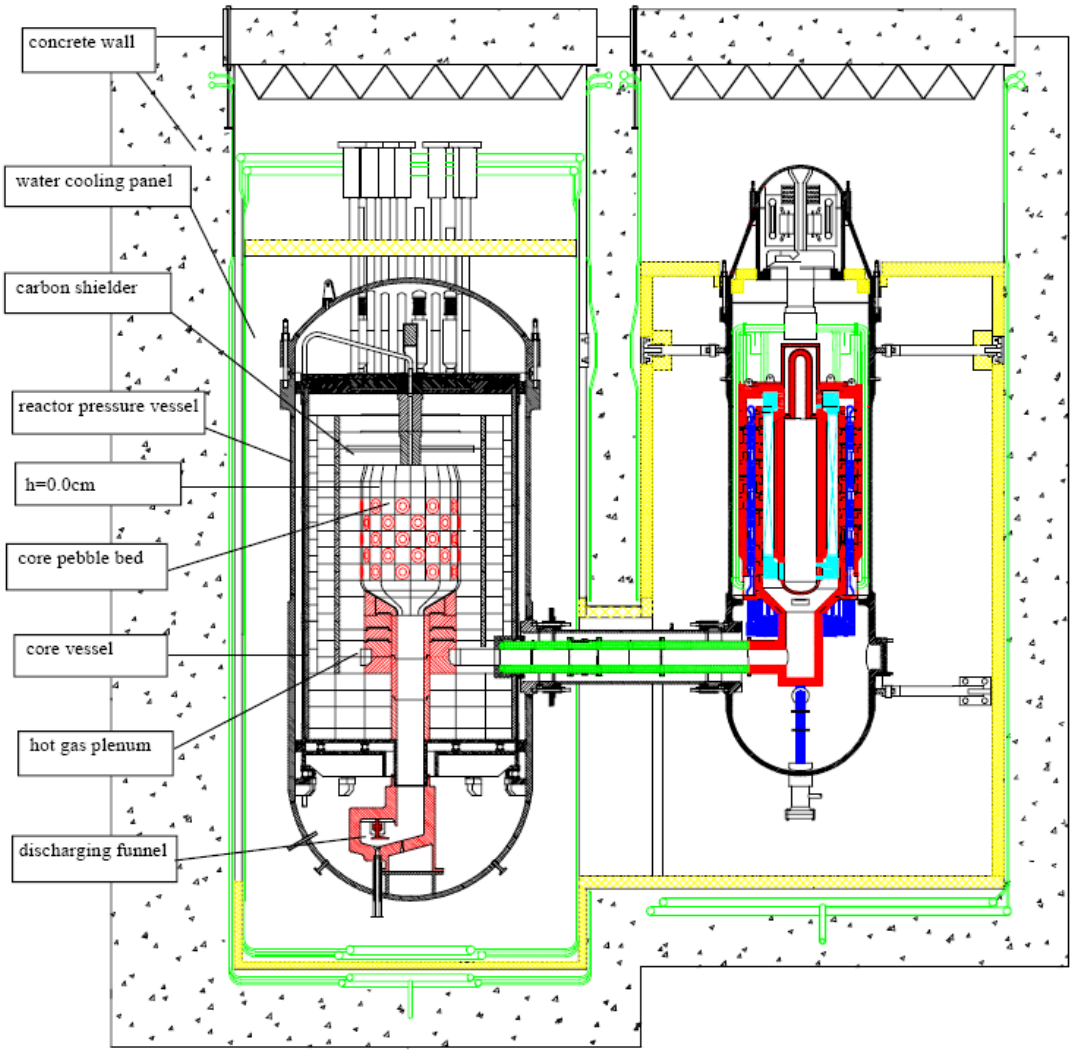

Figure 1.2: The layout of the HTR-10 [8].

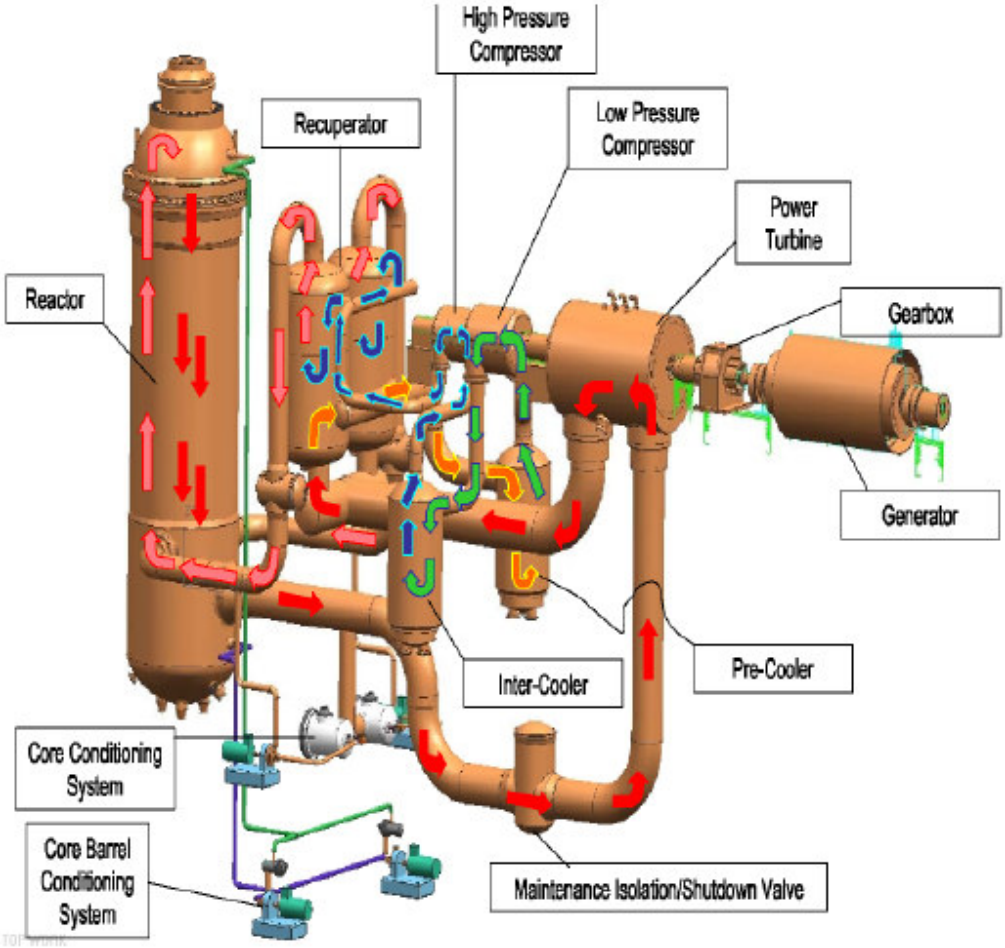

Figure 1.3: The PBMR Plant [9].

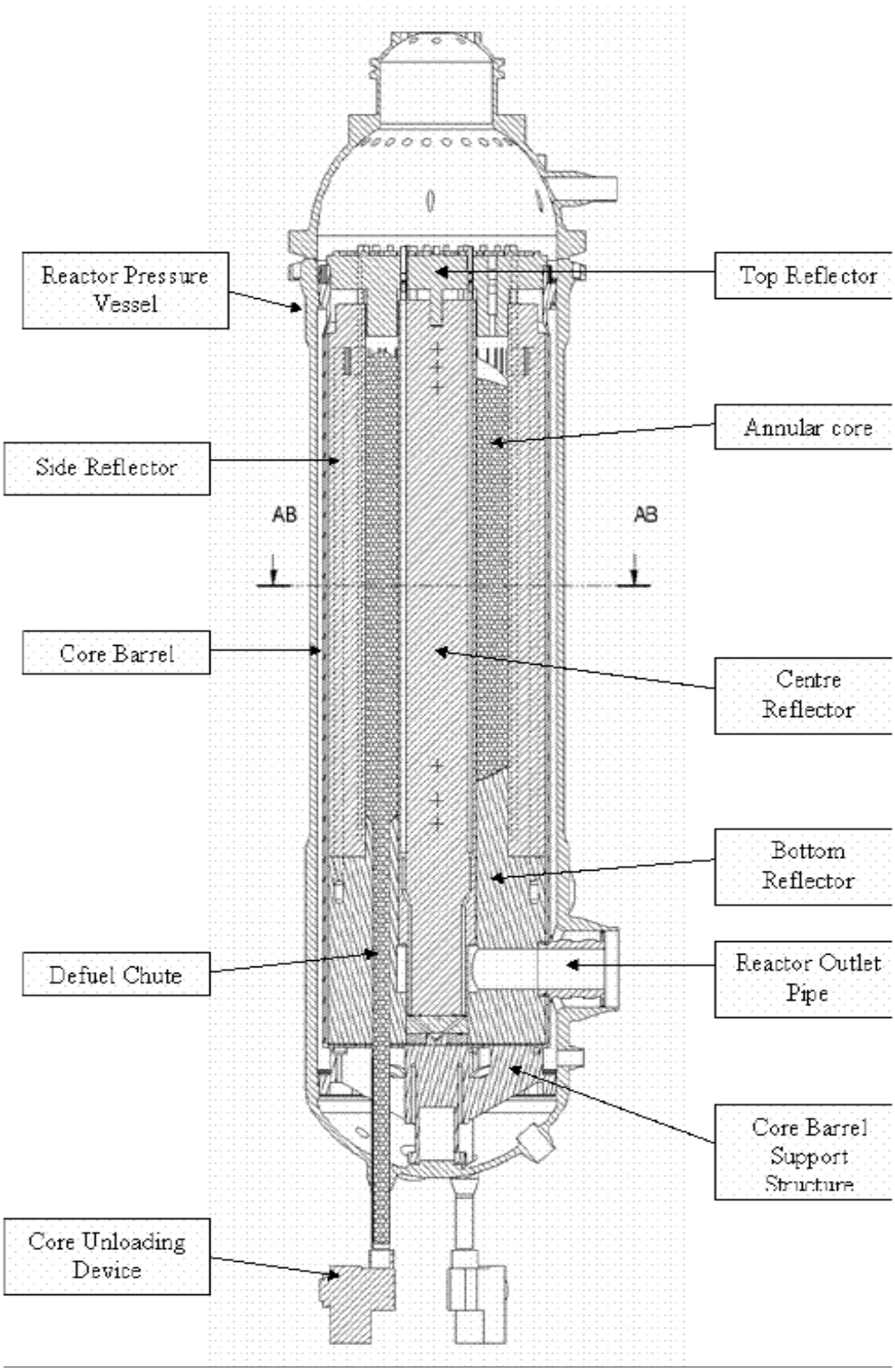

Figure 1.4: Layout of the PBMR [10].

The second category is the Prismatic Fuel Reactor concept which uses the same design of the coated particle as the pebble bed reactor, except that they are shaped into different configurations. The prismatic fuel design has coated particles mixed with matrix graphite and formed into a cylindrical fuel compact (Figure 1.5).

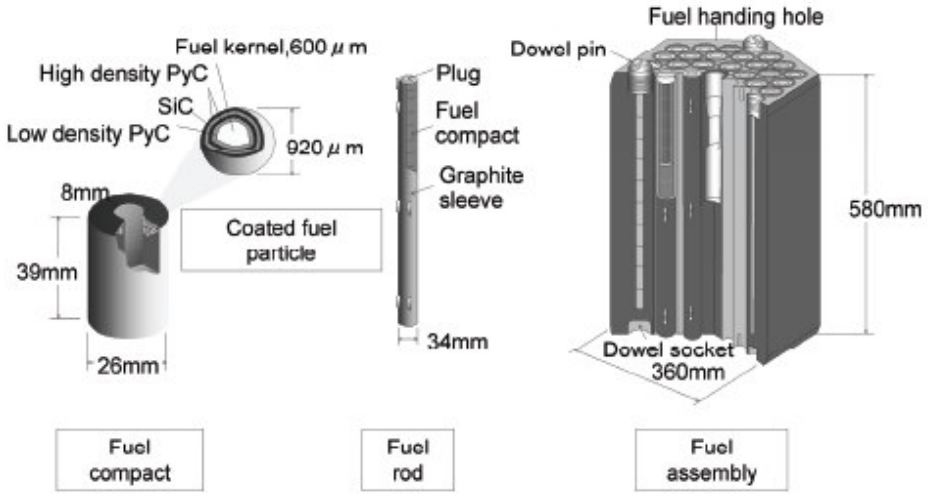

Figure 1.5: The structure of the HTTR fuel assembly [11].

These compacts are loaded into fuel channels in a hexagonal graphite fuel element. The prismatic fuel reactor requires periodic refuelling and shutdowns. The coolant exit temperature for the prismatic fuel concept is about 850 ºC. Compared to the **L**ight **W**ater **R**eactors (LWR's), the thermal efficiency is high due to high temperature operation. An example of such a reactor is the "Fort Saint Vrain Generating Station" that was operated from 1979 to 1989 in the USA and the **H**igh **T**emperature **T**est **R**eactor (HTTR) in Japan (Figure 1.6). These plants have a capacity of 842 and 30 MW thermal respectively. Similarly to the pebble bed concept, the primary coolant is helium.

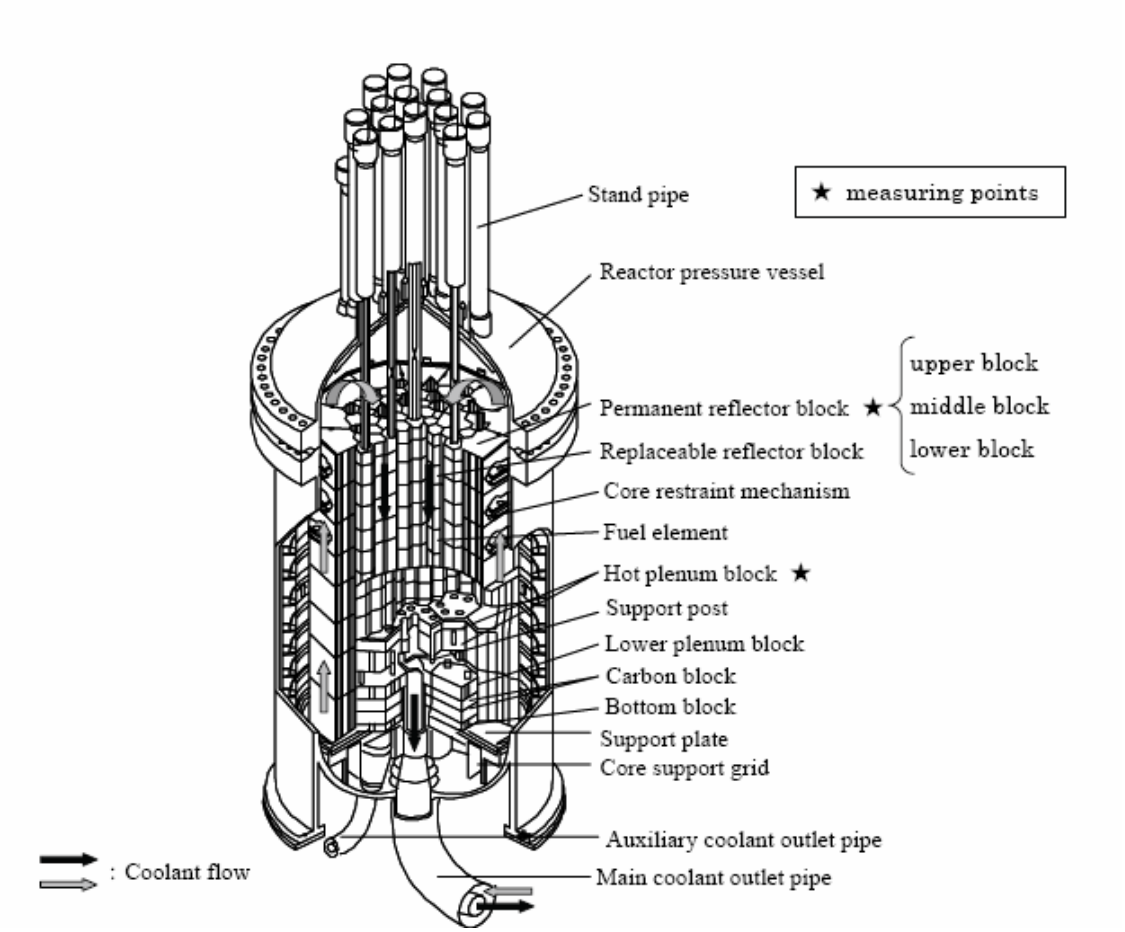

Figure 1.6: Layout of HTTR in Japan [11].

The third category is the "**V**ery **H**igh **T**emperature Gas-cooled **R**eactor (VHTR)" concept which provides the potential for process heat application such as coal gasification and hydrogen production (Figure 1.7). That is, it can be used to produce hydrogen and oxygen through water splitting, which is particularly well suited for coal to liquids and coal to methane processes to maximize carbon efficiency and minimise the carbon dioxide emissions [12]. The VHTR can produce hydrogen from only heat and water by using thermo-chemical iodine-sulphur (I-S) process or heat, water and natural gas by applying the steam reformer technology to core outlet temperature. It can also generate electricity with high efficiency, over 50% at 1000ºC, compared with 47% at 850ºC in the GT-MHR or PBMR. VHTR can also be deployed in refineries and petrochemical industries to substitute large amounts of process heat at different temperatures, including hydrogen generation for upgrading heavy and sour crude oil [6]. It is characterized by high temperature operation with coolant exit temperature above 900ºC or operational fuel temperature above 1250ºC. The international community, which includes the European (France, Belgium, Italy), Union council (Spain, Germany, Netherlands), Switzerland, USA, South Korea (**K**orean **A**tomic **E**nergy **R**esearch **I**nstitute (KAERI)), Japan and South Africa are exploring this VHTR concept [13] and Brinkmann [5].

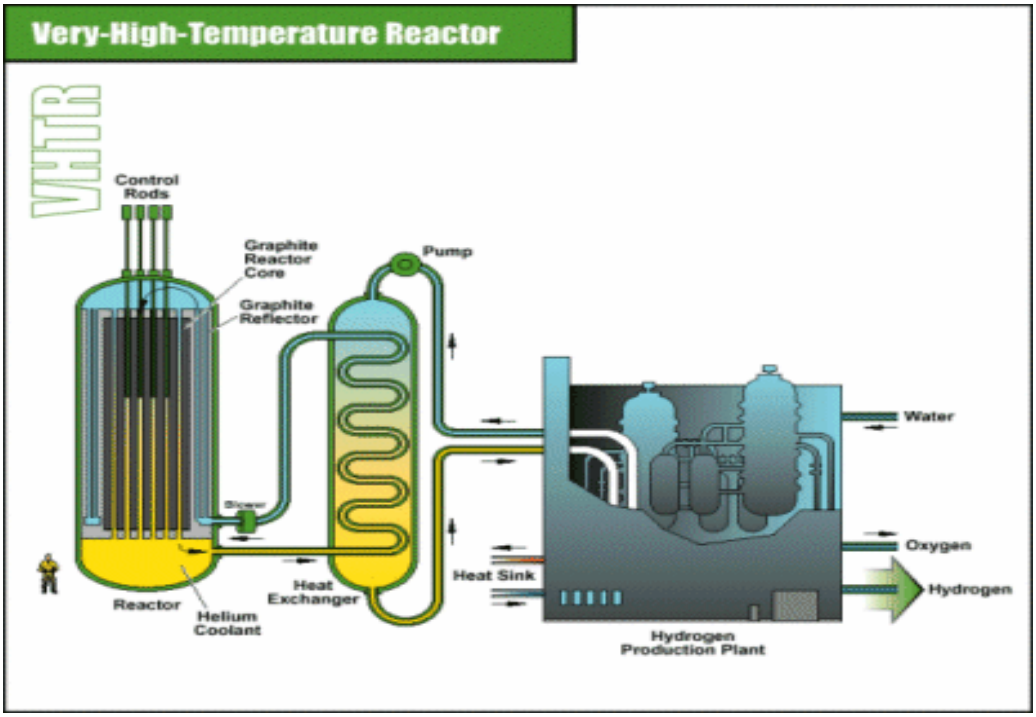

Figure 1.7: VHTR [6].

The fourth category is called the "Gas cooled fast reactor" concept characterized by the breeding of fissile material and has the option to use several fuel designs including both prismatic fuel and fuel pins. This concept uses a direct Brayton cycle gas turbine and the coolant exit temperature is estimated to be around 850ºC [6].

The current literature reviews and conferences [14] (for example a recent HTR-2008 conference that was held in the USA), indicated that the Pebble Bed Modular Reactor concept is presently the subject of research worldwide as an improvement over the conventional LWR type. The Pebble Bed Modular Reactor concept has been identified as one of the "Generation IV Nuclear Energy Initiatives" due to several advantages over the LWR type and these advantages include the passive safe design and proliferation resistance [15] which are discussed in section 1.2.

1.2. The inherent safety of the High Temperature Gas Cooled Modular Reactor (HTGR)

The main inherent safety characteristics of the HTR's are mainly due to several features which include:

- The use of refractory coated particles embedded in the graphite which retains fission products. The Silicon Carbide (SiC) layers have greater heat resistance,

corrosion resistance [16] and provide a unique robustness of the first barrier for fission products.

- The strong negative temperature coefficient of the core, which tends to passively shut the reactor down as temperature increases above the normal operating temperature [17].
- The following are PBMR specific characteristics in terms of nuclear stability and nuclear safety:
    - Heat generation limited by small amount of excess reactivity in-core;
    - Large neutron migration length for neutron stability;
    - Strong negative temperature coefficient limits reactivity excursions;
    - Excess reactivity of 1.3% $\Delta k/k$ allows 40 to 100 % load following at 10%/minute;
    - The temperature coefficient is always negative with strong immediate effect due to Doppler broadening;
    - Full control rod withdrawal without scram will not cause excessive fuel damage;
    - Total loss of coolant will not cause catastrophic fuel failure, as is the case for most other reactor designs.
- The helium used as a coolant in HTGR is chemically inert, has very high heat capacity and thermal conductivity (compared to other gases) and remains single phased under all conditions as compared to LWR reactor types [6]
- The use of graphite with high temperature stability and long response time as a moderator. Unlike the LWR types the moderation is not reduced in case of the loss of coolant (since for LWR water is used as both a coolant and moderator). HTGR has less parasitic capture in the moderator. For example the capture cross section of graphite is about a factor of 165 times less than that of H_2O used in LWR types [18]. However, the effectiveness of the moderating nuclide (or molecule) in moderating neutrons also depends on the relative probability that collision will result in a scattering reaction rather than a capture reaction. Hence graphite is a more effective moderator compared to water with a moderating ratio of about 192 and 71 for graphite and water respectively [18]. The moderating ratio is defined as the ratio of the macroscopic slowing down power to the macroscopic cross section of absorption.
- The HTGR experiences a very slow temperature transient if the active cooling is lost (during a depressurized loss of forced cooling, it takes about 48 hours for fuel spheres to reach the temperature peak), because of the high heat capacity of the graphite core structures and fuel matrix graphite. The response times are very long (days) as compared to minutes in LWR during LOFC. The power density is low (less than 10 MW/m^3 compared to at least 50 MW/m^3 for LWR). For example, for the PBMR reactor, the power density is about 4.78 MW/m^3.
- Heat transfer mechanisms are passive and do not require helium coolant pressure.
- Annular core geometry provides for a short heat transfer path to the outside of the Reactor Pressure Vessel (RPV) resulting in acceptable fuel temperatures (Figure 1.8). The transfer processes within the core, as indicated in Figure 1.8 are natural convection heat transfer between the fuel spheres and helium coolant, the radiative heat transfer between the adjacent fuel spheres, the heat conduction

inside the fuel spheres, the heat convection in the helium coolant and heat conduction from the core to the reflector.

- The efficiency is well above 40% as compared to the LWR reactor (~32%).

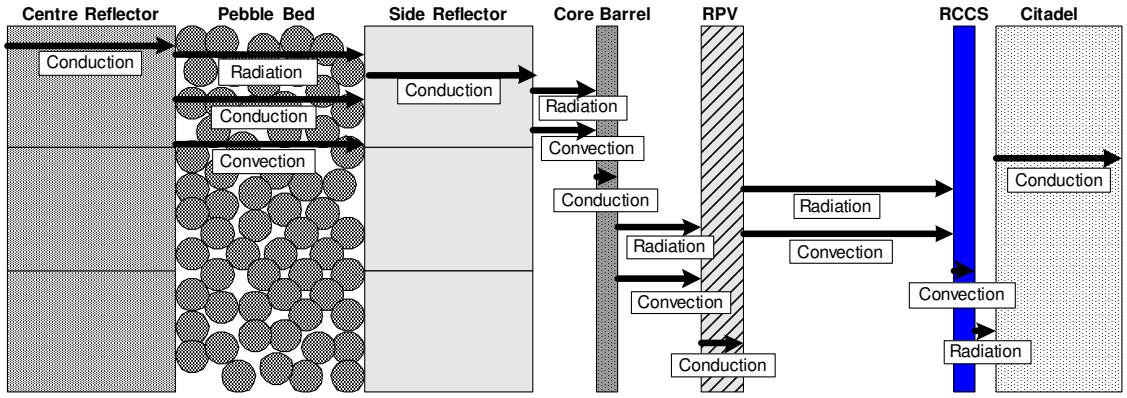

Figure 1.8: PBMR passive heat transfer [19].

Section 1.2 above highlighted the advantages of the HTGR compared to a LWR. However, the HTGR technology does have disadvantages as well. Despite the fact that on-line refueling can be seen as a major benefit because of reduced off time and low excess reactivity, these aspects are negated because on-line refueling is the main source of dust production in the pebble bed reactor. The studies and experiments have shown that during the operation of the AVR reactor in Germany, the dust was transported from the core to other parts of the primary circuit and deposited on the components [20]. The dust is highly radioactive due to the activation product ^{60}Co and fission products ^{137}Cs and ^{90}Sr attached to dust particles, hence the very high observed plant source terms in the AVR. The dust re-circulated in the power conversion unit can cause high worker dose levels during normal operation and maintenance activities [21]. Unlike the HTGR, the PBMR is using the direct cycle gas turbine. This implies that the turbine forms part of the contaminated primary circuit. The radiation protection of workers during maintenance period becomes most important, maintenance by remote control may be necessary [14].

Considering all the advantages and disadvantages stated above, section 1.3 will provide the reasons why South Africa and other international communities (like China, South Korea, Japan, etc.) continue to invest an enormous amount of time and money investigating the HTGR concept.

1.3 Why A High Temperature Reactor?

The high temperature reactor is an energy source which can be used in many ways for the supply of heat (process heat application) and electrical power. It is distinguished by the following special features:

- Favorable safety characteristics through the utilization of passive inherent characteristics in the event of accidents.

- Any core melt down can be ruled out by the use of ceramic instead of metallic material for fuel elements and core structures [17]. There are no active systems or operator intervention or off site emergency response required.
- No evacuation of the population in the case of hypothetical accidents, i.e. because of the improbability such accident scenarios need no longer be taken into consideration in the design [22].
- Simple operating procedures; the operating team has plenty of time for intervention in the event of an accident. For example, during the loss of coolant accident without any operator intervention, it will take 48 hours for the fuel sphere to reach a temperature of about 1600°C (refer to chapter 4). Considering the fact that the PBMR core contains about 452 000 fuel sphere in the core, only 7% of these fuel elements in the core will be exposed to temperatures approaching 1600°C. For the PBMR, this 7% must be quantified in term of the dose to the workers and to the public.
- Low radiation exposure of the workers (approximately 50 to 100 times lower than in the other nuclear power plants [22]). HTGR are extremely safe with respect to the retention capability of fission product by coated the particles.
- Simple fuel cycle; waste management through direct final storage, i.e. no reprocessing required, but still possible [22, 23].
- Continuous loading and discharging of fuel elements, i.e. high time availability because no downtime for refueling is required. It enhances effective utilization of fuel and minimization of the discharged waste.
- Higher thermal efficiency than modern conventional plants (i.e. for PBMR efficiency is about 41%).
- Apart from power generation and combined heat and power generation all heat requirements with temperatures up to 950°C can be satisfied.
- Economically competitive alternative with innovative and advanced technology.
- The PBMR technology is an unattractive target for the diversion of weapon-usable material and acts of terrorism. The proliferation resistance characteristics of HTGR and PWR were evaluated using the International Project on Innovative Nuclear Reactors and Fuel Cycles (INPRO) methodology. The results show that the proliferation resistance of HTGR (e.g. Gas Turbine Modular Helium Reactor (GT-MHR)) is higher than that of the PWR 24].

Section 1.4 provides a brief description of the PBMR reactor core and layout as currently used by the analyses performed to provide support and justifications of the chosen fuel management scheme, which is the purpose of this dissertation. However, the PBMR 400 MW design used in this dissertation is in the process of being replaced by cylindrical reactor with steam generator due to the too high temperatures described in this dissertation.

1.4 The PBMR layout and description

The Pebble Bed Modular Reactor (PBMR) is a helium-cooled, graphite moderated high temperature reactor with direct cycle. The design for the PBMR consists of a vertical steel reactor pressure vessel (Figure 1.4). This pressure vessel acts as a barrier against

fission product release to the environment. The pressure vessel is lined with the core barrel assembly and layered graphite core structures (i.e. central reflectors, side reflectors, top and bottom reflectors. The core barrel assembly supports the graphite core structures during normal plant operation and during accident conditions (i.e. seismic event). The graphite core structures define and maintain the reactor annular core geometry. The main function of the reflector is to reflect neutrons back into the core, thus increasing the neutron economy of the core. The side and central reflectors define boundaries for the pebble bed and provide channels for the reactivity control rods and shutdown system (small absorber spheres situated in the inner central reflector) respectively and also provide pathways for helium coolant flow and remove the heat deposited during power operation of the core (as illustrated in figures 1.9 and 1.10).

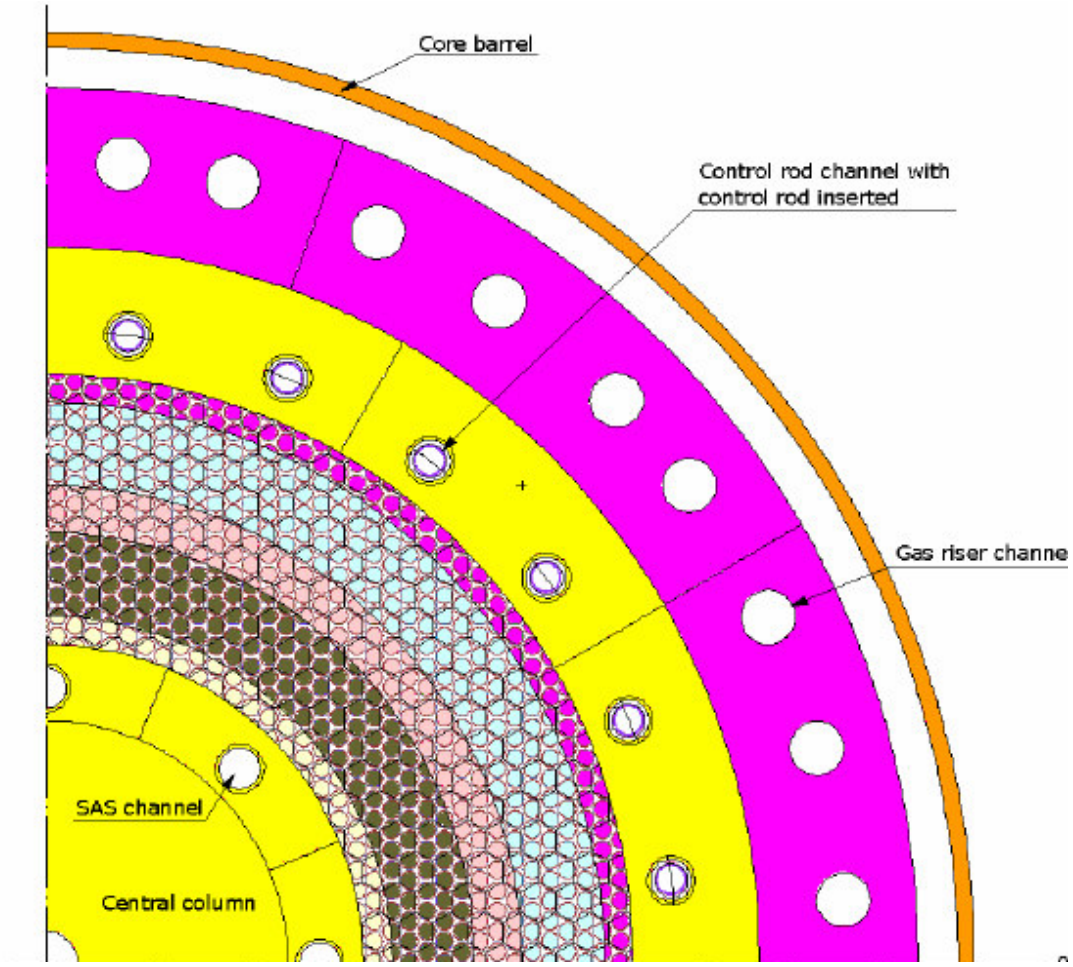

Figure 1.9: A cross section of a quarter of PBMR reactor core, where SAS refer to the Small Absorber Spheres [25].

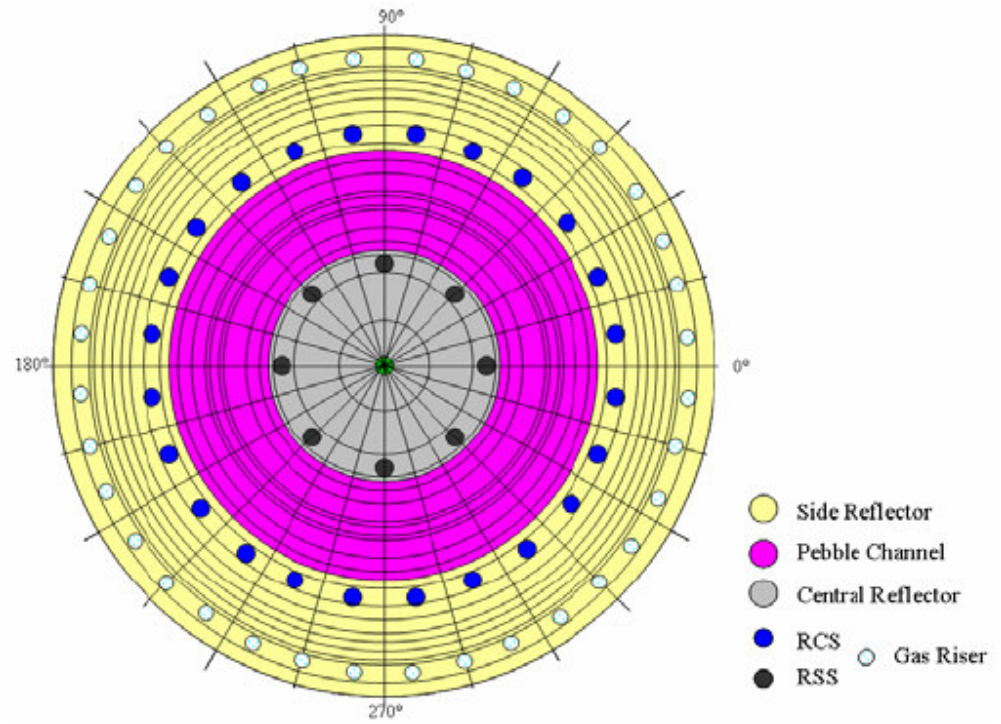

Figure 1.10: Radial cross section of the PBMR core, where RCS and RSS refer to the Reactivity Control System and Reserve Shutdown System respectively [26].

The top reflector provides neutron absorption and shielding of the core and protects the core barrel top plate from high temperature. The bottom reflectors provide channels for the cooling gas and protect the core barrel from high temperature gas exiting the core. The reactor is 3.7 m in diameter and 11.0 m high. Helium enters the reactor at a temperature of 500ºC and a pressure of about 90 bars and leaves the core at a temperature of 900ºC. When fully loaded, the PBMR reactor core contains about 452 000 fuel spheres.

Each fuel sphere or pebble is coated with a 5 mm thick layer of graphite (known as the fuel free region) and contains some 15000 coated TRISO particles each 0.92 mm in diameter as illustrated in figure 1.1. The fuel sphere contains 9 g of UO_2 enriched up to 9.6%. The central kernel of the TRISO particle is 500 µm in diameter and these kernels are surrounded by a porous carbon buffer layer to contain gaseous fission products and then by two pyrolytic graphite layers and a Silicon carbide (SiC) structural layer which prevent release of fission products.

The reactor criticality is maintained during the PBMR operation by removing depleted fuel spheres from the bottom of the reactor core and replenishing with fresh fuel at the top of the core. The fuel spheres leaving the core are measured, those exceeding the reference burn-up would be removed to the spent fuel storage tanks and others would be recycled (on average times). The fuel sphere burn-up is measured by **B**urn-**U**p **M**easurement **S**ystem (BUMS) which is connected to the operational control system. The BUMS performs spectroscopic analyses of photons radiated from irradiated fuel sphere to

determine the inventory of specific radio nuclides. Irradiated fuel emits gamma rays of various energies and intensities, as well as neutrons. For a fission product to be useful for the purpose of burn-up measurement, it must have long half life. The half life must be sufficiently long to ensure that radioactive decay does not cause significant departure from a linear relationship between activity and burn-up. For exact determination of the peak area in the gamma spectrum, a certain minimum counts must be accumulated. The longer the half life of a nuclide the smaller the activity will be. In order to accumulate sufficient data in short time available the concentration of relevant nuclide in the fuel element must be as high as possible. Thus nuclides with high fission yields are desirable and it is preferable that all it's precursor should have short half lives. And have high probabilities for emission of photon during radioactive decay. The photon peak of fission product nuclide should preferably not be interfered with by photon peaks produced by other fission product nuclides present in irradiated fuel at the time of measurement. The specific radio nuclide such as Cs-137 and/ ratio of Cs-134/Cs-137 are used by the BUMS. It has a half life of about 30.07 yrs and high fission yield. But it does not emit photon during decay. However, it decays to Ba-137m with high probability photon emission (661.6 keV) and has half life of about 2.6 minutes. So the measurement of Ba137m provides an indirect measurement of Cs137.

At 9.6% enrichment, the fuel sphere burn-up is estimated to be 90 000 MWD/Ton. The PBMR reactor unit would produce 400 MWth which would be converted at 41% efficiency to 165 MWe. However, PBMR has proposed design changes and are now focusing on the 200 MWth indirect steam cycle. Several technical challenges may have lead to this design changes and some of these challenges will be discussed in chapter 4. The PBMR 400 MW design input data, the methodology and assumptions and treatment of findings (results) will be described in chapter 4 of this dissertation.

1.5 Motivation and Study definition

Selecting an effective in-core fuel management plan for the reactor yields minimum energy costs for an electricity utility. This process forms the central part of the nuclear fuel management. This selection requires integration of the economic analyses with all the technical analyses on core neutronics, thermal hydraulics and accident analyses. These involve identification of the critical parameters from core neutronics design, thermal hydraulics and accident analyses that play a role in fuel management analyses and optimization of the fuel economy. For this dissertation, the focus will be on the parameters that play an important role for "in-core" fuel management. These parameters are identified as follows:

- Fuel Enrichment (Safety and economics)
- Heavy metal content in the fuel element (Safety and economics)
- Number of fuel passes, on-line refuelling (Safety and economics)

The above mentioned parameters have significant impact on core physics parameters such as:

- Maximum fuel temperature during normal operation and accident conditions (Safety)

- Average discharge fuel burn-up (Safety and economics)
- Power peaking factors (Safety)
- Reactivity worths (shut down capability) of the Reactor Control System (RCS) and Reserve Shutdown System (RSS, Safety)

These parameters provide a basis for fuel performance during normal operation and accident conditions. They also impose limits on core operating conditions to ensure fuel integrity and regulatory limits. An optimum combination of these parameters assists in selecting the "preferred" fuel management plan which strikes a balance between the economics and safety (operating and energy costs). This also involves a great deal of technical judgement derived from previous reactor operating experience.

For the PBMR reactor, there are only a limited number of specific operating requirements. These requirements are based on reactor and power optimization studies as well as reactor fuel operating limit and the operating technical specifications which provide the specific operational parameters for normal operation and accident conditions. These operating technical specifications are well established prior to reactor fuel loading or start-up of the reactor. They form part of the safety case submission to the regulatory authorities. The core physics parameters such as the discharge burn-up are selected to minimize the fuel cost within the constraints imposed by other operating requirements. Selecting a design margin on the other hand requires at least a quantitative evaluation of the relationship between fuel integrity and the fuel operating parameters such as power density, peaking factor, burn-up, fluence, temperature and fuel response to operational transients. If the plant is operated closer to the performance limit, the design margins are reduced and the risks of fuel failure increase. Operating with large design margin on the other hand, implies higher operating costs. Since the fuel costs are a relatively small fraction of the total energy cost, the compromise between the fuel operating costs and the risks of fuel failure is usually weighted heavily to reduce the probability of fuel failure (nuclear safety overrides commercial gain). Fuel failure probability is a function of fuel design characteristics, manufacturing specification and reactor operating conditions. Although the general fuel failure mechanism is known, many physical phenomena contributing to fuel failure are not thoroughly understood at the moment and due to this, conservative design and operating practice is required. These general failure mechanisms are:

- Kernel migration.
    - However, for the PBMR fuel the low power density and homogeneous fuel distribution does not provide sufficient strong temperature gradient.
- Fission products attack on the coating.
    - Example of fission product attack is the attack of the SiC by palladium.
- Pressure vessel failure.
    - The build-up of pressure inside the particle coatings is due to the generation of fission gases results in tensile stress in the SiC. If this stress exceeds the strength of the layer, the result is a simultaneous failure of the coating layer.

    - Neutron induced pyrolytic carbon cracking.
    - Debonding due to shrinkage cracks that develops in the inner pyrolytic carbon layer during irradiation/
    - Kernel swelling.
- SiC thermal dissociation.
    - This thermal dissociation may result in degradation of SiC integrity with respect to fission product release after extended times at temperatures in excess of those found in modular reactors. The thermal dissociation can progress to complete SiC degradation as temperature exceeds approximately 2200°C. Design selections which limit core temperatures to less than 1600°C ensure that the coating failure by dissociation is small.
- As fabricated defects.

Taking into consideration, the abovementioned mechanisms, the PBMR is expected to fail at very high temperature, burn-ups and fluence levels. From fuel management point of view, it is important to qualitatively understand the fuel failure mechanism as well as the fuel spheres operating conditions so that the plant operating limits can be achieved. The constraints imposed on these core physics parameters can result in violation of the fundamental safety functions. These fundamental safety functions include the containment of fission products, reactor shutdown capability and heat removal. The variation of the fuel management parameters such as enrichment and heavy metal loadings can result in the constraints on the core physics parameters such as burn-up, temperature, shutdown capability, peaking factor and power density. And these constraints will challenge the fundamental safety functions, that is higher burn-up and temperatures for example can challenge the confinement of fission products or increased enrichment level can even result in reduced shut-down capability and these constraints are described below.

This dissertation describes various phases of in-core fuel management. The first phase of the in-core fuel management involves coordinating fuel operating requirements with the overall energy generation planning effort carried out by each and every nuclear facility. This includes assessment of the enrichment, heavy metal content, and operating cycle which has impact on energy generating costs or fuel costs per energy generated by a reactor unit. These costs also depend on the nuclear plant refuelling scheme and operating mode, for example, the choice not to circulate in the core (OTTO,**O**nce-**T**hrough -**T**hen **O**ut) scheme [15] or multi pass scheme. The OTTO scheme does not re-circulate fuel elements in the core. The fuel goes into the core only once and a multi-pass scheme involves recirculation of fuel elements up to 10 times (until the targeted burn-up is achieved). For the PBMR, the fuel elements will be re-circulated up to 6 times before being discharged into the spent fuel tanks.

The second phase of the in core fuel management consists of the refuelling mode and reactor control plan that meets both the energy and refuelling requirements. These include detailed neutronics and thermal hydraulic evaluations to ensure that the technical operating specification and other constraints that may be imposed by the reactor are met.

Although the online refuelling used in the pebble bed allows a minimum reactivity inventory and may enhance total availability, it is a complex system that must be operated reliably at a rapid sphere transit rate. The current design suggests about 90 000 MWD/T of burn-up and 6 cycles through the core for a given sphere; with 9 grams of heavy metal fuel per sphere. The discharged burn-up is also subjected to constraints in terms of the fuel failure probability increasing with the discharged fuel burn-up and it has an impact on the power distribution. An increased fuel burn-up involves a gradual build-up of fission products in the fuel which results in an increased internal gas pressure and gaseous fission product release.

Even with the online refuelling, there is a need to keep the reactor shutdown during the most reactive condition (cold) and xenon free. The shut-down margin must be assured at all operating conditions of the plant. The details of these are discussed later in the dissertation (chapter 4, section 4.4.).

In addition, it is necessary to evaluate the consequence of anticipated operational occurrences (AOO) such as unplanned outages or maintenance, full core reload or off load and repairs of components prior to a planned outage period. A contingency plan is required in case an incident occurs in the plant.

The next section focuses on PBMR design constraints and interaction between the fuel operating parameters that are important during in core fuel management. These parameters include the fuel enrichment and the fissile content per fuel element, number of fresh fuel elements in circulation, the techniques used to control excess reactivity during reactor cycle and load follow. For the PBMR core, the reactor is always a mixture of fresh fuel spheres and partially spent fuel spheres.

The above mentioned parameters like, online refuelling (number of passes), fuel enrichment and heavy metal loadings have been selected because of their impact on fuel management and on the passive safety feature for the operation of the pebble bed core due to their impact on the fuel temperature, power peaking factors, burn-up etc. The assurance that the fission products release by the facility are below the design and regulatory limits must be given and these should include uncertainties due to fuel defects (fuel qualification), heavy metal contamination in the fuel sphere and power peaking.

Chapter 2

Theoretical Background

Fuel management studies require broad knowledge of parameters affecting reactor operation. These parameters are derived from the reactor physics design and analyses such as power distribution, reactor control and fuel depletion. The analytical model used for in-core fuel management analyses should be in a position to perform the evaluations of reactor multiplication, reactor control characteristics, spatial power distribution, excess reactivity, effects of fuel depletion and fission product build ups for the entire life of the fuel in the core. These evaluations will provide information and statistics on the fuel economics, fuel performance and operating requirements. The evaluation of reactor control characteristics must be performed to ensure that excess reactivity is adequate at all times and that at each operating point the plant operating technical specifications are satisfied. The evaluation of the power distribution and its interaction with the reactor control is performed so that thermal operating limits are not exceeded. That is, the fuel temperature may put some constraints on the retention capability of the fission products as plant safety must not be compromised. The balance between the operating limits and fuel management optimization is what differentiates between a good and a bad fuel management and can result in the minimum or maximum costs to the power utility depending on what has been specified as design margin. That is why the neutronics and thermal hydraulics analyses are performed for all the operating conditions (normal operation, anticipated occupational occurrence (AOO) and accident condition) to derive the plant safety and operating limits. This chapter will describe the neutron transport theory and the approximation of this transport theory (that is diffusion equation) as being used by the numerical model for the in-core fuel management analyses. It will also describe the treatment of neutron spectrum effects and their interaction with the space dependent neutron flux. The chapter will describe the neutron life cycle, the generation of "group constants" that can be used with space and energy averaged neutron fluxes to yield the neutron reaction rates of interest within the reactor and will also extend to the treatment of reactivity control mechanisms which are an important aspect of fuel management (including a short description of the reactor core capability).

2. Neutron life cycle

From the birth of a neutron by fission to its absorption in the core, neutron undergoes several processes. These processes are used to explain the neutron life cycle. The neutron population in any given volume depends on the processes that add and remove neutrons from the volume. The behaviour of the neutron population in a reactor is given by the rate of change of neutron production in reactor less the rate of change of neutron removal. For a steady state reactor condition, the rate of neutron removal equals to the rate of neutron production. This rate of change of neutron population has impact on the steady state condition of the reactor. For the purpose of this discussion, the neutron life cycle can be explained by making the following assumptions:

- All neutrons are born as fast neutrons
- Some fast neutrons can be absorbed by fuel and cause fast fission
- Some fast neutrons can leak out of the reactor
- Some fast neutrons can be resonantly captured while slowing down
- Some thermal neutrons can leak out of the reactor
- Some thermal neutrons can be absorbed by non fuel material
- Some thermal neutrons can be absorbed by fuel and not cause fission
- All the remaining thermal neutrons are absorbed by fuel and cause thermal fission

By comparing the number of neutrons produced by fission in one generation to the number of neutrons produced in the next generation, an indication of the rate of change of neutron population can be derived and is defined as the neutron multiplication factor and can be expressed mathematically as follows:

$$K_{eff} = \frac{\text{neutron production from fission in one generation}}{\text{neutron absorption in the preceeding generation}}. \qquad 2.1$$

This K_{eff} determines whether the neutron population is increasing, decreasing or remains constant. If the number of neutrons produced by fission in one generation equals the number of neutrons produced in the previous generation, $K_{eff} = 1$. This indicates the steady state condition and the reactor power will remain constant and it is said to be critical. However, if the $K_{eff} > 1$, that is the number of neutrons produced in one generation is greater than the number of neutrons produced in the previous generation, then the reactor power is increasing and the reactor is said to be super-critical. And if the $K_{eff} < 1$, the number of neutrons produced in one generation is less than the number of neutrons produced in the previous generation, the reactor power will decrease and the reactor is said to be sub-critical. The starting point of the neutron generation process is taken to be the birth of all fast neutrons from a thermal fission event and represents the numerator in the K_{eff} formula. The six factor formula is used to describe the processes that occur during neutron life cycle (figure 2.1) and is given by the following mathematical expression:

$$K_{eff} = \varepsilon p f \eta P_{NLF} P_{NLT}. \qquad 2.2$$

where $\varepsilon =$ Fast fission factor
$p =$ Resonance escape probability
$f =$ Thermal utilization factor
$\eta =$ Reproduction factor
$P_{NLF} =$ Fast non-leakage probability
$P_{NLT} =$ Thermal non-leakage probability

It should be noted that, for an infinitely large reactor, a lower fraction of neutron leakage

is expected (that is P_{NLF} and P_{NLT} are very high). The four factors (ε, p, f, η) from equation 2.2 are completely independent of the size and shape of the reactor and give the inherent multiplication ability of the fuel and moderator materials without regard to leakage and also accurately represent the infinite multiplication factor ($K_\infty = \varepsilon p f \eta$ (four factor formula)).

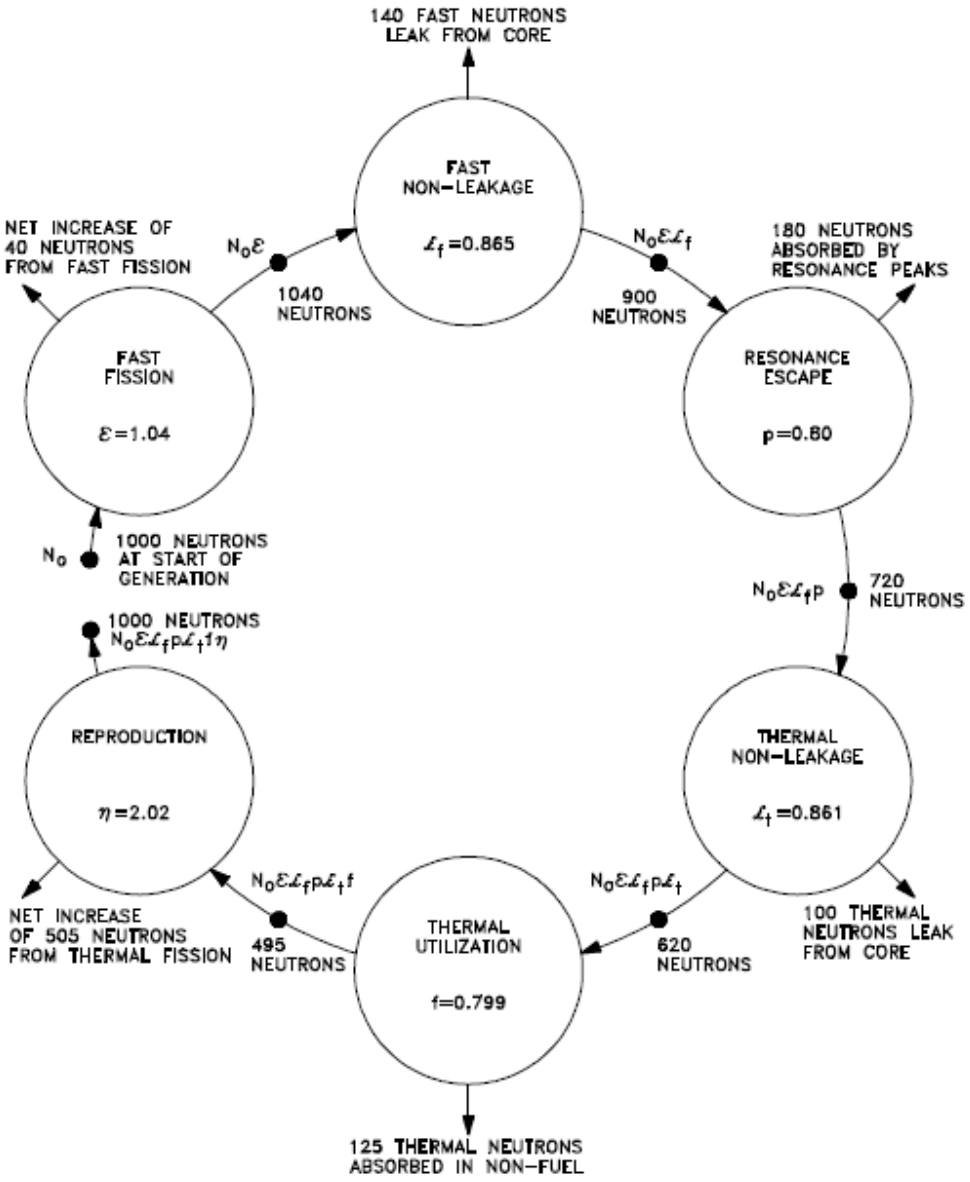

Figure 2.1: Neutron life cycle for a critical reactor (Keff = 1).

2.1 Description of the neutron life cycle

For a finite reactor, these factors are described as follows:

2.1.1 Fast Fission Factor: ε

There are appreciable number of fast neutrons that cause fission in U-235, U-238 and Pu-239. These fissions are known as fast fissions and they result in additional fast neutron production above the thermal fission. The fast fission factor ε, accounts for the neutrons produced by fast fission and is given by equation:

$$\varepsilon = \frac{\text{Fast neutrons produced by all fissions}}{\text{Fast neutrons produced by thermal fission events}}. \qquad 2.3$$

Because the fast fission factor represents a net gain in neutron population, the fast fission factor is slightly greater than 1, typically 1.03 to 1.10. In order for fast fission to occur, the neutrons must reach the fuel while they are still fast. Taking into consideration that the fuel is ceramic kernel or pellets and the fission occur within the kernels, so there is high probability that this fast fission will occur. Also considering the fact that neutrons do not slow down appreciably until they reach the moderator and once these neutrons are in the moderator the likelihood of reaching fuel again and causing fast fission is very small due to the rapid slowing down process. Since the fast fission of U-238 generally requires a neutron with energy greater than 1.8 MeV while U-235 can fission when absorbing a neutron of any energy from fast to thermal. Because delayed neutrons are born with an average energy of about 0.5 MeV, fast fission of U-238 is primarily a function of the prompt neutron fraction. Even though U-235 makes up a small percentage of the total volume in a commercial reactor core, a large fraction of fast fission occurs with U-235 because of its wider fission energy spectrum (Figure 2.2). In reactors employing rather massive, widely separated fuel elements, most of the fast fission in a given fuel element is produced by fission neutrons which originates in that element, since the neutrons quickly slow down below the fast fission threshold once they leave the fuel element and enter the moderator. However, for the case of small closely spaced fuel elements, many fission neutrons which originate in one element may cause fission in another. In such a case the fast fission factor may depend strongly on the density of the moderator between fuel elements, increasing with decreasing moderator density. The major parameters affecting the fast fission factors are fuel atomic density, fuel diameter and moderator ability to slow neutrons down. These parameters are controlled by the fuel or reactor design such that changes in the fuel and moderator temperatures do not significantly affect ε. The burn-up is significantly affected because during reactor operation depletion of U-235 in the fuel takes place which the results in the decrease fraction of fast fission from U-235. This impact is relatively small and may vary from fresh fuel to depleted fuel.

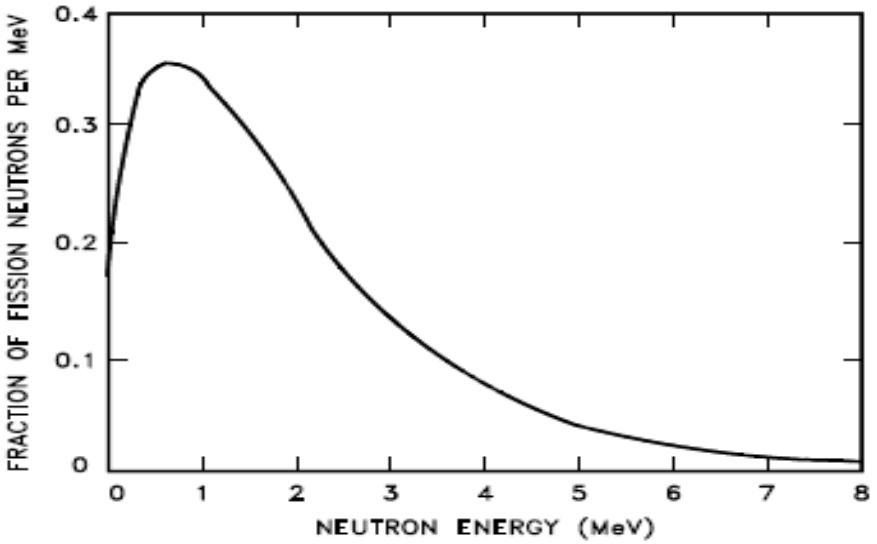

Figure 2.2: Fission Spectrum for thermal neutron induced fission in Uranium -235 [27].

2.1.2 Fast Non-leakage Probability: P_{NLF}

As fast neutrons produced by fission begin their slowing down process, there is a possibility that a neutron will be lost from the core via leakage. The fast non leakage probability P_{NLF} represents that fraction of fast neutrons that do not leak out of the core and is given by the equation:

$$P_{NLF} = \frac{\text{Fast neutrons that start to slow down}}{\text{Fast neutrons produced from all fission events}}. \qquad 2.4$$

The fast non-leakage probability represents a net loss of neutron population, i.e. a percentage of neutrons that remains in the core. The ability of fast neutron leakage depends on how far the neutron can travel before its next interaction. This depends on the moderator density. The effects of decreased moderator density would be to increase the area that neutrons can leak out of the reactor, whereas, a density increase makes the area smaller. Because of the physical size of the commercial reactor, the effects from moderator density on P_{NLF} are minor and are often neglected.

2.1.3 Resonance Escape Probability: p

As the neutrons move, they collide with the nuclei of fuel and non-fuel material and moderator in the reactor losing part of their energy in each collision and slowing down. While they are slowing down through the resonance region of uranium-238, which extends from about $6\,eV$ to $200\,eV$, there is a chance that some neutrons are captured. The probability that a neutron will not be absorbed by a resonance peak is called the "resonance escape probability". "*p*" is defined as the ratio of the number of neutrons reaching thermal energies to the number of fast neutrons that starting to slow down. This

ratio is shown below.

$$p = \frac{\text{The number of neutrons that reach thermal energy}}{\text{The number of fast neutrons that start to slow down}}. \qquad 2.5$$

The value of the resonance escape probability is determined by the fuel to moderator arrangements and the amount of enrichment of uranium-235. To undergo resonance absorption, a neutron must pass close enough to a uranium-238 nucleus to be absorbed while slowing down. In a homogeneous reactor the neutron slows down in the region of the fuel nuclei and this condition is easily met. This means that a neutron has a high probability of being absorbed by Uranium-238 while slowing down; therefore, its escape probability is lower. In a heterogeneous reactor, however, the neutrons slow down in the moderator where there are no atoms of Uranium-238 present. Therefore, it has a low probability of undergoing resonance absorption and its escape probability is higher.

The resonance escape probability represents a net loss of neutron population and it is affected by moderator to fuel ratio, fuel temperature, fuel enrichment and burn-up. That is, an increase in the moderator concentration will cause the neutrons to slow down more effectively, which spend less time in the resonant region, and this will result in a decrease in the probability of resonance absorption. p varies with changes in fuel temperature and burn-up. An increase in temperature will cause the resonance absorption to increase (refer to section 2.2) and hence decreasing p. During the reactor core life, a fraction of U-238 will be transformed into Pu-240 via neutron capture. These will increase the resonance capture over the core life and results in a decrease p. The increase in fuel enrichment will have minor effect on the resonance escape probability due to a decrease in U-238 concentration that results in a decrease in the amount of neutron absorption in U-238. Resonance absorption is affected by the time it takes for the neutrons to slow down to thermal energies and this time is inversely proportional to the moderator density. Further discussion on resonance absorption is given later in this chapter.

The product of the fast fission factor and resonance escape probability (εp) is the ratio of the number of fast neutrons that survive slowing down (thermalization) compared to the number of fast neutrons originally starting the generation.

2.1.4 Thermal Non- Leakage Probability: P_{NLT}

The thermal non-leakage probability represents the probability that a thermal neutron will not leak out of the core and is given by:

$$P_{NLT} = \frac{\text{Thermal neutrons absorbed in the core}}{\text{Fast neutrons that become thermal neutrons}}. \qquad 2.6$$

This factor is impacted by the same parameters as the P_{NLF} and the effects of the parameters is less due to the distance that the neutron travels in thermal energy range which is much less than that of a fast neutron. Like P_{NLF} the thermal non-leakage

probability P_{NLT} decreases with an increase in void coefficient. For an infinite reactor, P_{NLT} is neglected due to the relative size of the reactor and for a finite reactor P_{NLT} is approximately one and does not influence the value of K_{eff}.

2.1.5 Thermal Utilization Factor: f

Since all materials in the reactor absorb neutrons to some extent, careful selection of the reactor material, control of neutron absorption is accomplished and non-fuel absorption is minimised. The thermal utilization factor is the ratio of the number of thermal neutrons absorbed in the fuel to the number of thermal neutrons absorbed in the core and is given by:

$$f = \frac{\text{Thermal neutrons absorbed in the fuel}}{\text{Thermal neutrons absorbed in the core}}.$$

The thermal utilization factor *(f)* represents a net loss in neutron population.

.

$$f = \frac{V_{fuel}\phi\Sigma_a^{fuel}}{V_{fuel}\phi\Sigma_a^{fuel} + V_{\text{mod}}\phi\Sigma_a^{\text{mod}} + V_o\phi\Sigma_a^{o}}.$$

where $fuel$ = Reactor Fuel
Mod = Moderator
O = Other thermal neutron absorbers in the core
V = Volume
ϕ = Thermal Neutron Flux
Σ_a = Macroscopic absorption cross section

Assuming that the flux in the fuel, the moderator and other materials is the same, *f* reduces to:

$$f = \frac{\Sigma_a^{fuel}}{\Sigma_a^{fuel} + (\frac{V_{\text{mod}}}{V_{fuel}})\Sigma_a^{\text{mod}} + (\frac{V_o}{V_{fuel}})\Sigma_a^{o}}. \qquad 2.7$$

An increase in enrichment will increase *f* by increasing the ratio of U-235 to U-238 atoms. This is due to the fact that the thermal neutron macroscopic cross section for U-235 is greater than that of U-238. Over a core life, as the burn-up increases, the ratio of U-235 to U-238 will decrease causing a decrease in *f*. *f* is also affected by the withdrawal or insertion of the control rods. The insertion of the control rods will cause the absorption of other material to increase and hence decreasing *f*. *f* is one of the factors that a reactor operator can manipulate to control the effective multiplication factor K_{eff}.

2.1.6 Reproduction Factor: η

η represents the number of fast neutrons produced from fission compared to the number of thermal neutrons absorbed in the fuel and is given by the following equation:

$$\eta = \frac{\text{Fast neutrons produced by thermal fission events}}{\text{Thermal neutrons absorbed in the Fuel}}.$$

$$\eta = \frac{\nu^{235}\Sigma_f^{235} + \nu^{239}\Sigma_f^{239}}{\Sigma_a^{235} + \Sigma_a^{238} + \Sigma_a^{239}}. \qquad 2.8$$

where $\nu =$ The average number of neutrons produced for each neutron absorbed

$\Sigma_f =$ Macroscopic fission cross section

$\Sigma_a =$ Macroscopic absorption cross section

η represents the net gain in the neutron population and it varies with fuel enrichment and burn-up.

In order to control the reactor power, the operator must be able to control the thermal neutron population. The only way this can be achieved is by varying the values of the factors affecting neutron population. Figure 2.1 shows a typical relative influence of the six factors on the neutron population in the neutron life cycle.

As already stated, the non-leakage factors are insignificant and this leaves the four factor formula for reactor control. Although the fast fission factor and the reproduction factor are important for neutron production, both are reactor design dependent and remain essentially constant. For example, during the reactor operation, as uranium-238 depletes, plutonium is produced and these changes tend to counter balance the value of the fast fission factor ε, remains fairly constant. Thus, the only parameters that have significant changes to the reactor control parameters are the resonance escape probability (p) and the thermal utilization factor (f) through the ratio of the moderator atoms to fuel atoms.

The following section will describe the neutron transport equation and this equation describes the interaction of neutrons with matter. This equation and an approximation of this equation is used by many nuclear reactor analysts to assess the reactor core behavior.

2.2 Neutron Transport

The basic equation that describes the interaction of neutrons with matter is called the neutron transport equation. This has also been referred to as the conservation equation for angular neutron density as function of position, direction of motion and neutron energy. It also provides the exact description of the neutron population in a reactor and forms the central part of nuclear reactor analyses and is the foundation of the analytical model used for fuel management. It is the starting point for the diffusion theory and it is an essential tool for fuel management studies. The transport equation has major drawbacks, as it is

usually very difficult to solve the "transport equations" for even the simplest model problem due to massive analytical work and computational time.

Since the ultimate goal for a reactor analyst is to determine the neutron population distribution in a reactor, one requires accounting for the motion of the neutrons about the core and their interaction with the nuclei in the core. One can start by defining the neutron density at any point r in the reactor $N(r,t)$ as the expected number of neutrons in space d^3r about r at time t. The word "expected" is used in the definition to indicate that this is a "statistical description" and only the "mean" or "average" density distribution is calculated, since the actual neutron density $N(r,t)$ will be obtained through measurements that fluctuate about the "mean" value. The neutron density is of interest as it gives indication of the neutron population and allows us to calculate the rate at which nuclear reactions occur at any point in time in the reactor. This neutron density is different for various neutron energies E in the reactor and can be defined with respect to both the energy E and position r. When characterizing the individual neutrons in terms of neutron position r, energy E (or speed $\upsilon = \sqrt{2E/m}$) and time at which the neutron is observed, one must take into consideration the direction of motion of the neutron. Hence the "angular" neutron density $N(r,E,\hat{\Omega},t)$ can be redefined as the expected number of neutrons in space d^3r about r, energy dE about E moving in the direction $\hat{\Omega}$ in a solid angle $d\hat{\Omega}$ at time t. The term "angular" is used mainly due to the fact that the neutron density $N(r,E,\hat{\Omega},t)$ depends on velocity spherical coordinate angles θ and ϕ specifying neutron direction $\hat{\Omega}$ (Figure 2.3). The exact equation for angular neutron density $N(r,E,\hat{\Omega},t)$ in a reactor can be derived by simply balancing various mechanisms by which neutrons can be lost or gained in an arbitrary space within the reactor. At any point in time, the rate of change of angular neutron density can be given by a dynamic equilibrium:

$$\frac{\partial}{\partial t}\left(\int_V N(r,E,\hat{\Omega},t)d^3r\right)dEd\hat{\Omega} = gain\ \ in\ V\ - loss\ \ from\ V\ . \qquad 2.9$$

where

$\frac{\partial}{\partial t}\left(\int_V N(r,E,\hat{\Omega},t)d^3r\right)dEd\hat{\Omega}$ = the rate of change of neutrons in volume V with energy dE about E moving in the direction $\hat{\Omega}$ in $d\hat{\Omega}$.

The mechanism for neutron loss and gain can be classified as follows:

- Neutron gain:
    1. Via an external neutron source and through fission
    2. Via leakage or streaming of neutrons into the volume of interest V
    3. Via scattering collision in a volume that changes energy E' and direction $\hat{\Omega}'$ into the energy E and direction $\hat{\Omega}$ of interest.

- Neutron loss:
    4. Via neutron leakage out of the volume of interest
    5. Via absorption or scattering collision from the energy E and direction $\hat{\Omega}$ of interest to energy E' and direction $\hat{\Omega}'$

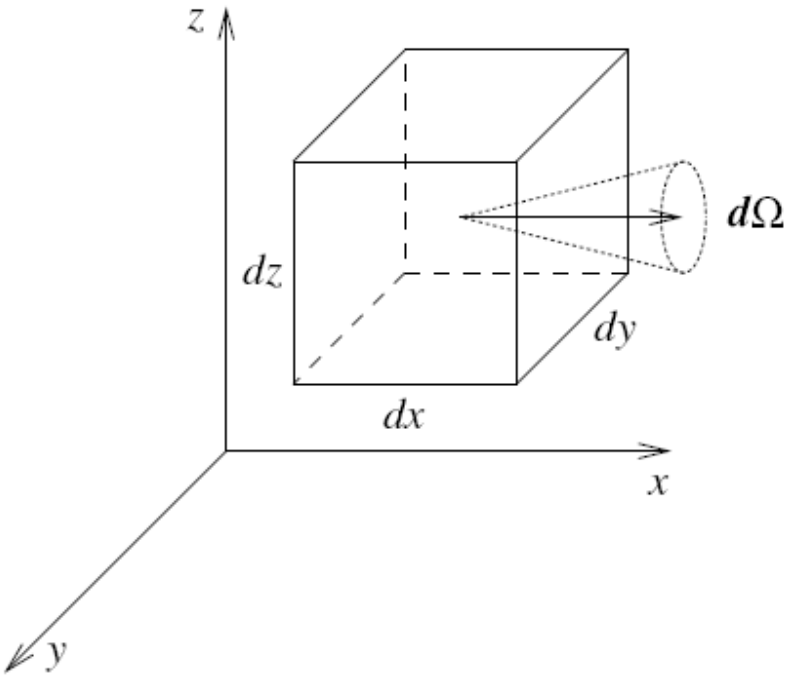

Figure 2.3: Particle located inside an infinitesimal volume dV and moving in the direction of the x-axis, the energy of the particle lies within some space interval [E, E+dE] of the energy space [28].

The neutron balance relationship described in equation (2.9) is discussed in several textbooks such as Duderstadt and Hamilton [27] and Stacey [18] and has the following mathematical expression:

$$\frac{\partial N(r,E,\hat{\Omega},t)}{\partial t} + \upsilon\hat{\Omega}\cdot\nabla N(r,E,\hat{\Omega},t) + \upsilon\sum_t N(r,E,\hat{\Omega},t) = \int_{4\pi} d\hat{\Omega}'\int_0^\infty dE'\upsilon'\sum_s(E'\to E,\hat{\Omega}'\to\hat{\Omega})N(r,E,\hat{\Omega},t) + S(r,E,\hat{\Omega},t) \quad . \qquad 2.10$$

where

$\frac{\partial N(r,E,\hat{\Omega},t)}{\partial t}$ = the rate of change of the number of neutrons in volume V with energy dE about E moving in the direction $\hat{\Omega}$ in $d\hat{\Omega}$

$\upsilon\hat{\Omega}\cdot\nabla N(r,E,\hat{\Omega},t)$ = the rate at which neutrons leak out of the surface

$\upsilon\sum_t N(r,E,\hat{\Omega},t)$ = the rate of neutron absorption and scattering at point r

$\int_{4\pi} d\hat{\Omega}' \int_0^{\infty} dE' v' \Sigma_s(E' \to E, \hat{\Omega}' \to \hat{\Omega}) N(r, E, \hat{\Omega}, t)$ = the rate of neutron scattering from $E', \hat{\Omega}'$ to $E, \hat{\Omega}$

$S(r, E, \hat{\Omega}, t)$ = the rate of source neutron appearing in space d^3r about r, energy dE about E and in the direction $\hat{\Omega}$ in a solid angle $d\hat{\Omega}$.

Starting from the left hand side of equation 2.10, the second and the third term refer to the neutron losses through the net neutron leakage from the volume (item 2 & 4) and scattering and absorption collision (item 5) respectively. And on the right hand side of equation 2.10, the second and the first term respectively refer to neutron gain due to neutron source (item 1) and scattering collision in a volume that changes energy E' and direction $\hat{\Omega}'$ into the energy E and direction $\hat{\Omega}$ of interest (item 3). Note that Σ_t and Σ_s refer to the total macroscopic cross section and the scattering macroscopic cross section respectively. This equation 2.10 is known as the neutron transport equation [27]. Focusing on the right hand side of equation 2.10, the source term $S(r, E, \hat{\Omega}, t)$ can be rewritten as

$$S(r, E, \hat{\Omega}, t) = S_{ext}(r, E, \hat{\Omega}, t) + S_s(r, E, \hat{\Omega}, t) + S_f(r, E, \hat{\Omega}, t) \qquad 2.11$$

where

$S_{ext}(r, E, \hat{\Omega}, t)$ = External source

$S_s(r, E, \hat{\Omega}, t)$ = Scattering source

$S_f(r, E, \hat{\Omega}, t)$ = Fission sources

The external source $S_{ext}(r, E, \hat{\Omega}, t)$ is independent of the neutron flux, it is just the rate at which neutrons are emitted into the volume of interest by an external source. It should be noted that angular neutron density $N(r, E, \hat{\Omega}, t)$ has seven independent variables $(r = x, y, z; E, \hat{\Omega} = \theta, \phi; t)$, since it contains derivatives in space and time as well as integral over angle and energy. The presence of these derivative, suggests that the initial and boundary conditions for angular neutron density must be specified. These boundary conditions depend on the area of interest, for example in an infinite system the neutron leakage at the boundary is zero. That is, there will be no neutrons entering the system from the outside ($N(r, E, \hat{\Omega}, t) = 0$). Hence, one requires that the angular neutron density at the boundary surface disappears for all "inward directions" The initial conditions may be selected to be a description of the initial value of the angular neutron density for all positions, energies and directions:

$$Initial\ condition: N(r, E, \hat{\Omega}, 0) = N_0(r, E, \hat{\Omega}),\ \ all\ \ r, E, \hat{\Omega}$$

The neutron transport equation (2.10) as described above together with its associated boundary conditions can be rewritten in terms of the angular neutron flux

($\phi(r,E',\hat{\Omega}',t) = \upsilon N(r,E,\hat{\Omega},t)$, where υ is the neutron speed) as follows:

$$\begin{aligned}&\frac{1}{\upsilon}\frac{\partial\phi(r,E,\hat{\Omega},t)}{\partial t} + \hat{\Omega}\cdot\nabla\phi(r,E,\hat{\Omega},t) + \Sigma_t\,\phi(r,E,\hat{\Omega},t)\\&= \int_{4\pi} d\hat{\Omega}'\int_0^{\infty} dE'\Sigma_s(E'\to E,\hat{\Omega}'\to\hat{\Omega})\phi(r,E,\hat{\Omega},t) + S(r,E,\hat{\Omega},t)\\&Initial\ condition: \phi(r,E,\hat{\Omega},t) = \phi_0(r,E,\hat{\Omega})\\&Boundary\ condition: \phi(r_s,E,\hat{\Omega},t) = 0\ \ if\ \hat{\Omega}\cdot\hat{e}_s < 0,\ \ all\ r_s\ on\ S\end{aligned} \qquad 2.12$$

where r_s denotes a point on the surface S (surface of the boundary). It is apparent that the neutron transport equation provides an essentially exact description of the neutron distribution within the reactor. The solution to this equation would result in the angular flux $\phi(r,E,\hat{\Omega},t)$ which would contain essential information required for the prediction of the reactor core behaviour. As mentioned above, the neutron transport equation has seven independent variables $(x, y, z, E, \theta, \phi, t)$ and the dependence of the macroscopic cross sections on position due to a non-uniform structure of most reactors (extremely complex) and dependence of cross sections on energy implies that it is unrealistic to attempt solving the neutron transport equation. Even if the number of spatial and angular variables were reduced to simpler geometry, the energy dependence of the cross sections generally precludes solving the transport equation except for unrealistically simple cross section models such as constant cross sections [29]. To make the transport equation more amenable to numerical and analytical treatment, an approximation is made and this approximation may entail the removal of the energy dependent variables or as another example, one may choose to remove the spatial and angular dependence to derive the energy dependent neutron flux similar to the slowing down equation (P1- approximation [27]). A direct numerical solution to the transport equation can be achieved by making use of the "discrete ordinate approach" described in Duderstadt and Hamilton [27], where the transport equation is made discrete with respect to all variables and coupled equations are solved numerically in all discrete phase space. An analytical solution to the transport equation may be derived by making use of the multi-group diffusion theory for scalar neutron flux along with energy group averaged cross sections. This approach to neutron transport is used by many textbooks (that is Duderstadt and Hamilton [27] and Stacey W.M [18]. The diffusion approximation is adopted by most reactor applications. A significant proportion of analysis utilizes the diffusion theory constants that have been derived from the transport equation and yield the same reaction rates as the transport equation. This neutron diffusion equation is defined as follows [27]:

$$\begin{aligned}&\frac{1}{\upsilon}\frac{\partial\phi}{\partial t} - \nabla\cdot\left[D(r,E)\nabla\phi(r,E)\right] + \Sigma_t(r,E)\phi(r,E,t)\\&= \int_0^{\infty} dE'\Sigma_s(E'\to E)\phi(r,E',t) + S(r,E,t)\end{aligned} \qquad 2.13$$

where

$\phi(r,E)$ = the scalar neutron flux density per unit energy per unit volume at a

space point r and energy E ($neutrons/cm^2 s$)

$D(r,E)$ = neutron diffusion coefficient at space point r and energy E (cm)

$\Sigma_t(r,E)$ = total macroscopic reaction cross section for neutrons at space point r and energy ($\Sigma_t = \Sigma_c + \Sigma_f + \Sigma_s$) where c, f, s refer to the capturing, fission and scattering cross sections (cm^{-1})

$\Sigma_s(r, E' \to E)$ = macroscopic cross section for the transfer of neutrons from E' to energy E at the space point r ($1/cm$)

The scalar neutron flux $\phi(r,E)$ is the number of neutrons times the velocity per unit volume per unit of energy and the cross section is the interaction probability per unit path length. This diffusion equation is also referred to as "the conservation of neutron" equation. The left hand side of the diffusion equation (2.12) represents the neutron losses by leakage and neutron interactions respectively. And the right hand side represents the neutron production through fission and scattering respectively.

The diffusion theory is an approximation of reality. It is based on Fick's law and it is assessed as being equivalent to the assumption that the net current of the neutrons per unit area in space, $J(r,E)$ is proportional to the gradient of the scalar flux and that the proportionality constant is the diffusion coefficient:

$$J(r,E) = -D(r,E)\nabla\phi(r,E) \qquad (2.14)$$

where

$J(r,E)$ = The net current of neutrons per unit area point r and energy E

$D(r,E)$ = Neutron diffusion coefficient at a space point r and energy E (cm)

$\nabla\phi(r,E)$ = The gradient of the scalar neutron flux density

For equation (2.13) to be valid, one assumes that the angular flux density varies linearly. That is, the flux density $\phi(r,E)$ is expected to be nearly isotropic in direction. However, near free surfaces (such as voids), absorber materials (control rods) or a neuron source, the flux density is anisotropic in direction and it is not well represented by a simple linear variation. For these situations, the diffusion approximation is poor. For example, near a point source, the flux density as calculated by diffusion varies as $1/r$, while the transport theory gives the correct $1/r^2$ variation [29]. For cases where flux gradient is large (anisotropy), the diffusion equation is adjusted to yield reaction rates that agree with the transport theory calculations, for example the Method of Equivalent Cross Section (MECS)[30]. This approximation has been validated (tested) for many reactor applications and the results were satisfactory [30].

In the nuclear reactor, neutrons have energies spanning from 10 MeV down to thermal (less than 0.1 MeV). The analytical solution to equation (2.13) can be achieved by a discrete ordinate method such that the multi-group fluxes $\phi_{gn}(r)$ represent the total flux of

the neutron with energy E in a group. This will give rise to a set of diffusion equations describing the neutron in each energy group. These equations are coupled to one another as neutrons experience changes in energy from group to group as they are moderated by scattering collision. Each energy group must be defined in order to adequately describe the nuclear reactor by also taking into consideration the dependence of the neutron cross-section on energy E. Most calculations can accurately predict the reactor behaviour by making use of "few-group" diffusion equations. This is achieved through a careful choice of the energy average cross section that characterizes the neutrons in each group. This chapter will not provide a heuristic derivation of the multi-group diffusion equation as this is described by Duderstadt and Hamilton [27]. The energy dependent diffusion equation (2.13) is converted to the multi-group diffusion equation (or approximation) to eliminate the energy variation, thereby making the model more amenable to numerical solution.

One of the important parameters when performing the fuel management is the reaction rates within a typical volume-energy element is defined as follows:

$$R^{i}_{xg}(r) = \int_{E_g}^{E_{g-1}} N^{i}(r)\sigma^{i}_{x}(E)\phi(r,E)dE. \qquad 2.15$$

$=$ is the number of nuclear interactions of type x in an isotope i in neutron energy group g at space point r in volume V per second unit volume,

where the terms within the integral are defined as follows:

$N^{i}(r)$ = the atomic density of isotope i at a space point r in a volume V

$\sigma^{i}_{x}(E)$ = microscopic cross section for the reaction type x with isotope i at neutron energy E

$\phi(r,E)$ = neutron flux density at energy E and space point r

For the purpose of this discussion, the nuclear reaction rates will be defined in terms of the nuclear cross section data, geometry and composition of the fuel in the core. Consider a typical fuel element volume in the reactor, this volume could be a length of the fuel rod with surrounding moderator or a larger volume such as the fuel assembly. This fuel element is subdivided into sub-volumes which enable the users to calculate the reaction rates within the volumes for each small range of neutron energies between E_g and E_{g-1}. The energy range will start at E_0, where the number of fission neutrons with energies greater than E_0 is negligible, and extends to thermal energy. The range between E_g and E_{g-1} will be called the energy group g. Note that as the energy indexing g in equation 2.15 above increases, the energy E_g is decreasing. The diffusion equation as defined above is such that the energy group within each homogeneous region has linear differential equations (Homogeneous region being that a region consists of identical typical volume elements). Each term within the linear differential equation preserves individual reaction rates. The coefficients in the diffusion equation are called the "multi

group" diffusion theory constants or multi group macroscopic cross sections. The diffusion in each energy group and each region consists of identical volume elements expressed as

$$\frac{1}{\upsilon}\frac{\partial \phi_g}{\partial t} - \nabla \bullet D_{gn} \nabla \phi_{gn}(r) + \Sigma_{tgn}\phi_{gn}(r,t) = \sum_{\substack{g'=1 \\ g' \neq g}}^{G} \Sigma_{gg'n}\phi_{g'n}(r,t) + \chi_g \sum_{g'=1}^{G} v_{g'}\Sigma_{fg'n}\phi_{g'n}(r,t) + S_g \quad . \qquad 2.16$$

where $\phi_{gn}(r,t) = \int_{E_g}^{E_{g-1}} \phi(r,E,t)dE'$ and the diffusion coefficient D_{gn} is defined as

$$D_{gn} = \frac{1}{3[\Sigma_{agn} + (1-\mu_0)\Sigma_{\mathrm{sgn}}]} \quad . \qquad 2.17$$

where μ_0 is the average cosine of the scattering angle in a volume n in energy group g. The other terms in the equation are defined as follows for each volume element n:

Σ_{tg}	=	Total macroscopic cross section including the capturing, fission and removal by scattering in energy group g
Σ_{ag}	=	Macroscopic absorption cross section in group g
Σ_{sg}	=	Macroscopic scattering cross section in group g
χ_g	=	Fraction of fission neutron born in group g
$v\Sigma_{fg'}$	=	Neutrons per fission times the fission cross section in group g
$\Sigma_{gg'}$	=	Macroscopic cross section scattering of neutron from group g' to group g
S_g	=	Source term due to an external source in group g
υ_g	=	Neutron speed characterising group g
D_g	=	Diffusion coefficient for group g

The equation 2.16 is the multi-group diffusion equation which describes the neutron balance in a specific group by balancing the ways in which neutrons can enter or leave the specific group. This balance equation (2.16) can be read as follows:

$$\begin{bmatrix} Time\ rate\ of \\ change\ \ of \\ neutrons\ in \\ group\ \ g \end{bmatrix} + \begin{bmatrix} change\ due \\ to \\ leakage \end{bmatrix} + \begin{bmatrix} total\ absorption \\ for\ a \\ group \end{bmatrix}$$

$$= \begin{bmatrix} neutrons \\ scattering \\ \text{into} \\ group\ \ g \end{bmatrix} + \begin{bmatrix} fission \\ neutron \\ source \\ for \\ group\ \ g \end{bmatrix} + \begin{bmatrix} source \\ neutrons \\ appearing \\ in\ \ group\ \ g \end{bmatrix}$$

This equation (2.16) results in an explicit expression for group constants $D_g, \chi_g, \Sigma_{fg}, \Sigma_{sg}, \Sigma_{sg'g}, \Sigma_{ag}, \Sigma_{tg}$ *and* υ_g and these constants must be determined. These constants are still dependent on the space and time. To calculate these constants one needs to know the neutron flux $\phi(r, E, t)$ in order to approximate the intra-group fluxes.

2.3 Evaluation of multi group constants

There are two general classes of group constants used in reactor analyses namely; the few group and multi group constants and the latter are based on the subdivision of the energy range between 0 and E_0 into a larger number of groups to minimize the energy dependence of $\phi(r, E)$ within the group. The few group constants are based on the use of ten or less groups to cover the entire energy spectrum. This is normally sensitive to the changes in geometry, fuel isotopic composition and temperature. Large computer programmes have been developed to evaluate the macroscopic group constants for diffusion theory calculations. These programmes solve the energy dependent neutron transport in a varying degree of approximations and also evaluate the variation of group constants with fuel burn-up, power density and moderator temperature and density.

In order to evaluate multi-group constants, one requires the nuclear dataset. This nuclear dataset consists of continuous data of each reaction cross section of interest for isotopic material used in the reactor. In some cases, cross section dataset is identified by parameter for well defined analytical functions such as Breit Wigner single level formula for resonance reaction [27]. The most widely used nuclear dataset that is currently available and has been used in V.S.O.P code is the ENDF-IV/V (Evaluated Nuclear Data File) [25]. This data is developed from the basic experimental data as well as theoretical calculations and represents the combined technical judgement of cross section experts from different organisations. The nuclear datasets such as ENDF formats and libraries are decided by Cross Section Evaluation Working Group (CSEWG) as part of the cooperative effort of national laboratories, industries and universities. The ENDF format provides a representation of neutron cross sections and distribution, photon production for neutron reaction, charged particle production from neutron reactions, photon-atomic interaction data, thermal interaction data, thermal neutron scattering data, radionuclide production, decay data (including fission products), and so on. The ENDF system was developed for the storage and retrieval of evaluated nuclear data to be used for applications of nuclear technology. These applications control many features such as the choice of material, the data used, the format used and testing required before the library is released. The ENDF system is logically divided into formats and procedures. These formats describe how data sets are arranged in the libraries and give the formulas needed to reconstruct physical quantities such as cross sections and angular distributions from the parameters in the library. The procedures are generally imposed by a particular organization and the library sanctioned by the CSEWG referred as ENDF/B [31]. Other organisations may use different procedures; however they face the risks that their libraries will not work with processing codes sanctioned by CSEWG. The nuclear data such as ENDF/B library are maintained by National Nuclear Data Centre (NNDC) and contains recommended evaluation for each material. For example, when a user is

interested in performing a reactor physical calculation or performing shielding analyses specific evaluated dataset required (e.g. all neutron induced reactions, covering the full range of incident neutron energies for each material etc). The choice of the data is made on the basis of requirements of applications, conformance of the evaluation of the formats, procedures and performance in testing. The ENDF/B datasets are revised or replaced only after extensive review and testing. These datasets may be revised or replaced when experimental data for particular material becomes available or when integral tests show that the data give erroneous results or when the user requirements indicate a need for a more accurate data or a better representation of the data for a particular material. The new or revised datasets are included in new releases of the ENDF/B library. Once the evaluated dataset have been prepared in ENDF format, they can be converted to forms appropriate for testing and actual applications using the widely used processing codes such as INJOY, PREPRO2002, AMPX-77. For example, processing codes such as INJOY or PREPRO2002 can be used to generate averaged cross sections for use in the neutronic calculations from the ENDF library. These codes include functions such as resonance reconstruction, "Doppler" broadening, multi-group averaging and/or rearrangement into specified interface formats [32] and [31]. To be specific, PREPRO2002 can be used to produce the temperature dependent, linearly Interpol-able in energy, tabulated cross sections in the ENDF/B-IV formats. The steps required and codes used to produce linearly Interpol-able tabulated cross sections in the ENDF/B-IV are described by Cullen DE [32]. All ENDF/B evaluations go through at least some testing before being released as part of the library. The testing includes the use of codes maintained by NNDC and visual inspection by reviewer to assure that the evaluation conforms to the current formats, procedures and benchmarks (when available to evaluate the usefulness of the evaluation for actual application).

For cases where resonance reactions contribute to reaction rate, the contribution of that resonance will be induced in the multi-group cross section library. Each cross section is defined [27] as

$$\sigma_{xg}^{i} = \frac{\int_{E_g}^{E_{g-1}} \sigma_x^i(E) F(E) dE}{\int_{E_g}^{E_{g-1}} F(E) dE}. \qquad (2.17)$$

where σ_{xg}^{i} is obtained from the nuclear dataset. Usually when developing a multi-group library one constructs a neutron spectrum that approximates a specific reactor type. For example, in thermal reactors, the shape of the fission spectrum could be used for neutron energies above 1 MeV (Figure 2.2). The numerical $\frac{1}{E}$ slowing down spectrum in a non-absorbing material with constant cross section could be used in energy range between thermal and fast energies. The group width must be specific enough so that the choice of the neutron flux $F(E)$ has negligible small effects on microscopic group cross section values. For different reactor types, different multi-group constants or structures are utilized in order to emphasize the different energy ranges of interest.

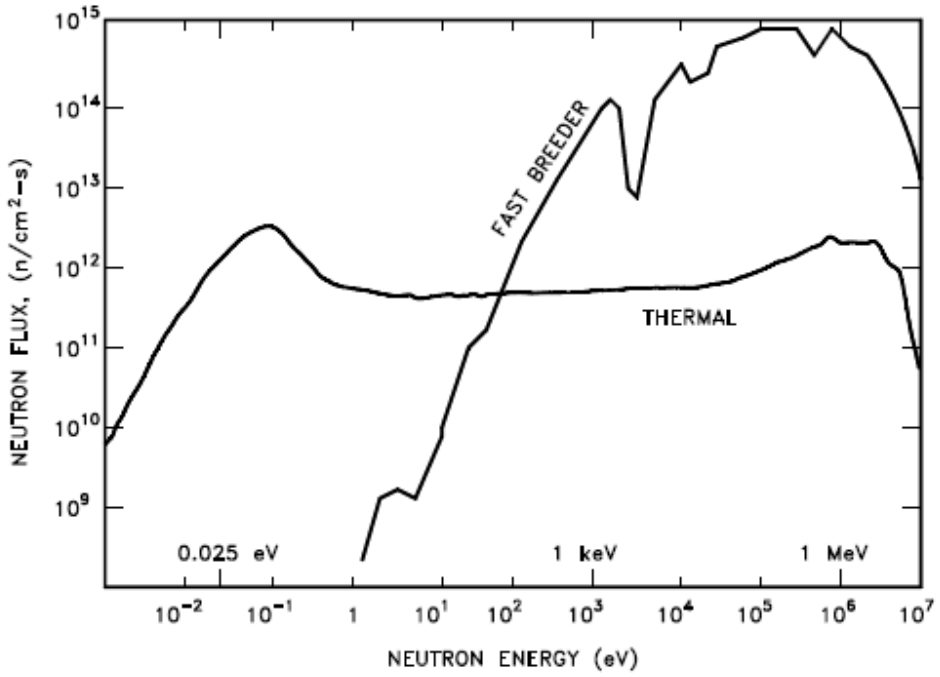

Figure 2.4: A comparison between the neutron spectrum of the thermal reactor and fast breeder reactor [18].

The main difference among reactor types arises from differences in the neutron energy distribution or spectrum, which causes differences in the neutron-nuclear reaction rates and the competition for neutrons. For thermal and fast reactors, the majority of the neutron-nuclear reaction corresponds to the thermal and fast energy range (E<1 eV and E> 1 keV respectively. The representative neutron spectra for the thermal and fast reactors are shown in Figure 2.4. There are important physics differences between the thermal and fast reactors. For example, the neutron capture to fission ratio is lower and the number of neutrons produced per fission is larger for fast reactors than thermal reactors. These generally results in a larger value for the multiplication factor (k) for a given amount of fuel in a fast reactor than thermal reactor and to be specific, a smaller critical mass of fuel in a fast reactor than in a thermal reactors. Because of larger neutron-nuclear reaction rates in thermal neutrons than for fast neutrons, the mean distance travelled by a neutron before absorption is greater for fast reactors than in thermal reactors. This implies that the detailed distribution of fuel, coolant and control elements has a much greater effect on the local competition for neutrons in thermal reactors than in fast reactors and that the neutron population in different regions of the core are more tightly coupled in fast reactors than in thermal reactors. Hence the fast breeder reactor, a more closely spaced energy structure in the energy range between 10 keV to 1 MeV is required as compared to thermal reactors. The energy distribution from fission is essentially the same for both reactions, so the difference in the curve shapes may be attributed to the neutron moderation or slowing down effects. For the breeder reactor, no attempt is made to thermalize or slow down neutrons and hence an insignificant number

of neutrons exist in the thermal range. In the thermal reactors the flux in the intermediate energy region (1 eV - 0.1 MeV) has approximately a $1/E$ dependence. This $1/E$ is caused by slowing down process, where elastic collisions remove a constant fraction of neutron energy per collision at higher energies than at lower energies. The fact that neutrons lose a constant fraction of energy per collision causes a "build up" at lower energies and hence a greater number of neutrons exist at lower energies as a result of this build-up. The thermal neutron energy at some temperature can be characterized by Maxwell-Boltzmann distribution (Figure 2.2). The energy of most thermal neutrons is close to the most probable energy, but there is a spread of neutrons above and below this value ($\upsilon_p = \sqrt{\frac{2kT}{m}}$). where k is the Boltzmann constant (k =1.38×10^{-16} erg/K), T is the absolute temperature (in Kelvin (K)), υ_p is the most probable velocity of the neutron (cm/sec) and m is the neutron mass.

The thermal reactor group energy structure is selected carefully such that a very finely structured multi-group calculation can be solved. These calculations take into consideration the treatment of resonance absorption since this is one of the primary mechanism for neutron loss in fast and thermal reactors. This resonance absorption enters into the multi group diffusion equation through the fast multi group absorption cross sections, hence accurate estimation of these group constants are important because a flux depression is expected at those energies in the vicinity of a strong resonance. The analysis of such flux depression plays a critical role in the determination of the multi-group constants. That is, small inaccuracies in the treatment of resonance absorption can propagate sizable errors in the estimation of both fuel depletion and fertile-to–fissile conversion (U-238, Th-232 to Pu-239, U-233 respectively). The most important feature of the microscopic multi-group cross sections library is that the cross section and resonance parameters are independent of the geometry and composition.

2.3.1 Resonance Absorption

Cross-sections depend on the relative speed between the neutron and the target nucleus. As nuclei themselves are in thermal motion the relative speed can either be greater or less than the neutron speed. This difference in the relative speed gives rise to a "Doppler shift" effect in resonance cross section behaviour (Breit Wigner Resonance cross section formula) [27]. The dependence of this cross section on energy at different temperatures is depicted in Figure 2.5. It can be seen that as temperature increases, the resonance broadens while its peak amplitude decreases. Hence the resonance cross sections that have been averaged over the distribution of nuclear velocities are referred as "Doppler-Broadened" cross sections.

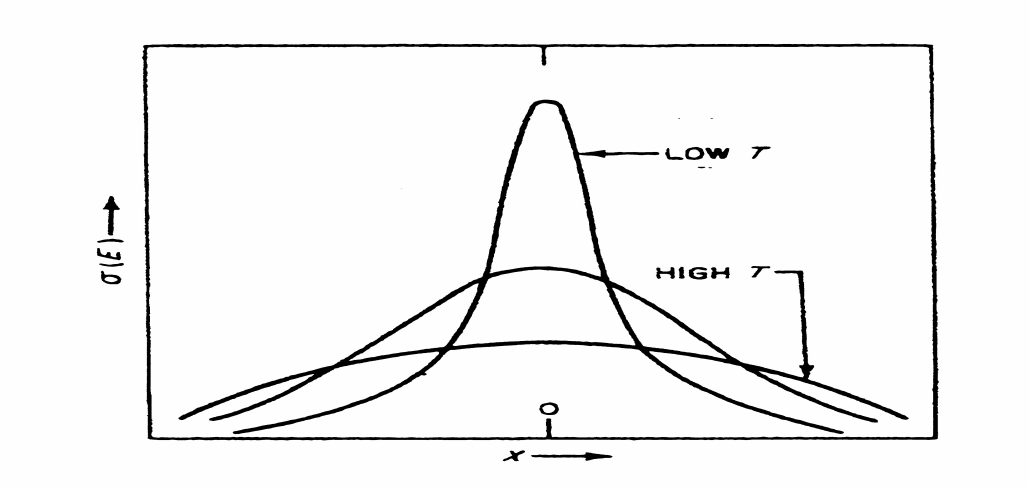

Figure 2.5: Doppler Broadening [27].

In a nuclear reactor, as the neutrons slow down from fission energies, they will experience an appreciable probability of being absorbed in the numerous sharp capture resonances which characterize heavy nuclei such as U-238 or Th-232. Such resonance absorption is an important phenomenon in a nuclear reactor as it affects the reactor multiplication factor, fuel burn-up, reactor controls and reactor kinetics. As this resonance absorption in fertile material (U-238 or Th-232) can lead to the production of fissile material (Pu-239, U-233), an accurate analysis of resonance absorption is important. There are several different types of resonance absorption and the most important one, in a thermal reactor, is the absorption in the well resolved low energy resonance of the fuel material such as 6.6 eV in U-238 (Table 2.1 [27]). This table highlights the resonance data for several low lying resonances of U-238 which are significant in thermal reactors. The number of collisions in table 2.1 is given in terms of lethargy (u) and the nucleus mass (A). The neutron lethargy or logarithmic energy decrement is a dimensionless logarithmic ratio of the energy of source neutron to the energy of neutron after a collision and is expressed as follow $u = \ln\left(\frac{E_0}{E}\right)$ and E_0 is the maximum neutron energy. The average lethargy gain or the average logarithmic energy loss of a neutron in a collision with a nucleus of arbitrary mass number A (e.g.U-238) is given by

$$\xi = 1 + \frac{\alpha}{1-\alpha}\ln\alpha.$$

$$= 1 - \frac{(A-1)^2}{2A}\ln\left(\frac{A+1}{A-1}\right).$$

$$= 1 - \frac{(238-1)^2}{2x238}\ln\left(\frac{238+1}{238-1}\right)$$

$$= 8.379871x10^{-3}$$

For example, the number of collision in table 2.1 below is calculated as follows

$$\langle \# \rangle = \frac{u}{\xi} = \frac{\ln(\frac{E_0}{E})}{\xi} = \frac{\ln(\frac{2x10^6}{6.67})}{8.379871x10^{-3}} = 1504.92$$

Above several keV in fertile material (and as low as 50 eV in fissile materials) the resonance structure becomes so finely detailed that resonances can no longer be individually resolved. Treatment of resonance absorption in the region of unresolved resonance is more complicated and requires the use of a nuclear model to describe the resonance structure

E (eV)	$\sigma_0(b)$	Number of collisions from 2 MeV to E (eV)
6.67	2.16E+05	1504.90
20.90	3.19E+04	1368.62
36.80	3.98E+04	1301.11
66.54	2.14E+04	1230.43
102.47	1.86E+04	1178.91
116.85	1.30E+04	1163.23
165.27	2.41E+03	1121.86
208.46	8.86E+03	1094.15

Table 2.1: Resonance data for several low lying resonance of U-238

An accurate treatment of resonance absorption is essential to reactor criticality calculation, since this is the primary neutron loss mechanism in both thermal and fast reactors. This process enters into the multi-group diffusion equation (2.11) through the fast multi-group absorption cross section Σ_{ag} and accurate estimate of this group constant must be investigated. In the vicinity of strong absorption there will be a depression in the neutron flux at those energies (Figure 2.6) and such flux depression is of considerable importance in the determination of the multi-group constant. A rigorous treatment of resonance absorption would attempt to determine the flux by solving the transport equation directly or by Monte Carlo techniques [27] and such techniques are too expensive for use in routine design analyses. Since the spatial variation in neutron flux has strong influence on the resonance absorption, using the slowing down equation, the neutron flux can be defined as [27]:

$$\phi(E) = \frac{\Sigma_s(E_0)}{\Sigma_t(E_0)} \frac{S_0}{E\Sigma_t(E)} P(E) \qquad 2.18$$

where

Σ_s = Macroscopic scattering cross section

Σ_t = Total macroscopic cross section

S_0 = Rate at which source neutrons are emitted at each energy E_0

$P(E)$ = The probability that a source neutron is not absorbed while slowing down from energy E_0 to E (resonance escape probability)

In an infinitely large absorber, the resonance escape probability [27] is given by

$$P_{total} = \prod_i p_i = \exp\left[-\frac{N_A}{\xi \Sigma_s} \sum_i I_i \right]. \qquad 2.19$$

where

P_{total} = Total resonance escape probability

p_i = Resonance escape probability for any single well resolved resonance located at an energy E_i

I_i = Effective resonance integral for the *i*th resonance

= $\int_{E_i} dE \sigma_\gamma^A(E)\phi(E)$ (where $\phi(E) \sim \frac{1}{E}$)

ξ = The average lethargy gain per collision

$\sigma_\gamma^A(E)$ = Capture cross section

N_A = Absorber concentration

The resonance escape probability increases with the moderator density. The resonance is more effective in absorbing neutrons if the resonance energy E_0 is lower (Table 2.1). Since the neutron collision density is proportional to $1/E$, at lower energies, the neutrons will experience more collisions with absorber nuclei and therefore higher probability of being absorbed. For this reason, the most significant resonance in thermal reactor occurs in low lying resonance of fertile material such as 6.6 eV resonances in U-238. Therefore, the microscopic cross section is temperature dependent through the "Doppler Broadening" mechanism. However, since the area under the resonance (Figure 2.5) is essentially temperature independent, the resonance peak drops with temperature and the broadened resonance increases the energy range over which absorption occurs. This effect outweighs the slight lowering of the resonance peak and gives rise to an enhanced absorption with increasing temperature. This effect arises due to "the self shielding" (Figure 2.6). That is the effect where the strong absorption of the resonance tends to shield the absorber nuclei from neutrons with energy ($E \sim E_0$) and results in a flux depression. As the temperature increases, the resonance peak decreases thereby decreasing self-shielding and hence flux depression and increasing resonance absorption (i.e. energy integration reaction rate $\Sigma_a(E)\phi(E)$).

The evaluation of self shielding factors as described assumes that the energy dependence of the scalar neutron flux within an energy group is very small and the flux is resolved in space and energy. This assumption is not valid in the vicinity of neutron absorption or

scattering resonances. Using the neutron absorption resonance in U-238 at 6.67 eV as an example, the cross section varies from 1 barn to an upper limit of about 10000 barns at the peak of resonance. Near the resonance peak all neutrons produced in the moderator are absorbed near the surface of the fuel sphere and hence neutron absorption at the surface of the fuel shields material inside the fuel (that is, the interior of the fuel element experience flux depression since the majority of the neutrons are absorbed at the sphere surface and cannot reach the interior). Figure 2.6 illustrates an extreme case of the spatial self shielding. And the flux depression corresponds to the peak absorption cross section (this is called energy self shielding) and this varies with temperature of the material due to the Doppler effects.

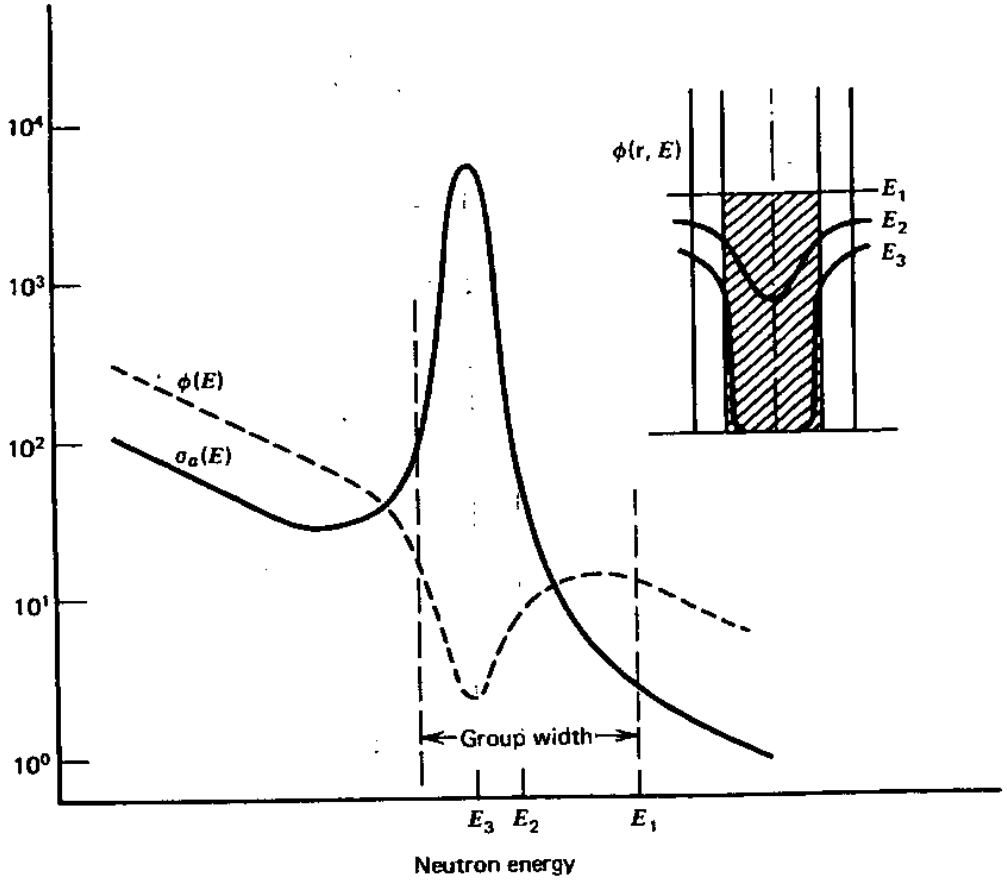

Figure 2.6: Space-Energy flux depression in the neighbourhood of resonance [33].

Analytical techniques have been developed to solve this heterogeneous resonance absorption problem. Most techniques assume that the shape of the cross section can be described by the Breit –Wigner single level formula and that the resonances are not overlapping. The neutron source is also assumed to be spatially uniform within the fuel as well as the surrounding homogeneous mixture of absorber and moderator. So the resonance escape probability P_{gn} is calculated for each resonance energy group and the total resonance absorption in all the materials is equated to the sum of the reaction rate in resonance material:

$$\sum_i R^i_{xgn} = \frac{q_{gn}(1-\prod_i P^i_{gn})}{\prod_i P^i_{gn}} \qquad 2.20$$

where

q_{gn} = is the neutron slowing down past the energy E_g in a volume element n per unit time per unit volume

P^i_{gn} = is the probability that a neutron will not be absorbed in the isotope i in the energy group g in a volume element n

A detailed description of the analytical technique is given in Duderstadt and Hamilton [27] and by Honeck HC [34]. On completion of the evaluation of these techniques in a heterogeneous system, the reaction rates are then calculated and hence the macroscopic group constants are evaluated.

2.3.2 Few group constants

The above mentioned group constants can later be used to calculate the multiplication factors and reaction rate distribution for a reactor system made up of a uniform array of fuel element cells (refer to flow diagram Figure 2.9). The regions of the reactor that are not made up of fuel will be treated by calculating group constants for these regions in the same manner as used for fuel regions within the limitation of the diffusion theory. Once these group constants have been calculated for each material type of volume element n, a set of simultaneous equations (2.15) is solved numerically for all regions making up the reactor. These calculations will result in the largest eigenvalues λ corresponding to the system multiplication factor and scalar flux at each space point r and each energy group g. The number of energy groups required for the generation of a multi-group constant is in the order of 100 to 200 and multiplication with the energy group points could result in very high computational costs especially if one is interested in the detailed spatial distribution. This is the main reason why smaller energy groups are used in fuel management analyses and reactor analyses codes. For these codes, smaller numbers of energy groups are used in which the neutron spectrum $F(E)$ is subjected to significant variations within each energy group. To derive the "few group constants", the neutron spectrum $F(E)$ is subjected to significant variations within each energy group. These group constants can be accomplished in two fold via the suppression of spatial variation of the scalar flux and the multi-group criticality equation is solved for uniform medium to obtain either an infinite medium neutron spectrum or finite buckling neutron (B^2) spectrum. The buckling (B^2) is a measure of neutron leakage. There are two types of buckling, namely the geometric and material buckling. The geometric buckling is a measure of neutron leakage while material buckling is a measure of neutron product less absorption. For a homogeneous steady state reactor (critical reactor) the geometric buckling is equals to the material buckling. The multi group equation (2.16) is replaced by

$$-\nabla D_g \nabla \phi_g = D_g B^2 \phi_g . \qquad 2.21$$

The solution of g homogeneous simultaneous equations results in the neutron spectrum within each type of material volume element. The selection of B^2 and the control condition within each material type is important and it is desirable to calculate the neutron spectrum for a set of conditions close to criticality. For fuel elements situated in a region where the leakage is small, an absorption cross section corresponding to control material is used to bring production and loss into balance. And for the fuel situated at the periphery, the use of B^2 is used to represent the net loss of fast neutrons and this is important as the neutron spectrum is sensitive to B^2 and the quantity of control material. For example, in the LWR, an increase in B^2 will result in a decrease in high energy spectrum relative to low energy since most neutron leakage occurs at higher energies. But an increase in control poison has reverse effects since most control absorption occurs at lower energies. The second step for accomplishing the few-group constant is by collapsing the energy groups. The group subdivision points for coarse groups must occur at a break point between multi-group points as shown in Figure 2.7. The few group criticality equation yields identical eigen-values to that for multi-group criticality equation. When the few group constants are used in a spatial calculation they result in a considerable reduction of computational costs as compared to multi-group. It should be noted that this collapsing of multi-group constants is not done without loss of accuracy. However, if two adjacent regions in spatial calculation have different spectra within the coarse group, the reaction rates calculated near the boundaries result in errors. If the spectrum differences are small or if the fraction of the total core volume is within a few mean free paths of such boundaries is small, then there is high probability that the error will be negligible. The validity of the few group approach depends on the fraction of the core volume that is in an "asymptotic" spectrum. The errors associated with collapsing of few groups are usually evaluated empirically by performing and comparing few group calculations with multi-group calculation on a one dimensional simulation. The selection of the number of groups to use in few groups calculation depends on the reactor type and the amount of neutron spectrum variations within the problem. An extreme case may be a single group which covers the entire spectrum. This is valid in large reactors containing a single type of fuel, but can yield significant errors if there is a spatial variation in concentration of fissile isotopes or fuel inventory.

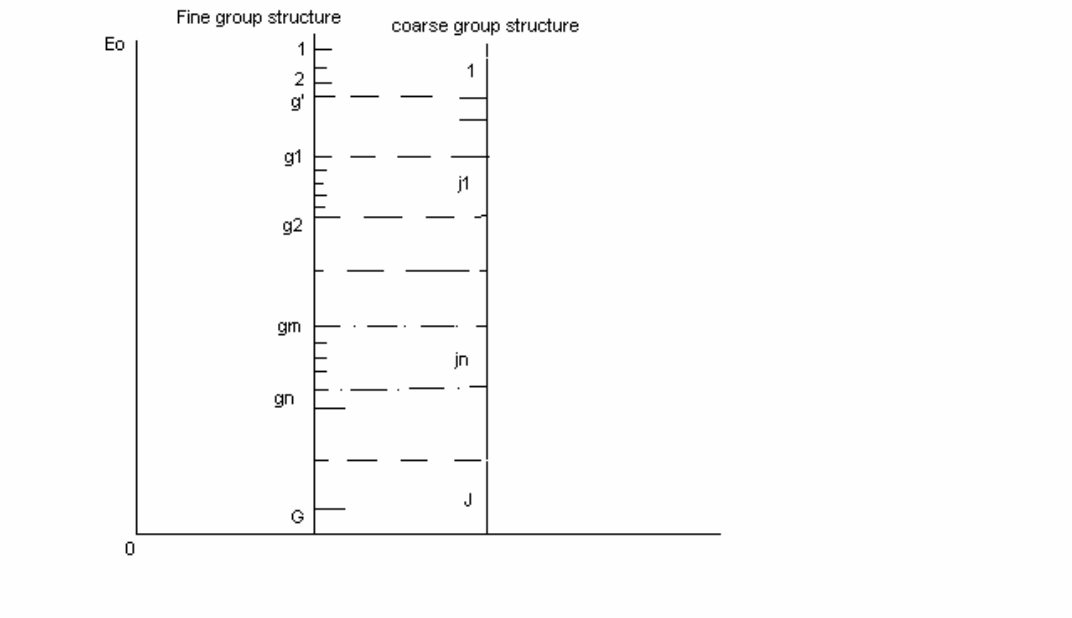

Figure 2.7: Collapsing of the multi-group to few-group constant [33].

The use of two groups is common in thermal reactors [27] where the energy break point E_b between groups is selected as the energy above which up-scattering collisions is neglected (since neutrons can never gain energy during collision that is, $E_f = (\frac{1-\alpha}{2})E_i$, where E_f refers to the average final energy of a neutron undergoing an elastic collision and E_i refers to the initial energy of the neutron and $\alpha = \left(\frac{A-1}{A+1}\right)^2$, where A is the mass of the nucleus). These groups are called the fast and thermal energy groups. Another common energy group structure consists of four energy groups. In these groups, subdivision of the fast group into three groups, the first of which extends to the U-238 fission threshold, the second extends to the upper energy of resolved resonance region. These four energy groups are called the fast, slowing down, resonance and thermal groups. Figure 2.8 illustrates the group structure for the two cases.

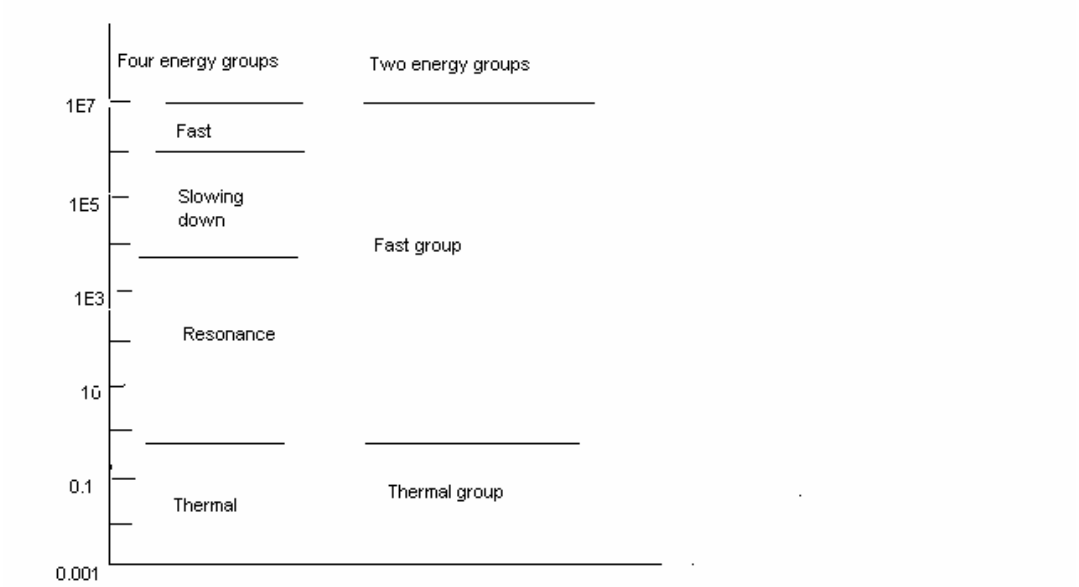

Figure 2.8: Typical structure for a few group reactor calculations [33].

The four group calculations are usually adequate to account for the severe core reflector spectrum difference. Fast reactors most frequently use a larger number of coarse groups since both the conversion ratio and the reactivity feedback effects are quite sensitive to spectrum changes. And computational costs are compensated for by the fact that considerably fewer spatial mesh points are required in a fast reactor due to longer mean free paths for fast neutrons. The next section illustrates as an example, the use of one and two group approximation to illustrate a variety of fuel management concepts. Most fuel management models are confined to one or two groups. The two group diffusion equations are defined as follows:

$$-\nabla\bullet(D_1\nabla\phi_1)+(\Sigma_{a1}+\Sigma_{R1})\phi_1=\frac{1}{\lambda}(\nu\Sigma_{f1}\phi_1+\nu\Sigma_{f2}\phi_2). \qquad 2.22$$

$$-\nabla\bullet(D_2\nabla\phi_2)+\Sigma_{a2}\phi_2=\Sigma_{R1}\phi_1 \qquad 2.23$$

$$\overbrace{E_2=0eV\text{--------}E_1=1.86eV}^{THERMAL-GROUP}\overbrace{\text{--------------}E_0=10MeV}^{FAST-GROUP}$$

Where

Σ_{R1} = The group transfer cross section from fast to thermal group.

Comparing equations (2.22) and (2.23) with the general multi group equation (2.16) has indicated the following simplifications:

(i) The fission fraction in group one is assumed to be unity and that for group two is zero

(ii) Scattering from group two to one is negligible

Both of these assumptions are accurate reflection of physical reality in thermal reactors. If a uniform medium equation is assumed and using equation (2.21) to convert the differential equation to algebraic criticality equation, the following relationship for reactor eigenvalue or multiplication constants is obtained.

$$\lambda = \frac{v\Sigma_{f1}}{\Sigma_{a1} + \Sigma_{R1} + D_1 B^2} + \frac{\Sigma_{R1} v\Sigma_{f2}}{(\Sigma_{a1} + \Sigma_{R1} + D_1 B^2)(\Sigma_{a2} + D_2 B^2)}. \quad 2.24$$

where λ refers to the effective multiplication constant (K_{eff}). In diffusion theory, the non leakage probability for energy group j for a bare homogeneous region is given by

$$P_{NL} = \frac{1}{1 + L_j^2 B^2}. \quad 2.25$$

where

$$L_j^2 = \frac{D_j}{\Sigma_{aj} + \Sigma_{Rj}}. \quad 2.26$$

Then the eigenvalue or the multiplication constant can be rewritten as follows:

$$\lambda = \frac{v\Sigma_{f1}}{\Sigma_{a1} + \Sigma_{R1}} P_{NL1} + \frac{\Sigma_{R1} v\Sigma_{f2}}{(\Sigma_{a1} + \Sigma_{R1})(\Sigma_{a2})} P_{NL1} P_{NL2}. \quad 2.27$$

and each of the cross section ratios in equation (2.27) has a physical meaning in terms of the neutron multiplication constant in the infinite medium of the material in question.

$$K_1 = \frac{v\Sigma_{f1}}{\Sigma_{a1} + \Sigma_{R1}}. \quad 2.28$$

where K_1 refers to the number of fast neutrons produced per neutron removed from group1

$$P_R = \frac{\Sigma_{R1}}{\Sigma_{a1} + \Sigma_{R1}}. \quad 2.29$$

where P_R is the resonance escape probability (that is the probability of neutron being scattered from group 1 to 2)

$$K_2 = \frac{v\Sigma_{f2}}{\Sigma_{a2}}. \quad 2.30$$

where K_2 refers to the number of fast neutrons produced per neutron absorbed in group 2. The total multiplication factor for an infinite uniform system is given by

$$K_\infty = K_1 + P_R K_2. \quad 2.31$$

The effective multiplication factor in a finite uniform system is given by

$$K_{eff} = K_1 P_{NL1} + P_R K_2 P_{NL1} P_{NL2}.$$

2.32

By using equations (2.21) and (2.23) it follows:

$$D_2 B^2 \phi_2 + \Sigma_{a2} \phi_2 - \Sigma_{R1} \phi_1 = 0. \qquad 2.33$$

By rewriting group 1 flux in terms of group 2 it follows:

$$\phi_1 = \frac{(D_2 B^2 + \Sigma_{a2})}{\Sigma_{R1}} \phi_2. \qquad 2.34$$

Similar expressions such as Σ_a and $\nu\Sigma_f$ can be derived as follows:

$$\Sigma_a = \frac{\Sigma_{a1}\phi_1 + \Sigma_{a2}\phi_2}{\phi_1 + \phi_2}. \qquad 2.35$$

By substituting equation (2.34) into (2.35) and eliminating ϕ_2, equation (2.35) reduces to

$$\Sigma_a = \frac{\Sigma_{a1}[\frac{D_2 B^2 + \Sigma_{a2}}{\Sigma_{R1}}]\phi_2 + \Sigma_{a2}\phi_2}{\frac{D_2 B^2 + \Sigma_{a2}}{\Sigma_{R1}}\phi_2 + \phi_2}.$$

$$= \frac{\phi_2\left(\Sigma_{a1}\frac{D_2 B^2 + \Sigma_{a2}}{\Sigma_{R1}} + \Sigma_{a2}\right)}{\phi_2\left(\frac{D_2 B^2 + \Sigma_{a2}}{\Sigma_{R1}} + 1\right)}.$$

$$= \frac{\Sigma_{a1}(D_2 B^2 + \Sigma_{a2}) + \Sigma_{a2}\Sigma_{R1}}{(D_2 B^2 + \Sigma_{a2}) + \Sigma_{R1}}.$$

$$= \frac{\Sigma_{a1} D_2 B^2 + \Sigma_{a2}(\Sigma_{a1} + \Sigma_{R1})}{D_2 B^2 + \Sigma_{a2} + \Sigma_{R1}}. \qquad 2.36$$

and

$$\nu\Sigma_f = \frac{\nu_1\Sigma_{f1}\phi_1 + \nu_2\Sigma_{f2}\phi_2}{\phi_1 + \phi_2}.$$

$$= \frac{\nu_1\Sigma_{f1}(\frac{D_2 B^2 + \Sigma_{a2}}{\Sigma_{R1}}\phi_2) + \nu_2\Sigma_{f2}\phi_2}{[\frac{D_2 B^2 + \Sigma_{a2}}{\Sigma_{R1}}]\phi_2 + \phi_2}.$$

$$= \frac{\phi_2\left(v_1\Sigma_{f1}\dfrac{D_2B^2+\Sigma_{a2}}{\Sigma_{R1}}+v_2\Sigma_{f2}\right)}{\phi_2\left(\dfrac{D_2B^2+\Sigma_{a2}}{\Sigma_{R1}}+1\right)}.$$

$$= \frac{v_1\Sigma_{f1}(D_2B^2+\Sigma_{a2})+v_2\Sigma_{f2}\Sigma_{R1}}{D_2B^2+\Sigma_{a2}+\Sigma_{R1}}. \qquad 2.37$$

Similarly, the group constants can be given as

$$D = \frac{D_1\phi_1+D_2\phi_2}{\phi_1+\phi_2}$$

$$= \frac{D_1\dfrac{D_2B^2+\Sigma_{a2}}{\Sigma_{R1}}\phi_2+D_2\phi_2}{\dfrac{D_2B^2+\Sigma_{a2}}{\Sigma_{R1}}\phi_2+\phi_2}.$$

$$= \frac{\phi_2\left(D_1\dfrac{D_2B^2+\Sigma_{a2}}{\Sigma_{R1}}+D_2\right)}{\phi_2\left(\dfrac{D_2B^2+\Sigma_{a2}}{\Sigma_{R1}}+1\right)}.$$

$$= \frac{D_1(D_2B^2+\Sigma_{a2})+D_2\Sigma_{R1}}{D_2B^2+\Sigma_{a2}+\Sigma_{R1}}.$$

D, Σ_a and $v\Sigma_f$ represent the collapsed the group constants from two energy group into one group. A similar but a more complex expression can be derived for more than two groups of neutrons [27]. The above mentioned sections have described the techniques for calculating group constants later to be used in the fuel management analyses. These techniques include the use of computer codes to evaluate the asymptotic neutron spectrum and spatial self shielding effects for specific reactor conditions.

2.4 Reactivity effects

For an operating reactor, there are several numbers of spatial power variations feedback phenomena that give rise to significant changes in the reactor composition and temperatures which result in significant changes in reaction rates and reaction rate ratios. As an example the changes in Xe-135 concentration with the local power density and the change in U-238 temperature with power density resulting in the broadening of U-238 neutron absorption resonances. These changes in coolant and fuel temperatures can give rise to significant changes in few group constants. Another example is small changes in the control poison can alter the group constants. These changes occur in the reactor on a day to day basis and these changes must be accounted for by the computer model. One way of accounting for the incremental changes in the group constants is by calculating

the asymptotic neutron spectrum and associated few group constant over a range of expected composition and temperatures. These changes can be fitted into a polynomial fit or set tables that are obtained from the spectrum calculation. Since changes in group constants due to Doppler effects take place in the resonance region only and can be confined to Σ_a and Σ_{R1}. Using the two group theory as explained above, one can further assume that the group one flux remains constant with changes in fuel temperature such that an increase in the resonance absorptions is compensated for by an equal but opposite reduction in removal to group two and that the change in the remaining group one constants is negligible ($\Delta\Sigma_{a1} = \Delta\Sigma_{R1}$, $\Delta v\Sigma_f = 0$ and $\Delta D_1 = 0$). The relationship between the group constants and the power density is difficult to develop as it requires a series of neutron spectrum calculations as well as evaluation of the fuel to coolant heat transfer [27]. And if a reliable measurement system is available for the power coefficients then the data can be used to develop a relationship between group constants and power density. If we assume that reliable measurements are available for a large reactor with a single fuel type, uniform flux and power density, then the relationship between the multiplication factor and the removal cross section Σ_{R1} in a uniform reactor can be described as

$$\frac{dK_{eff}}{dQ} = P_R K_2 P_{NL1} P_{NL2} \frac{1}{\Sigma_{R1}} \frac{d\Sigma_{R1}}{dQ}. \qquad 2.38$$

Q refers to the reactor power. If both sides of equation (2.38) are divided by K_{eff} then equation (2.38) becomes

$$\frac{1}{K_{eff}} \frac{dK_{eff}}{dQ} = \left(\frac{P_R K_2 P_{NL1} P_{NL2}}{K_1 P_{NL1} + P_R K_2 P_{NL1} P_{NL2}} \right) \frac{1}{\Sigma_{R1}} \frac{d\Sigma_{R1}}{dQ}. \qquad (2.39)$$

Assuming that equation (2.39) equals to the power coefficients and that $P_{NL2} = 1$ then, equation (2.39) reduces to

$$\begin{aligned} \frac{d\rho}{dQ} &= \left(\frac{P_R K_2 P_{NL1}}{K_1 P_{NL1} + P_R K_2 P_{NL1}} \right) \frac{1}{\Sigma_{R1}} \frac{d\Sigma_{R1}}{dQ}. \\ &= \left(\frac{P_R K_2}{K_1 + P_R K_2} \right) \frac{1}{\Sigma_{R1}} \frac{d\Sigma_{R1}}{dQ}. \\ &= \frac{P_R K_2}{K_\infty} \frac{1}{\Sigma_{R1}} \frac{d\Sigma_{R1}}{dQ} \end{aligned} \qquad 2.40$$

and the change in Σ_{R1} caused by a change in power density can be approximated as

$$\Delta\Sigma_{R1} = \Sigma_{R1} \frac{K_\infty}{P_R K_2} (Q_0 - Q) \left. \frac{d\rho}{dQ} \right|_{Q_0}. \qquad 2.41$$

where $\frac{d\rho}{dQ}$ is derived from the experimental data and other parameters are determined from the few group theory. By dividing the above mentioned equation by the weighting factor that has been derived from the measurements, equation (2.41) becomes,

$$\Delta\Sigma_{R1} = \Sigma_{R1} \frac{K_\infty}{P_R K_2} \frac{(Q_0 - Q)}{w} \frac{d\rho}{dQ}. \qquad 2.42$$

where w is derived from the measured power distribution data using the perturbation theory techniques.

The previous subsections of this chapter described the techniques and procedures for calculating the few group constants for use in the reactor model and fuel management calculations. The flow diagram (Figure 2.9) summarizes separate components for analytical techniques used for determining the few group constants and their use in a computer model. Item 1, in Figure 2.9, provides the reactor geometry and composition required for each calculation. This geometry does not depend on time and fuel management alternatives to the reactor design. Item 2 is the multi-group neutron cross section library which consists of spectrum independent multi-group microscopic cross section and resonance parameters obtained from the basic data such as ENDF/B and JEFF etc. These data do not vary with time and reactor composition for a given type of reactor. Item 3 in the flow diagram represents that input that differentiates between various different fuel types including the specific composition of fuel to be loaded in the reactor such as moderator density, fuel temperature etc, for which the few group constants are required. Item 4 represents the calculation of neutron spectrum in a homogeneous system of specific composition and geometry of the fuel type used in the reactor. These also include the neutron energy spectrum used to obtain few group macroscopic constants appropriate for the system investigated. While items 6, 7, 8 represent an iterative process that results in power distribution, fuel temperature, moderator-density and control distributions consistent with the multiplication factor or criticality calculation determined. This process requires at least several iterations and a number of smart techniques developed for reducing computational requirements. Once an acceptable and converged power distribution is achieved, the model will continue to calculate the burn-up (item 9). Item 9 represents the spatial non-uniform depletion of fuel material over a finite time step based on the power distribution determined during the iterative process. For some codes, these steps utilize pre-calculated analytical fits or look-up tables of few group constants and fuel compositions as a function of burn-up. These look-up tables or fits are based on the neutron energy spectra determined at various burn-up levels. The time steps for each interval calculations is selected to be small enough so that there is no major change in the power distribution and that the computational costs are not excessive.

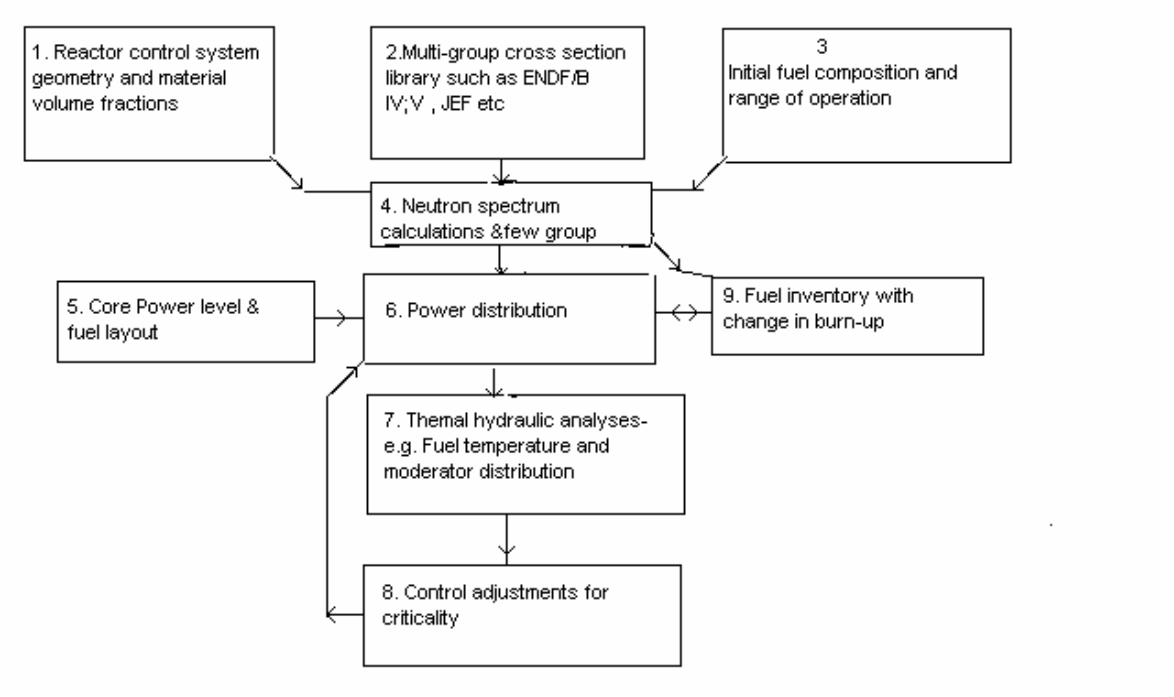

Figure 2.9: Flow diagram of a typical reactor model.

2.5 Determination of power distribution and criticality

The reactor core nuclear analyses cannot be performed independently without a strong interaction with the thermal hydraulics and structural analyses. Due to this, a number of constraints are placed on the core neutronics design, that is the core size and geometry is determined by thermal consideration since one needs to ensure that the power density is sufficiently low to prevent excessive temperature in the core. The core power calculations depend on parameters such as enrichment, core geometry, moderator to fuel ratio, control rods position and the fuel design. The power density will depend on the location of the fuel and time (burn-up and isotope production over core life time). Parameters such as "the ratio of peak to average power density" in the core, usually called hot channel or peaking factor are important to the thermal hydraulic engineer and allows for the determination of the thermal limitation on the core performance for a specific design. One will also notice a strong feedback from thermal core analyses due to core temperature as it is strongly linked to the resonance absorption which in turn affects the reactivity (Figure 2.5).

The relationship between the reactivity and core power was discussed in the previous section (equation 2.31). The reactivity control reaction time is important if the reactor is to be compensated for small reactivity transients caused by changes in temperature, loads and fission products poisons. The change in reactivity takes place between the fuel load temperature and zero power operating temperature, usually defined as "temperature defect ($\Delta\rho_{TD}$)" [27]. This result in coolant temperature specifically:

$$\Delta\rho_{TD} = \int_{T_1}^{T_2} \frac{d\rho}{dT} dT. \qquad 2.43$$

T_1 and T_2 refers to the loading temperature and zero power temperature respectively. Most of the water moderated reactors have a negative coolant temperature coefficient and temperature defect constitute a loss of reactivity with the exception of the heavy PWR using chemical shim which has a slightly positive coefficient at loading temperature. This power defect is a result of the change in reactivity that takes place between zero power and full power:

$$\Delta\rho_{PD} = \int_{0}^{P_0} \frac{d\rho}{dQ} dQ \qquad 2.44$$

and the power coefficient is due to temperature or density change that occurs in various reactor constituents with power level. For example for any reactor type, the power coefficient [27] is given by

$$\frac{d\rho}{dQ} = \frac{d\rho}{dT_f}\frac{dT_f}{dQ} + \frac{d\rho}{dT_s}\frac{dT_s}{dQ} + \frac{d\rho}{dT_m}\frac{dT_m}{dQ} + \frac{d\rho}{dT_c}\frac{dT_c}{dQ}. \qquad 2.45$$

Here *f, s, m* and *c* refer to the fuel, core structures, moderator and coolant respectively. For the reactor that uses uranium dioxide as fuel material, the first term ($\frac{d\rho}{dT_f}\frac{dT_f}{dQ}$) is a major contributor to the power coefficient. This is due to the fact that the low thermal conductivity of the ceramic material results in a larger value of $\frac{dT_f}{dQ}$ and the Doppler broadening of the resonances in U-238 causes high value of $\frac{d\rho}{dT_f}$. However, the PBMR is not directly coupled to coolant and hence only reactivity coefficient due to fuel (Doppler), moderators and reflectors are critical.

2.6 Evaluation of core capability and changes

As part of the in-core fuel management and in order to select an optimum fuel management, one needs to perform an evaluation of reactivity and control requirements, power distribution analyses and the core capability evaluation. The first two items were already discussed in the previous section and the focus of this section will be on the evaluation of core capabilities and changes; that is the depletion analyses as one expects the core composition to change with time. This core composition is complicated by the fact that the time and spatial variations in the isotopic composition depends on the flux distribution which itself depends on the core composition. These changes in core composition occur relatively slowly (can be a matter of day or months) so that the reactor can always be kept in a critical state by control element adjustment. These changes in composition can be classified in twofold, namely; the short term composition changes due to fission products build-ups (e.g. Xe-135 and Sm-149) that affect the operation of

the reactor (e.g. during load following) and the longer term fuel depletion as these is determined by the burn-up and fuel loading requirements.

2.7 Fission product poisoning and its effects on reactor operation

Fission products generated at the time of fission decay to produce a variety of fission products. Some of these fission products have very high neutron absorption cross section and have substantial impact on the reactor design and operation. These fission products poison such as Xe-135 and Sm-149 have impact on the thermal utilization factor, multiplication factor and reactivity.

2.7.1 Production and Removal of Xe-135

Xe-135 has a $2x10^6$ barn neutron absorption cross section. Xe-135 is produced directly by fission, but is more commonly a product of Tellurium-135 (Te-135) decay chain shown below:

$$^{135}_{52}Te \xrightarrow[19.0\ sec]{\beta^-} {}^{135}_{53}I \xrightarrow[6.7\ hrs]{\beta^-} {}^{135}_{54}Xe \xrightarrow[9.1\ hrs]{\beta^-} {}^{135}_{55}Cs \xrightarrow[2.3x10^6\ yrs]{\beta^-} {}^{135}_{56}Ba\ (Stable).$$

The fission yield for Xe-135 is about 0.3% while the Te-135 is about 6%. The half life for Te-135 is so short that it can be assumed that Iodine-135 (I-135) is produced directly from fission. I-135 is not a strong neutron absorber but decays to form neutron poison Xe-135. Ninety five percent of all the Xe-135 produced comes from the decay of I-135. Therefore the half life of I-135 plays an important role in the determination of the amount of Xe-135 concentration. The rate of change of Iodine concentration is equal to the rate of production minus the rate of removal. This is expressed in the equation below.

$$\begin{bmatrix}\text{The rate of change}\\ \text{of Iodine Concentration}\end{bmatrix} = \begin{bmatrix}\text{Yield from}\\ \text{Fission}\end{bmatrix} - [\text{Decay rate}] - \begin{bmatrix}\text{Iodine}\\ \text{absorption}\end{bmatrix}.$$

$$\frac{dN_I}{dt} = \gamma_I \Sigma_f^{Fuel} \phi - \lambda_I N_I - \sigma_a^I N_I \phi \qquad 2.46$$

where

N_I = I-135 concentration

γ_I = Fission yield of I-135

λ_I = decay constant for I-135

Σ_f^{Fuel} = Macroscopic fission cross section for fuel

ϕ = Thermal cross section

σ_a^I = Microscopic cross section for I-135

Since σ_a^I is very small, the absorption rate (or the third term) may be ignored and the

expression for the rate of change of Iodine concentration is modified as shown below:

$$\frac{dN_I}{dt} = \gamma_I \Sigma_f^{Fuel} \phi - \lambda_I N_I. \qquad 2.47$$

Equilibrium is achieved when the rate of production of Iodine equals the rate of Iodine removal. The Iodine concentration remains constant and is designated $N_I(eq.)$. The following equation for the equilibrium concentration can be determined from the preceding equation by setting the two terms equal to each other and solving for $N_I(eq.)$.

$$N_I(eq.) = \frac{\gamma_I \Sigma_f^{Fuel} \phi}{\lambda_I}. \qquad 2.48$$

Since the equilibrium Iodine concentration is proportional to the fission reaction rate, it is also proportional to the reactor power level. Hence the rate of change of Xenon concentration is equals the rate of production minus the rate of removal. Recall that 5% of Xe-135 comes directly from fission and 95% comes from the decay of Iodine. The rate of change of Xenon concentration is expressed by the following equations.

$$\begin{bmatrix} The\ rate\ of\ change \\ of\ Xenon\ Concentration \end{bmatrix} = \begin{bmatrix} Xe-135 \\ Yield\ from \\ Fission \end{bmatrix} + \begin{bmatrix} Iodine \\ Decay\ rate \end{bmatrix} - \begin{bmatrix} Xenon \\ Decay\ rate \end{bmatrix} - \begin{bmatrix} Xenon \\ absorption \end{bmatrix}$$

$$\frac{dN_{Xe}}{dt} = \gamma_{Xe} \Sigma_f^{Fuel} \phi + \lambda_I N_I - \lambda_{Xe} N_{Xe} - \sigma_a^{Xe} N_{Xe} \phi \qquad 2.49$$

where

N_I	=	I-135 concentration
N_{Xe}	=	Xe-135 concentration
γ_{Xe}	=	Fission yield of Xe-135
λ_{Xe}	=	decay constant for Xe-135
λ_I	=	decay constant for I-135
Σ_f^{Fuel}	=	Macroscopic fission cross section for fuel
ϕ	=	Thermal cross section
σ_a^{Xe}	=	Microscopic cross section for Xe-135

The Xenon absorption term refers to the neutron absorption Xe-135 by the following reaction:

$$^{135}_{54}Xe + {}^{1}_{0}n \longrightarrow {}^{136}_{54}Xe + \gamma$$

Xe-136 is not a significant neutron absorber therefore the neutron absorption by Xe-135 constitutes removal of poison from the reactor. The neutron absorption rate of Xe-135 is dependent on the neutron flux and Xe-135 concentration. The equilibrium concentration of Xe-135 is designated by $N_{Xe}(eq.)$ and is represented as shown below.

$$N_{Xe}(eq.) = \frac{\gamma_{Xe}\Sigma_f^{Fuel}\phi + \lambda_I N_I}{\lambda_{Xe} + \sigma_a^{Xe}\phi} \quad 2.50$$

For Xe-135 to be equilibrium, I-135 must also be in equilibrium. Substituting the expression for the equilibrium Iodine-135 concentration into the equation for the Xenon results in the following equation:

$$N_{Xe}(eq.) = \frac{\gamma_{Xe}\Sigma_f^{Fuel}\phi + \gamma_I\Sigma_f^{Fuel}\phi}{\lambda_{Xe} + \sigma_a^{Xe}\phi} \quad 2.51$$

$$= \frac{(\gamma_{Xe} + \gamma_I)\ \Sigma_f^{Fuel}\phi}{\lambda_{Xe} + \sigma_a^{Xe}\phi}$$

From this equation, it can be seen that the equilibrium Xe-135 concentration increases as the power increases because the numerator is proportional to the fission rate. This increase in Xe-135 with power level is non linear because the Xe-135 concentration directly affects the reactivity level in the core, the negative reactivity due Xe-135 concentration for different power levels or conditions are reported instead of Xe-135 concentration. For example, the excess reactivity during load following for the PBMR to cater for negative reactivity insertion due to Xenon concentration is about 1300 pcm.

2.7.2 Xe-135 Response to Reactor Shutdown

When the reactor is shutdown, the neutron flux is reduced to essentially zero. Therefore after shutdown, Xe-135 is no longer produced by fission and is no longer removed by absorption. The only remaining production mechanism is the decay of I-135 which was in the core at the time of shutdown. The only removal mechanism for Xe-135 is decay.

$$\frac{dN_{Xe}}{dt} = \lambda_I N_I - \lambda_{Xe} N_{Xe}. \quad 2.52$$

Because the decay rate of I-135 is faster than the decay rate of Xe-135, the Xenon concentration builds to a peak. The peak is reached when the product of the term $\lambda_I N_I$ is equal to $\lambda_{Xe} N_{Xe}$. The time at which the maximum negative reactivity occurs is calculated to be

$$t_{\max} = \frac{1}{\lambda_I - \lambda_{Xe}} \ln\left(\frac{\lambda_I}{\lambda_{Xe}}\right) \approx 11.1\ hrs. \quad 2.53$$

Subsequently, the production Xenon via the Iodine decay is less than the removal of Xenon decay and the concentration of Xe-135 decreases. The greater the flux level prior shutdown, the greater the concentration of I-135 at shutdown, therefore the greater the peak in Xe-135 concentration after shutdown.

2.7.3 Production and Removal of Samarium-149

Samarium-149 (Sm-149) is the second most important fission product poison because of its high thermal neutron absorption cross section of $4.1\,x10^4$ barns. Sm-149 is produced from the decay of Neodynium-149 fission fragment as shown in the decay chain below.

$$^{149}_{60}Nd \xrightarrow[1.72\ hrs]{\beta^-} {}^{149}_{61}Pm \xrightarrow[53.1\ hrs]{\beta^-} {}^{149}_{62}Sm\ (Stable)$$

The half life of Nd-149 is shorter than that of Pm-149 such that it can be assumed that Pm-149 is formed directly from fission. This assumption ignores the absorption of neutrons by Pm-149. The concentration of Pm-149 is determined as follows:

$$\begin{bmatrix} The\ rate\ of\ change \\ of\ Pm-149 \\ Concentration \end{bmatrix} = \begin{bmatrix} Pm-149 \\ Yield\ from \\ Fission \end{bmatrix} - \begin{bmatrix} Pm-149 \\ Decay\ rate \end{bmatrix}$$

$$\frac{dN_{Pm}}{dt} = \gamma_{Pm}\Sigma_f^{Fuel}\phi - \lambda_{Pm}N_{Pm}. \qquad 2.54$$

where

N_{Pm} = Pm-149 concentration
γ_{Pm} = Fission yield of Pm-149
λ_{Pm} = decay constant for Pm-149
Σ_f^{Fuel} = Macroscopic fission cross section for fuel
ϕ = Thermal cross section

At equilibrium, Pm-149 concentration is given by:

$$N_{Pm}(eq.) = \frac{\gamma_{Pm}\,\Sigma_f^{Fuel}\phi}{\lambda_{Pm}}. \qquad 2.55$$

The rate of change of Sm-149 formation is described as follows:

$$\begin{bmatrix} The\ rate\ of\ change \\ of\ Sm-149 \\ Concentration \end{bmatrix} = \begin{bmatrix} Sm-149 \\ Yield\ from \\ Fission \end{bmatrix} + \begin{bmatrix} Pm-149 \\ Decay\ rate \end{bmatrix} - \begin{bmatrix} Sm-149 \\ Absorption \end{bmatrix}.$$

$$\frac{dN_{Sm}}{dt} = \gamma_{Sm}\Sigma_f^{Fuel}\phi + \lambda_{Pm}N_{Pm} - N_{Sm}\sigma_a^{Sm}\phi \qquad 2.56$$

where

N_{Pm} = Pm-149 concentration
N_{Sm} = Sm-149 concentration
λ_{Pm} = decay constant for Pm-149
Σ_f^{Fuel} = Macroscopic fission cross section for fuel
ϕ = Thermal cross section
σ_a^{Sm} = Microscopic cross section for Sm-149

However, the fission yield for Sm-149 is nearly zero hence the rate of change of Sm-149 is given by:

$$\frac{dN_{Sm}}{dt} = \lambda_{Pm}N_{Pm} - N_{Sm}\sigma_a^{Sm}\phi. \qquad 2.57$$

At equilibrium, Sm-149 concentration is given by:

$$N_{Sm}(eq.) = \frac{\lambda_{Pm}N_{Pm}}{\sigma_a^{Sm}\phi} = \frac{\gamma_{Pm}\Sigma_f^{Fuel}\phi}{\sigma_a^{Sm}\phi} = \frac{\gamma_{Pm}\Sigma_f^{Fuel}}{\sigma_a^{Sm}}. \qquad 2.58$$

This expression for equilibrium Sm-149 concentration illustrates that the equilibrium Sm-149 concentration is independent of the neutron flux and power level. The Sm-149 concentration will undergo a transient following power level change but will return to its original value.

2.7.4 Samarium-149 Response to Reactor Shutdown

Since the neutron flux drops to zero after shutdown, the rate of change of Sm-149 product becomes the following:

$$\frac{dN_{Sm}}{dt} = \lambda_{Pm}N_{Pm}. \qquad 2.59$$

Because Sm-149 is not removed by decay, it presents problems that are somewhat different from Xe-135. Sm-149 is stable and can only be removed by neutron capture. After shutdown, the Sm-149 concentration builds up to a steady state level. Sm-149 poisoning is minor when compared to Xe-135 poisoning. Although Sm-149 has a constant poisoning effect during long term sustained operation, its behaviour during initial start-up, during post shutdown and restart periods requires special consideration in the reactor design. The negative reactivity worth of Sm-149 due to equilibrium Samarium poisoning is estimated to be:

$$\Delta\rho_{Sm} = -\gamma_{Pm}\frac{\Sigma_f^{fuel}}{\Sigma_a} = -\frac{\gamma_{Pm}}{\nu} \cong 0.00463. \qquad 2.60$$

where we have used the approximation that $K_{eff} \approx \nu\frac{\Sigma_f^{fuel}}{\Sigma_a} = 1$. The isotopic inventory of Sm-149 and Xe-135 concentration in the PBMR fuel sphere is estimated to be 8.94E-11 and 1.27E-11 atoms/cm^3.

2.8 Reactor Core Thermal Hydraulics

For any heterogeneous core configuration, there is a local variation of the neutron flux or power distribution in the core that must be taken into consideration. The previous section has already examined the variation of the flux in the vicinity of the fuel by using collision probability methods to compute the cell average group constant. Similar techniques are employed near absorber material. However there are other local spatial flux variations occurring due to the variation in core composition and playing an important role in the reactor design. The most important one is the local power peaking that occurs at the boundaries between the fuel and the reflectors. For the PBMR, this occurs in the first flow channel closer to the inner central reflector situated further away from the control rods. Since the thermal neutrons are reflected near the reflectors, one expects to see a larger thermal flux next to the reflectors and hence power density and peaking factor in the flow channel closer to these reflectors. The local flux near the channel will be considerably higher than the average flux in the region. One must take into consideration, the constraints on the core power density and power peaking so that the operational limits are not exceeded. Although the power density and peaking factors is lower for the HTGR as compared to the PWR, such effects must be accounted for in the HTGR core design. Most of the detailed calculations on the core power distributions are performed with 2-D and 3-D models. Accurate description of the power and flux distributions using the finite difference multi-group diffusion equation requires that the mesh spacing be at least comparable (or less than) the minimum neutron diffusion length in the core (0.5 cm in PWR and 4-5 cm in HTGR) even after core homogenization.

2.9 Reactivity control

Reactivity control is an integral part of nuclear fuel management and changes in reactivity due to power manoeuvring, fuel depletion, fission production build-up

(especially poison) must be compensated for (as described in Figure 2.9). The techniques used to control reactivity (changes in multiplication factor) must be reviewed and modified to best achieve operating objectives. This section will evaluate various phenomena that cause changes in the reactor multiplication and discuss the type of reactivity control to compensate for excess multiplication. These include the primary control method used in power reactor such as movable control absorbers. The total control requirements of nuclear reactor consists of individual components each being characterized by a reactivity worth value, the time scale associated with the reactivity changes. These control system must have the capability to render the reactor sub-critical during all operating conditions [35].

The reactivity control system (that is the control rods) will be used to compensate for xenon poisoning or fuel depletion and power defects. The control rods as mentioned above can also result in large local power density perturbation in the fuel adjacent to the control location following the control rod movement. And the changes in the gross reactor power shape also take place following the control rods withdrawal or insertion and these changes may results in an increased peak to average power density (Peaking factor) and a reduction in operating margin. On the other hand, the insertion of the solid absorber such as small absorber spheres in PBMR reactor core will insert negative reactivity in the core. Many reactivity control systems are distributed in a pattern so that the efficient reactivity control can be achieved within the flux peaking limitations as well as power shaping and hence satisfying the reactivity control requirements as per operating technical specification and the regulatory requirements. For this dissertation, the focus will only be on the movable control rods used to control the core reactivity. The movable control rods can be used for a variety of purposes that is to control reactivity during power manoeuvring or reactor shut down. The control rods have the greatest effects on the power distribution and the interaction between the control rods arrangement and the power distribution will be carefully evaluated as part of the safety analyses supporting information to be given to the regulator for license application. The PBMR core has partially inserted control rods at the top of the reactor core to compensate for power manoeuvring and reactivity feedback due to Xe-135 poisoning and to dampen the spatial power oscillation induced by Xe-135 [36].

2.10 Computational methods for solving the diffusion equation

The fine mesh diffusion theory calculations are capable of representing the geometric details of the reactor fuel element and the two dimensional problems are frequently simulated such that each fuel element in the core is represented by a spatial mesh point. For any realistic reactor calculation, one takes into consideration the non-uniformities corresponding to fuel, cladding, moderator, coolant, control elements, spatial variations in the fuel, coolant densities due to non-uniform power densities and temperature distribution. These complexities immediately force one to discard analytical methods in favour of direct numerical solution of the diffusion equation. Although a direct numerical solution can be performed on modern computers, it is extremely expensive to do particularly when a series of calculations would be required for a parameter study. In actual practice, one usually use few groups in reactor calculations. However, recalling the

very complicated dependence of the cross sections on energy (in particular, their resonance structure), it is apparent that the groups would have to be finely divided in order to yield meaningful results. This very finely structured multi-group calculation is performed to calculate the intra-group fluxes (usually relying on various models of neutron slowing down and thermalization). The group constants for this fine spectrum calculation are frequently taken to be just the tabulated cross section data averaged (with, for example, a 1/E weighting) over each of the fine groups. The intra-group fluxes are then used to calculate coarse group calculation (including spatial dependence). This scheme for first calculating a neutron flux spectrum and then collapsing the cross section data over this spectrum to generate few group constants is the most common method used today [27]. It should be noted that the spectrum calculations and the few group calculations depends on the reactor type and its operating conditions. That is, the fuel loading, isotopic composition, temperature and coolant conditions. In fact such group constants will have to be calculated in each region which the core composition varies appreciably because of the variation in enrichment or moderator density. For regions of the nuclear reactor that are not made up of fuel elements can be treated by calculating multi-group constants for these regions in the same manner used to obtain such constants in the fuel region within the limitations of the diffusion theory (that is taking into account reactivity adjustments such as the movements of the control rods).. For these cases, the physical structure of the fuel is no longer limited by the mesh spacing for the diffusion problem and the increase in the mesh spacing is restricted by the diffusion length or the pitch between the fuel elements. The intention of this section is to briefly describe the basis for the numerical techniques. There are several techniques that can be used to solve the diffusion equation; however the emphasis will only be on the finite difference method applied by the V.S.O.P code. The multi-group diffusion equation is first translated to the finite difference equation by making use of the Taylor expansion. These will result in a set of finite difference equations and this set of equations will be solved by making use of an iterative method. A detailed derivation of the finite difference equation from the multi-group diffusion equation and the numerical methods are described by Duderstadt and Hamilton [27].

Chapter 3

Code Description

A set of system parameters which will yield a safe, reliable and economical reactor operation at a rated power level over the desired core life time must be determined. To determine these parameters, a set of numerical models or codes may be required or used to simulate the reactor core behaviour. As we have already observed in chapter two nuclear analyses also interact with other aspects of the core design including structural analyses, thermal hydraulics analyses and economic performance. Consideration of these aspects will place a number of constraints on the nuclear reactor core design such as the core size, the geometry and the thermal aspects (that is, in order to achieve low power density and to prevent high fuel temperature in the core). The second aspect is the ability of the fuel elements to withstand the radiation damage, as well as thermal and mechanical stresses experienced in the reactor core. Given the reactor core configuration, nuclear analyses can be performed to determine the reactor core behaviour and to identify constraints on the core design. These analyses identify the range over which system parameters can be varied while still complying with the constraints placed on the reactor performance. To execute this, a detailed reactor core design can be used to determine the best suited system parameter that can yield optimum core performance consistent with the reactor core design constraints. It should be noted that the specific detailed design data is usually proprietary information by the reactor designer such as the PBMR PTY LTD, AREVA and Westinghouse. For the purpose of this study, PBMR PTY LTD has authorised a set of benchmark data [37]. The purpose of this chapter is to illustrate how the nuclear models are used to simulate the reactor core behaviour. This chapter will also provide background on the software or tools used for the in-core fuel management studies and also provides a brief description of the coding process followed by an in depth description of what each code is typically used for in relation to the critical parameters described in section 1.5. V.S.O.P.

3.1 Background on computer codes (V.S.O.P)

Very Superior Old Program (V.S.O.P.) is a system of proven computer codes linked together for the numerical simulation of nuclear reactor physics performance. The V.S.O.P. code is based on diffusion theory. The code is applicable to all thermal reactors including the Pebble Bed Modular Reactors. It was widely used for developmental work of High Temperature Reactor (HTR) with spherical fuel elements. This code was successfully applied to heavy and light water reactors, MAGNOX and RBMK. The code was developed by the research centre in Jülich (FZJ) former Kernforschunganlage Jülich (KFA).The first edition of V.S.O.P. code was published in 1980 [38]. This code was developed to help in understanding the high temperature pebble type technology and its physical behaviour. The V.S.O.P. code was also used to support the licensing of the German High Temperature Reactor (HTR) project and has been validated in the licensing process for the SIEMENS MODUL-200 pebble bed reactor by code to code comparison against the SIEMENS ZIRCUS code [39]. The code was also used by TŰV Hanover to check the validity of the ZIRCUS code and the validation has shown that V.S.O.P. is able

to describe the core physics of the pebble bed high temperature reactor in cold condition with sufficient precision [39]. The PBMR Pty Ltd used V.S.O.P. to perform a comparison with the criticality and control rods results obtained at the ASTRA facility [30]. Code to code benchmark studies were conducted using the V.S.O.P and other codes on the Chinese HTR-10 and the Japanese HTTR. INET (in Beijing), NRG, CEA and FZJ participated in these benchmarks [40].

The code was recently used to model the AVR reactor core and benchmarked against the "Melt wire Experiment" [41]. Currently this code is used in the design and licensing of the current commercial project such as the Pebble Bed Modular Reactor (PBMR) and the Gen IV reactors.

3.2 V.S.O.P capabilities

The application of the V.S.O.P. code implies processing of cross sections, the set-up of the reactor and of the fuel element, neutron spectrum evaluation, neutron diffusion calculation in two or three dimensions, fuel burn-up, fuel shuffling, fuel cycle costs, reactor control, and thermal hydraulics of steady states and transients. The neutronic calculations can be performed in up to three dimensions. The thermal-hydraulics part (steady state and time dependent) is restricted to HTRs and to two spatial dimensions.

The code enables the user to simulate reactor life from initial core loading, start-up, run-in phase and toward equilibrium core conditions. This includes in core monitoring of fuel characteristics and behavior until these spheres are discharged to the spent fuel storage. These characteristics include estimation of the fuel temperature, peaking factors, burn-up, cycle length (residence time), fluence, fuel inventory (isotopic composition), flux, reactor shut down margin etc. Repeated calculations of the different physics features ensure consistency in their feedback during the proceeding burn-up, the simulation of the fuel shuffling, and variations of the core power. Characteristics of the life history of the fuel elements (including the power level) are used to calculate the decay power. Reprocessing and closure of the fuel cycle can be simulated under consistent control of the mass flow of the fuel including the isotopic decay during periods of intermediate storage.

The status of the reactor at the end of each calculation can be saved and used as input to new investigations (these include third party codes like TINTE, Origen etc). The burn-up section of the code also allows the assessment of the impact of the most important "minor actinides" on the physics of the reactors and on the characteristics of spent fuel. In the burn-up calculation, a fission product chain of 45 fission products is explicitly modelled. After a specified number of burn-up steps of required length, single partial volumes all move one-step downwards along the flow line. Figure 3.1 below, illustrates the reactor core layout and flow lines as modelled by making use of V.S.O.P code [42]. While the bottom most partial volumes are being discharged, each of the different fuel sphere loads are being grouped together, mixed and reloaded according to the next higher fuel sphere load. The oldest loads are discharged to the spent fuel volume and fresh fuel spheres are loaded.

V.S.O.P allows for this stepwise calculation process to continue until equilibrium is reached, i.e. the results for each burn-up period are reproduced identically. The cycle achieved during the stepwise calculation process is termed the "equilibrium cycle". This cycle characterizes the biggest part of the reactor life. V.S.O.P also allows load follow calculations from reactor start-up through run-in phase towards an equilibrium cycle. The reactor simulation compromises a series of iteration between calculating the flux and burn-up followed by shuffling steps of fuel element in the core. In this way, the effect of the pebble flow is simulated. Through the use of pebble flow lines, the effect of axially variable flow velocities and varying flow paths is included in calculations. V.S.O.P assumes that the neutron spectra inside the different batches are very similar and the same sets of few group microscopic cross sections are used for the batches (6 batches in case of 6 passes) due to relatively long mean free paths of the neutrons within the pebble bed. This is achieved by first averaging the atomic densities of radio-nuclides for different batches and then using the same microscopic cross sections for 6 batches (in case of 6 passes) to determine the flux. These assumptions imply that the variation of flux within the batches is negligible. Figure 3.2 represent the thermal flux profile for the PBMR.

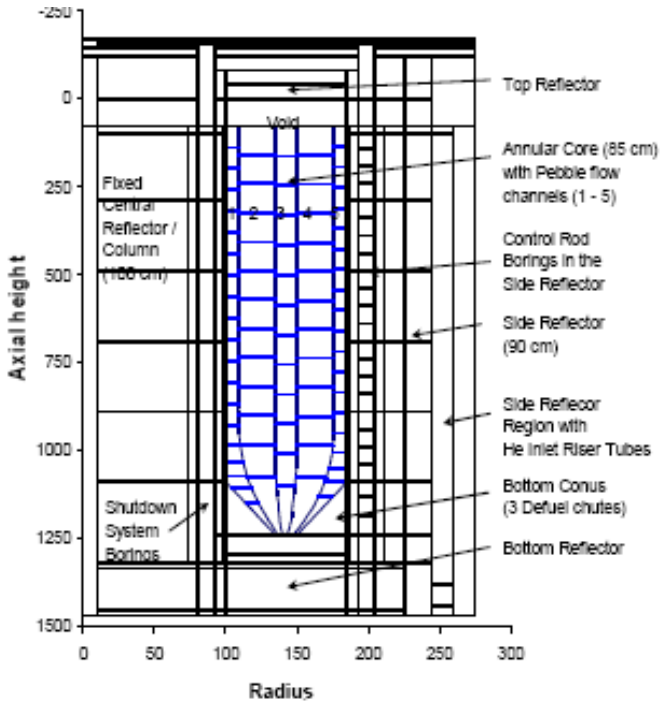

Figure 3.1: Reactor core layout as modelled by V.S.O.P including the flow lines [42].

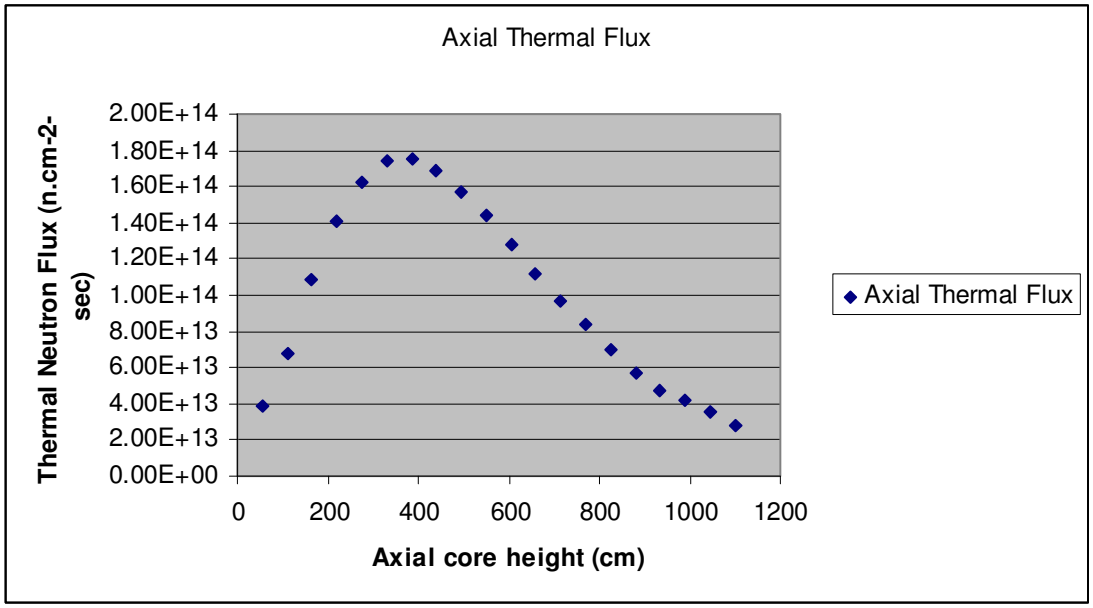

Figure 3.2: Axial flux shape for the PBMR core.

3.3 V.S.O.P code layout

Figure 3.3 shows a flow diagram of the computational process. This flow diagram describes how nuclear data is processed and the inter-connection between these sub-programs within V.S.O.P. All the arrows going into the codes are inputs needed by the codes. This code consists of cross section libraries and processing routines and neutron spectrum evaluation based upon the GAM [44] and THERMOS[34] code, two dimensional (2-D) and three dimensional (3-D) diffusion, depletion routines, in-core and out of pile fuel management; fuel cycles cost analyses and the thermal hydraulics of the pebble reactors.

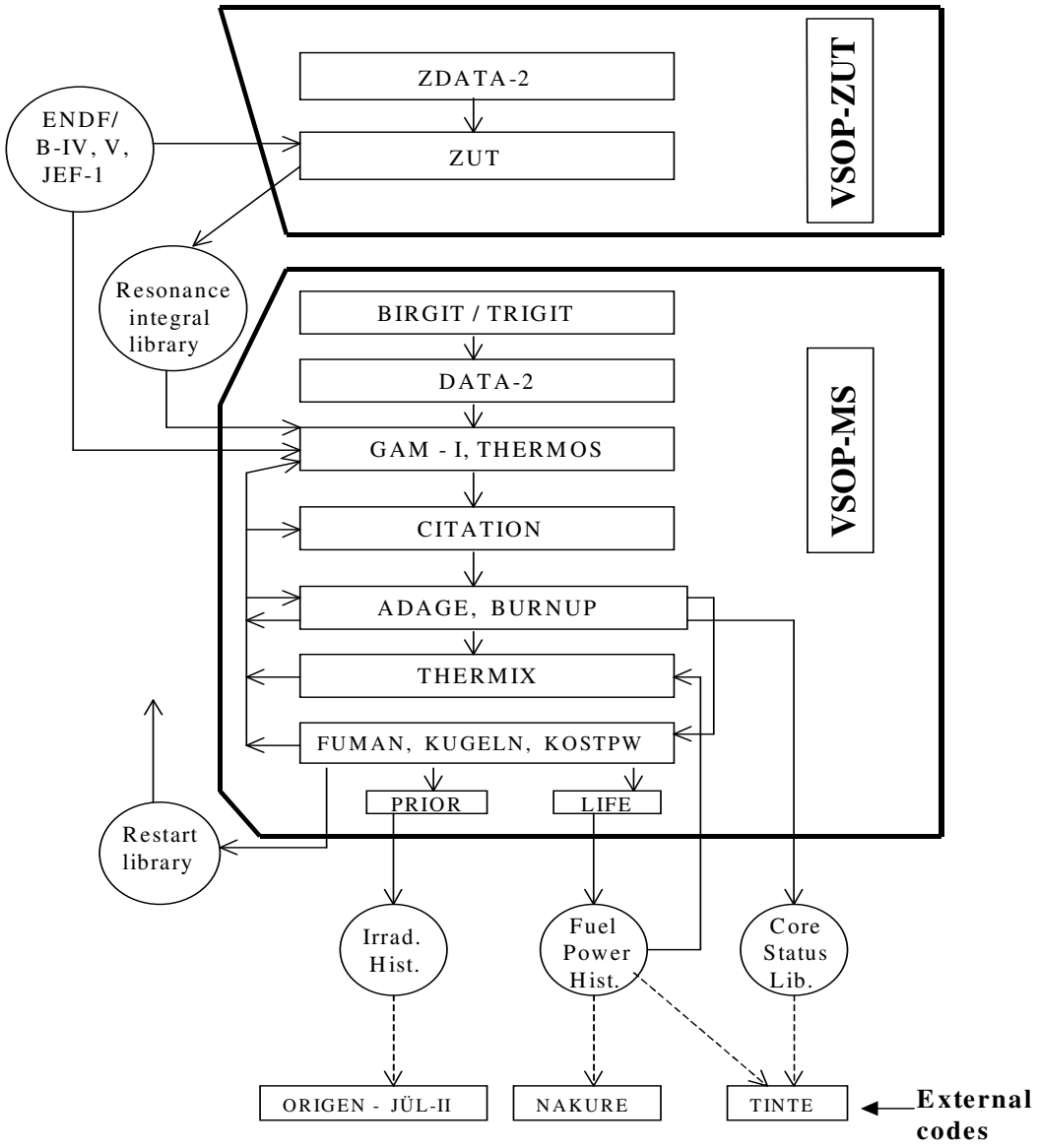

Figure 3.3: V.S.O.P basic programs.

3.3.1 Nuclear Data

The neutron energy ranges are split into four energy groups namely, the thermal, two epithermal groups and the fast energy group. Table 3.1 below highlights the energy ranges. Group 4 and 1 correspond to the thermal and fast energy group respectively and group 2 and 3 correspond to the two epithermal energy groups.

Group	Energy limits (eV)
4	0 - 1.86
3	1.86 - 29
2	29 - 0.1×10^6
1	$0.1 \times 10^6 – 10^7$

Table 3.1: Energy grouping within V.S.O.P

The code contains large cross section libraries (ENDF/B-V and JEF-1). Fast and epithermal data in a 68-group GAM structure are prepared for V.S.O.P from ENDF/B-V and JEF-1 libraries [43]. At present, the libraries consist of 190 nuclides needed in a calculation for each 68 energy subgroups. These energy groups range from 0.414 eV to 10 MeV in an equal lethargy spacing (integrated over a quarter of lethargy)

3.3.2 ZUT-DGL

As indicated in the flow diagram Figure 3.3, the sub code "ZUT-DGL" generates cross sections for resolved and unresolved resonances for U-238, PU-242 and Th-232. Prior to the running of the V.S.O.P code, the resonance absorption cross sections are prepared for fuel spheres for different absorber concentrations at different temperatures. The dependence of the resonance cross-sections on temperature and fuel burn-up is achieved by linear interpolation between the respective cross section sets [44].

For HTGR type of fuel (TRISO particles) as per figure 1.1 in chapter 1, the term "fuel lump" being referred to in the text and referenced document [44] is the kernel of the coated particles. Because of the particle size, the escape probability is close to 1 (for a small fuel lump), even for neutrons with energy close to the peak of strong resonance. The neutron can travel through many coated particles without any collision, whether through the coating or the kernels. That is, a neutron can travel from its place of birth (from kernel) whether through the coatings of the particles or passing through the outer shell of the fuel sphere (the fuel free zone) and enters into the outer shell of the next fuel sphere and passes through the matrix graphite and undergoes collision in any coated particles or even escape completely. Figure 3.4 below shows the escape probabilities from the coated particle.

ZUT-DGL also calculates neutron fraction leakage from the adjacent spectrum zone calculations and the buckling term from diffusion calculations over the whole reactor. The resonance integrals for isotopes Th-232, U-238 and Pu-242 are also calculated by

making use of the resonance data from ENDF/B-IV and –V. ZUT-DGL provides input to the GAM code (resonance integral). The resonance integral calculation is used for homogeneous distribution of resonance absorber in the finite volume of a lump. The transport equation is solved in very fine groups over the energy range of each resonance. The calculations also include the neutrons which are born in the kernel (lump), leave it, and are absorbed or scattered down in any other kernel of the same configuration. Excluded are those neutrons which leave the kernel and undergo scattering reactions outside the sphere. Nordheim [45] excludes these neutrons by geometric escape probability $P(E)$:

$$P(E) = \frac{P_0(E) \bullet (1-C)}{1-C \bullet (1-\Sigma_t^F(E)P(E))} \qquad 3.1$$

where

$P_0(E)$ = the probability that a neutron will escape from the kernel (lump) of origin
C = Dancoff factor
$\Sigma_t^F(E)$ = Total macroscopic cross section in the fuel.

For heterogeneous composition of the kernels (lumps), the escape probability is directly evaluated by numerical methods [44] described in detail by Rütten et.al, 1997[44] as well as Duderstadt JJ and Hamilton LJ [27].

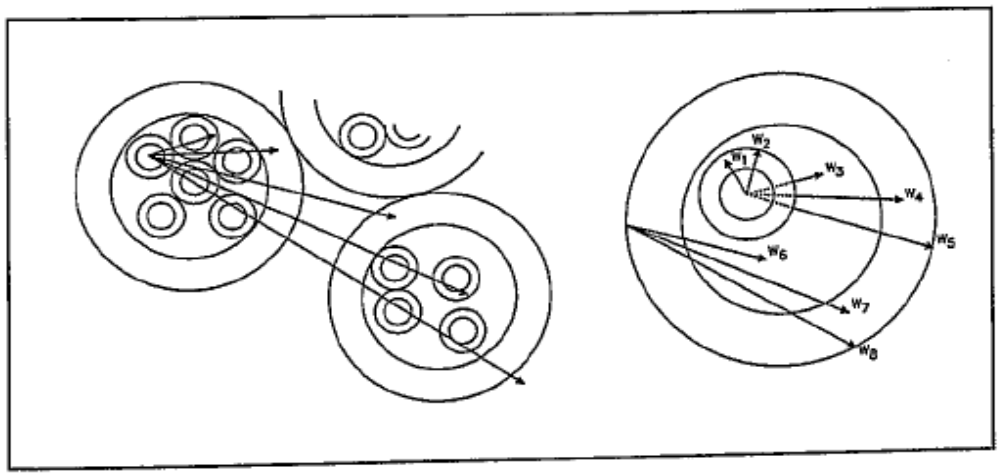

Figure 3.4: Break down of the neutron escape probability [44].

These parameters, namely neutron leakage, buckling term and resonance integral calculated by ZUT-DGL code play a critical role in the overall calculation of the reactor core criticality and the fuel economics calculations.

3.3.3 BIRGIT/TRIGIT

The two dimensional (2-D) and three dimensional geometric design of the reactor is calculated by making use of the BIRGIT and TRIGIT codes respectively. The V.S.O.P

code requires the material (fuel and reflector material composition) data to be loaded into the geometry. These geometric data and fuel material composition (as calculated by DATA-2) are provided as an input to V.S.O.P code. The code prepares the 2-D geometric design in *r-z* cylindrical coordinates. In V.S.O.P, the basic unit of the reactor material composition is called a **"batch**". For the first core loading, the reactor is subdivided into batches. The in-core batches are loaded with fuel material (calculated by DATA-2) and the ex-core batches with material of the reflectors. The calculation flow is individually calculated for every batch (the follow of burn-up, of fuel shuffling, of fuel-cost evaluation and of decay heat during accident simulations). The reactor core normally consists of a mixture of different types of fuel elements of different irradiation ages. That is, a batch will consist of homogeneous fuel elements with a specific irradiation age. And a mixture of this respective batches put together is called a layer. This layer really represents partial volumes of the reactor and may consist of batches with different irradiation ages (passes) or material compositions depending upon the fuel management scheme used by V.S.O.P code. These batches are grouped together forming "**spectrum zones**". The spectrum calculations are based on the averaged atomic densities of these zones and provide the broad group cross section for the respective batches. In a pebble bed reactor, the fuel elements move downwards in a given flow pattern or line which is obtained from the experimental research of the test facilities. The flow lines of spherical fuel elements through the reactor are input into BIRGIT/TRIGIT code. The shape of the layers and their shuffling fits into the flow lines. These flow lines describe the pebble movements in both radial and axial direction. The volume between the flow lines or flow channels is divided into layers. The number of layers in the flow channels determines the relative speed of the pebble flow. For example, a layer situated at the periphery (next to the reflectors) moves slower than the layer situated in the middle flow channel due to wall friction and also achieve high burn-up due to higher neutron flux (Figure 3.4). At the bottom, pebbles are discarded as spent fuel or mixed with new fuel and reload from five different burn-up (for 6 passes) conditions after each pass. Hence the fuel to be reloaded at the top layer is just an average from all discharge fuel from the previous pass.

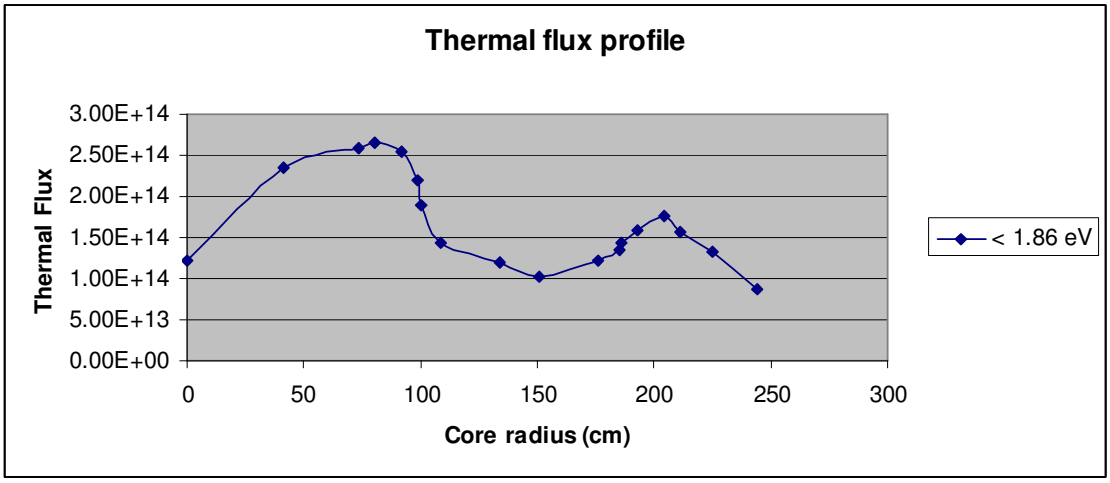

Figure 3.5: Radial thermal flux profile for the PBMR.

However, during reactor operation, the pebble circulation into any radial position in the

core is random. From Figure 3.5 show higher thermal neutron flux in the reflector at a radial distance of about 80 and 200 cm respectively. However the peak on the side reflector (at a radial distance of 200 cm) is lower than at 80 cm because, during normal operation, the control rods are partially inserted in the side reflector, hence the flux depression. BIRGIT/TRIGIT also prepares the mesh pattern for the 2-D or 3-D diffusion calculations (CITATION) and performs the transformation between the BIRGIT and the diffusion (CITATION) grids and the transformation for the thermal hydraulics grids.

3.3.4 DATA-2 code

For high temperature reactors both the spherical and prismatic fuel element design can be used. The DATA-2 code reads the fuel design specifications of the reactor and then calculates the atomic densities and fabrication costs. It also prepares the data set for GAM-1 and THERMOS code. These data sets are provided as an input to the V.S.O.P code. The V.S.O.P code requires atomic densities that are homogeneously distributed for many different batches in the reactor. It requires cross section and geometric input from BIRGIT/TRIGIT code. It provides fuel design specification input to ZUT code for resonance integral calculations and V.S.O.P.

3.3.5 GAM code

The GAM code was developed mainly due to the need for a procedure that would provide few of multi-group constants for the reactor calculation in a consistent manner. The code is using the resonance integral to generate these multi-group constants characterizing the absorption directly from the resonance integral (calculated by ZUT-DGL code). The group constants and their changes with temperature and atomic densities of influential nuclide are calculated by subroutine GAM. The dependence of resonance absorption cross sections on temperature is achieved by linear interpolation between the respective cross section sets. The changes of the constants for important radio nuclides are evaluated by using a self shielding factor (Note that self shielding is where the local neutron flux is depressed within a material due to neutron absorption near the surface of the material, Figure 2.6). There are two types of self shielding factors in V.S.O.P code, GAM namely; cross section self shielding and neutron flux self shielding factors. The cross section self shielding factors (SC) allow modification of the microscopic cross sections of the library. This might be desired to account for resonance shielding effects, for changes of the neutron energy spectrum within a fine group *g*, or for improved measurements of cross sections, respectively. The code allows input for different subsets of cross section-self shielding factors SC_g. They can be applied for any nuclide in any spectrum zone. The SC_g are multiplied to the respective cross sections σ_g of the energy group *g*.

The method used in GAM for calculation of resonance integral is the “quantitative method” developed by Adler [46]. The resonance absorption is calculated by a method developed by L.W Nordheim[45]. There are three methods that can be applied within the code, namely, P1 approximation equation, B1 approximation equation and the “moment method”. A full description of these methodologies is described by Joanou [47].

Using the fuel design data from the DATA-2 codes and the resonance integral data calculated by the ZUT code, GAM code performs an evaluation of the neutron flux for the 68 energy groups (0.414 eV - 10 MeV). The GAM code also calculates multi-group cross sections for a maximum of 32 fast groups and inelastic scattering. The cross sections of the resolved and unresolved resonances for radio nuclide U-238 and Th-232 are generated by the ZUT code.

3.3.6 THERMOS code

It performs one dimensional calculation in 30-energy groups ranging from 0 to 2.05 eV (thermal). The thermal data in 30 -group structure is collapsed from 96 THERMALIZATION libraries by a relevant neutron energy spectrum generated by the THERMALIZATION code. THERMOS code uses different spectrum calculations during normal operation and accident simulation. THERMOS code was developed by Honeck [34]. This code uses an "integral form" of the transport equation to calculate the spatially dependent thermal neutron spectrum in a cell characterized by 1- dimensional symmetry. This code was aimed at investigating the thermal neutron flux in a reactor lattice with the main emphasis on accurate prediction of the reaction rates. The method used in THERMOS relies heavily on the assumption of isotropic scattering using the energy dependent transport equation and assuming isotropic sources and scattering [34].

3.3.7 ADAGE (Actinide Depletion and Generation) and FEVER codes

During the reactor operation, the fuel composition or inventory will change as fissile isotopes are consumed and fission products are produced. This variation of fuel composition is caused by an exposure to neutron flux during the reactor operation. Therefore, calculation of the core multiplication factor and power distribution must be calculated repeatedly over the operating life of the reactor. The depletion analyses performed by "ADAGE and FEVER" codes are closely related to nuclear fuel management since one tries to optimise the fuel loading, fuel arrangement and fuel reloading in order to achieve the most economical power generation within the reactor core design constraints (with adequate safety margin) placed on the reactor operation (which is the main purpose of this dissertation). As discussed in section 1.5, the requirements for fuel loading are determined by taking into consideration the temperature, power reactivity defects, fuel depletion and fission product build up. The fuel burn up is simulated by an alternation procedure between the simulation of fuel shuffling and the evaluation of the space and energy dependent neutron flux resulting in the local depletion and production of fission products. Within V.S.O.P, the iteration step in between the shuffling of the fuel is called "Burn-up Cycle". This cycle is divided into large burn-up time steps which in turn are subdivided into smaller burn-up time steps. For large time steps, the spectrum calculation and diffusion calculations are performed repeatedly, whilst for the small time steps, the height of the neutron flux is readjusted to the core power for each time step as part of the logical and systematic calculation of the fuel burn-up. During the small time step calculations, the spatial distribution remains unchanged until the recalculation in the large burn-up time steps.

ADAGE and FEVER codes solve the burn up calculation equation for 28 heavy metal isotopes and determine the fission inventories in the fuel by making use of the normalised flux at its local position [44] for each small time step within the large time step. ADAGE code uses the "matrix exponential" method in the treatment of decay and transition schemes by constructing the transition matrix for 28 heavy metal isotopes listed in the ADAGE library which is used in the burn up section of the code [44]. This library contains the identification number for each isotope and decay constant including the information regarding the possible transition by α, β^-, β^+, decay by disintegration from the excited nuclear state to the ground state and by spontaneous fission. The ADAGE code is using the broad group cross section for neutron absorption, neutron induced fission and (n, $2n$) reaction from GAM-1 and THERMOS codes. The ADAGE library defines the heavy metal chain from Th-232 through Cm-244 according to the cross section data available from the GAM library. The burn-up of the fission products and fuel shuffling are covered by subroutine BURNUP, FUMAN and KUGELN which forms part of the FEVER code. The build-up history of up to 49 fission product nuclides in the fuel compositions is followed explicitly.

3.3.8 CITATION code

CITATION is a diffusion code. This code is applied for calculation of the criticality and neutron flux distribution. It is using as an input the macroscopic cross section data which are prepared from collapsed microscopic cross section and atomic densities. The basic nuclear library (ENDF-IV/V and JEFF) provides data in the form of the 96 energy group structure of the THERMALIZATION code. This data is condensed into 30 energy groups of the THERMOS using neutron spectrum which is representative of the reactor core. Depending on the user, the 3-D or 2-D model can be developed which use the diffusion calculation modules in the CITATION code that calculates the leakage term for different spectrum zones and energy groups.

3.3.9 THERMIX/KONVEK

The THERMIX code was developed for thermal hydraulics evaluation of the pebble bed HTR reactors in two dimensions. The code simulates the steady state and transient conditions. The code receives the power distribution of the reactor from the nuclear code (CITATION, FEVER) at a given point in time. The code provides the corresponding temperature profiles of the fuel and moderator averaged over the volume of the reactor spectrum zone for use in the neutronics calculation. The basic equations used by the THERMIX which complies with the conservation laws (energy, mass, momentum etc) are described by V.S.O.P manual, Rütten et.al, 1997[44].

3.3.10 FUMAN, KUGELN and BURNUP

The burn up of the fission products and the simulation of the fuel sphere movement (shuffling) are covered by the subroutines BURNUP, KUGELN and FUMAN. These subroutines form part of the FEVER code (refer to FEVER code, by Todt F)[44].

3.3.11 LIFE

The LIFE code prepares a library, which is used in calculating local decay power to be used by THERMIX. The code prepares the history of the fuel sphere in the core, this include, the burn-up, isotopic inventory of fission products and actinides and power profiles. This information is provided to the transient analyses model for further calculations.

3.3.12 PRIOR

PRIOR is used to calculate the fuel life history to be used in generating the entire fuel isotope composition.

Chapter 4

Fuel Management Calculation

The ultimate goal of the nuclear reactor design engineer is to design a reactor and the fuel element such that the reactor core and fuel elements can be utilized efficiently and that fission product releases in the primary coolant under normal operation and accident conditions are within the design limit. The fuel designers always strive to design fuel in such a way that it can accommodate both normal operation and transient conditions such as reactivity transients (e.g. control rods ejection), without any loss of integrity. That is, the fuel element retention capability of fission products can be guaranteed under all reactor core operating conditions. On the other hand, it is desirable to operate fuel at higher burn-up to reduce fuel costs. Therefore, the design of the fuel and operating limits must have sufficient margins to reduce the failure probability to a very low level. The PBMR fuel is using the German specification [37] and if one assumes that the PBMR fuel can be manufactured to be as good as the German fuel, then, one can take credit of the available experimental data which is representative of the PBMR operating conditions. These data indicate the three important parameters that contribute to fuel failure such as burn-up, fluence and temperature [48]. Hence, the reactor core must be designed such that it can produce the desired thermal power without exceeding the temperature limitation on the core components that might lead to fuel failure and releases of radioactive materials into the coolant. Such thermal limitations constitute the primary factors in determining the core size, since the critical mass of fissile material can theoretically operate at any power level if sufficient coolant is provided. Due to this, one first determines the core power density that can accommodate the intended primary cooling and then determines the reactor size necessary to meet the desired reactor thermal power output at that power density. Given the fuel geometry and core configuration (e.g. core volume) and taking into consideration the thermal hydraulic effects, one can perform nuclear analyses to determine the fuel inventory or fuel loading that allows the reactor to operate at the rated power over the desired core lifetime. That is why the nuclear analyses are intimately related to the thermal analyses. We have also seen (chapter 2, section 2) that the nuclear cross sections that determine the core multiplication depend sensitively on the temperature (Doppler effects). For this study, the core size and desired thermal power is already determined by PBMR PTY LTD and the core design data or specification is described in the PBMR report [37]. This reactor core design data can be used to perform reactor analyses and determine the reactor core behaviour including the core design constraints. The PBMR 400 MW design used in this dissertation is in the process of being changed to cylindrical reactor with steam generator due to the too high temperatures and others core design constraints described in this dissertation. Some of the results from the study have being used during the independent review of the PBMR and Source-Term discussions. These analyses will identify the range over which system parameters can be varied while still complying with the constraints placed on the reactor performance. To execute this, a detailed reactor core design can be used to determine the best suited system parameters that can yield optimum core performance consistent with the reactor core design constraints. This chapter will describe the design data and

evaluate the impact of the variations of the parameters specified in the design data to the in-core fuel management. That is, impact of the variation of parameters such as enrichment, heavy metal loadings and number of passes and their impact to safety and economics will be assessed. These imply taking into consideration the thermal limitations on core performance which entails keeping the fuel temperature below the safety limit (note that the design limit being referred to is enveloping the safety limit).

4.1 Description of the fuel and reactor core design model

As already described in section 1.4, the PBMR reactor with rated power level of about 400 MW has a reactor core diameter of about 3.7 m and an effective core height of about 11 m. The reactor consists of two sets of reflectors, namely the inner central reflector and the side reflector. The side reflector is about 90 cm thick and provides channels for 24 control rods whilst the inner central reflector has diameter of about 2 m and provides channels for the reserve shut-down system. During normal operation of the PBMR 400 MW reactor control rods will be partially inserted at 2 m from the bottom of the top reflector. These control rods are located at a radial distance of about 1.95 m. These control rods compensate for the excess reactivity in the core during operation of the plant. These 24 control rods are divided into two groups of twelve. The first group is inserted at the top of the core and the second group will travel from the top to the bottom of the core (That is, they will overlap with the 1st group). Each control rod has an effective height of 6.50 m. The PBMR reactor has an effective core volume of about 83.715 m^3 and contains about 451 000 fuel spheres with heavy metal loading of about 9 g and enrichment of about 9.6%wt U-235. The amount of coolant required to remove heat from the reactor at the rated power level of 400 MW is 192.7 kg/s and the reactor inlet and outlet temperatures of about 500 and 900 °C respectively [19;26].

The reactor core model fuel zone is subdivided into five flow channels. These five flow channels are divided into equi-sized partial volumes per flow channel (79), each of which contains a mixture of six different fuel element loads. These loads represent various passes through the core. The partial volumes in the core are appropriately grouped together to form spectrum zones for the spectrum calculations. The model is using spectrum zones 1 to 79 for the fuel region and spectrum zones 80 to 250 for the non-power generating areas. The main input parameters for the model such as the reactor cavity cooling system, reactor pressure vessel dimensions and core barrel are described in Table 4.1 and detailed design data is described by Mulder E [37]. The PBMR has already selected the multi-pass fuel management scheme with a circulation rate of about 6 (passes). This design data is used for both neutronics and fuel management studies.

Parameter	Units	Value
Core Thermal Power	MW	400
Core volume	m^3	83.715
Reactor Core height	m	11
Primary System Pressure	bars	89.5
Pebble Bed Packing Fraction	-	0.61
Mass Flow rate	kg/s	192.7

Parameter	Units	Value
Coolant inlet Temperature	° C	500
Coolant outlet Temperature	° C	900
Fuelling Regime	-	Multi pass (6x)
Central Column Diameter	m	2
Side Reflector Inner Radius	m	1.85
Barrel Outer Radius	m	2.925
RPV Inner Radius	m	3.10
RPV Outer Radius	m	3.28
RCCS Inner Radius	m	4.10
Helium Specific Heat	J/(kg K)	5195
Prandtl Number of Helium	-	0.66

Table 4.1: Main input parameters

In the PBMR spherical fuel element design, the fuel in the form of UO_2 kernels is contained in coated particles that are embedded in the graphite matrix forming the fuel zone of elements. This is represented by Figure 1.6. Each fuel element contains coated particles that are uniformly distributed in the graphite matrix, which together constitute the "fuel zone". This fuel zone is in turn coated with a layer of graphite that serves as a clad and moderator. The details of the fuel design are summarized in Table 4.2 and more details can be found in Mulder E [37].

Parameter	Unit	Value
Pebble Radius	cm	6.0
Thickness of the fuel free zone	cm	0.5
Enrichment	%wt	9.6
Density of the matrix graphite/ fuel free zone	g/cm^3	1.74
Heavy metal loadings per fuel pebble	g	9
Kernel diameter	µm	500
Kernel density	g/cm^3	10.4
Coating Materials		C/C/SiC/C
Layer thickness • Buffer layer thickness • Inner PyC layer thickness • SiC layer thickness • Outer PyC layer thickness	 µm µm µm µm	 95 40 35 40
Layer density • Buffer layer density • Inner PyC layer density • SiC layer density • Outer PyC layer density	 g/cm^3 g/cm^3 g/cm^3 g/cm^3	 1.05 1.90 3.18 1.90

Table 4.2: Fuel Specification

Section 4.2 will describe the model assumptions. These will include the assumption that

the in-core helium flow is evenly distributed and homogeneous distribution of the fuel in the core (that is homogeneous mixture of old and fresh fuel).

4.2 Model Assumptions

- During power operation a certain fraction of the heat generated during fission process is deposited not at the position where fission takes place, but is distributed through the fuel and core structures by transport of neutrons, fission and decay gammas. V.S.O.P code does not model this effect (non-local heat deposition).
- The helium bypass flow between the side reflector (SR) and the core barrel (CB) was not modelled.
- Helium mass flow rate was fixed at 192.7 kg/s.
- For the thermal hydraulics, the reactor cavity cooling system (RCCS) was fixed at 20 °C
- The helium pressure was fixed at 89.5 bars.
- The heat transfer coefficients at the top and the bottom of the core were set to 1.E-6 W/(cm^2.K) which implies thermal isolation at the top and bottom ends.
- Calculations were performed in a 2D R-Z cylindrical geometry.

4.3 Description of the constraints imposed by investigated fuel management parameters

For the reactor core to produce the desired thermal power without exceeding the limits, the thermal limitations must be specified, for example temperature limitations on the component that might result in the fuel failure and eventually the release of radioactive materials into the coolant. These thermal limitations constitute primary factors such as the reactor core size. From this, one can determine the core power density that can accommodate the intended primary cooling and the reactor core size necessary to meet the desired thermal power output at this power density. This study uses the rated power level, reactor size and dimensions already specified by PBMR PTY LTD. Our main task is to determine the optimum core performance level that can result in safe and economic reactor operation. This can be achieved by determining the optimum for the power peaking factors and power densities. However, the power density distribution also depends on other parameters such as leakage, fuel composition, uranium concentration, enrichment, burn-up, control rod effects, power distribution in the sphere etc. The reactor core is normally loaded with fuel elements that are identical in geometry, mechanical design, thermal-hydraulic design but may differ significantly in uranium concentration, enrichment, burn-up etc. These features are normally applied to reduce the core power density variation induced by leakage. And if not properly used, the effects may be opposite. The desire is to operate the plant at high temperatures in order to increase the plant efficiency and this result in the following core performance limitations:

4.3.1 Fuel temperature limitations

One of the principal limitations on the allowable power density in the reactor arises due to the desire to prevent the fuel temperature from exceeding its melting point at any point

in time. The PBMR is using the kernel that contains UO_2 which has a melting temperature of about 2800°C. It should be noted that the melting temperature varies with irradiation. In other words, the melting temperature tends to decrease with an increase in fuel exposure to radiation. So the fuel sphere exposed to very high burn-up can induce centreline melting and also has very high probability of failure (failure we are referring to the release of fission products). It should be noted that radiological limits will still be met if only few spheres exceeds the centreline melting temperature, however, attention must be paid in determining the impact of these failures to the amount of the radioactive material released during such an incident so that the normal operation or design base accident (DBA) limits in terms of fission product releases are not exceeded. The maximum fuel temperature achieved by spheres also depends on the linear power density and pebble thermal conductivity. So thermal limits imposed by the fuel melting can be expressed in terms of the maximum achievable power density in the core or power peaking factor. The power density and power peaking factor specific to PBMR form part of discussion of the study results. The thermal conductivity is also of major importance for calculating the temperature distribution and is a function of fast neutron dose and temperatures. This also holds for the graphite spheres as well as for the reflector graphite. The conductivity of non-irradiated graphite is a function of temperature. When irradiated by fast neutrons, the conductivity is reduced due to several mechanisms of material destruction or damage. The amount of reduction depends on the irradiation fluence, the irradiation temperature and the type of graphite. Based on the experimental data, graphite model data set and analytical are established. The graphite sphere (Nukem A3-3) data is taken from the work of Binkele [37, 44] up to a fast neutron fluence of approximately $6.09 \times 10^{21} cm^{-2}$ and a temperature up to 1 000°C. The PBMR will experience approximately $2.7 \times 10^{21} cm^{-2}$ during PBMR operation. Figure 4.1 shows the variation of graphite thermal conductivity with temperature and fluence. The graphite referred to by figure 4.1 is the reflector graphite as well as the graphite spheres used during the reactor start-up. The current experimental data on graphite for temperature and fluence levels representative of the PBMR conditions is insufficient. As part of the graphite qualification programme, the reflector and graphite sphere will be tested at the conditions that are representative of the PBMR operating condition and PBMR has scheduled this qualification tests (some of these tests form part and of the core structure ceramics (reflector graphite) life assessment). The PBMR reflectors are exposed to temperature far less than 1 000°C during normal operating conditions and graphite spheres are used for start-up only. The extrapolation reflected in figure 4.1 will results in reduced graphite thermal conductivity which in turn results in increased temperature. The validity of this extrapolation will be assessed through the graphite qualification programme. With respect to fuel temperature predictions for normal operation, a sensitivity and uncertainty analyses were performed on the most important parameters affecting the prediction of fuel temperature. These parameters include the increased helium leakage flow, power level in the reactor, helium heat capacity, thermal conductivity of the spheres, the helium mass flow rate, reactor inlet temperature of helium etc. The uncertainties evaluated were dominated by the variation of increased leakage flows followed by the variations of the power level. This implies that the helium heat convection is dominating the heat removal at steady state and therefore the graphite heat conduction correlation model is not anticipated to make significant difference to the steady state fuel temperature. The

graphite conduction correlation model is anticipated to make significant difference during accident condition. Figure 4.2 refers to the effective thermal conductivity of the pebble bed. This consists of three mechanisms namely, conduction, convection and radiation. The effective thermal conductivity referred by figure 4.2 is the total effective thermal conductivity of the pebble bed and is given by the following expression:

$$\lambda^T = \lambda_e^R + \lambda_e^g + \lambda_e^c . \qquad 4.1$$

where

λ^T = the total effective thermal conductivity of the pebble bed

λ_e^R = the effective thermal conductivity through voids radiation and solid conduction

λ_e^g = the effective thermal conductivity through convection and solid conduction

λ_e^c = the effective thermal conductivity through conduction and solid conduction

The effective conductivity λ_e^R is based on Zehner-Schülder. This model accounts for conduction within the fuel spheres and radiation in the voids. At high temperatures, the heat transfer via radiation dominates. Zehner-Schülder also estimates for gas and solid conduction (λ_e^g) and this model was tested by Prasad [8]. The last term in equation 4.1 (λ_e^c) is the prediction of thermal conductivity of the contact area for spheres in the pebble bed. However, the effect of gas convection on heat transfer is not included in the Zehner-Schülder correlation since THERMIX has a function for simulating the process of natural convection. The model for natural convection in the core is included in the calculation distribution of the pebble in order to take natural convection into account. The comparison of the effective thermal conductivity between the Zehner-Schülder correlation and the measured data mentioned that the effective thermal conductivity was slightly lower than the measured data. There are several conflicting articles regarding the validity of the Zehner-Schülder especially in the heat transfer in the near wall region (next to the boundaries or reflectors). The article reports an increase in the porosity near the boundaries resulting in a decrease in the number of contact points between the pebbles which affects the radiation and conduction through the pebble bed. However, the concluding remark from the IAEA technical document number 1163 [8] was that "the SANA experiment validated the THERMIX code and the effective thermal conductivity correlation modeling heat transfer mechanism in the pebble bed". The THERMIX code was deemed suitable for the gas cooled reactors [8]. PBMR has performed the experiments at the Heat Transfer Test Facility (HTTF) to assess the near wall effects and several other tests as part of the verification and validation of the codes. The results from these tests are not yet available in the public domain. Zehner-Schülder model was recommended for pebble bed at low and medium temperature levels. And the Robold model accounts for the heat transport through the openings between the pebbles of the

bed by radiation and the model is preferred for temperature above 1400°C. For the current analyses V.S.O.P. evaluate both models of Zehner-Schülder and Robold, respectively and applies the respective maximum of the two models [37, 44].

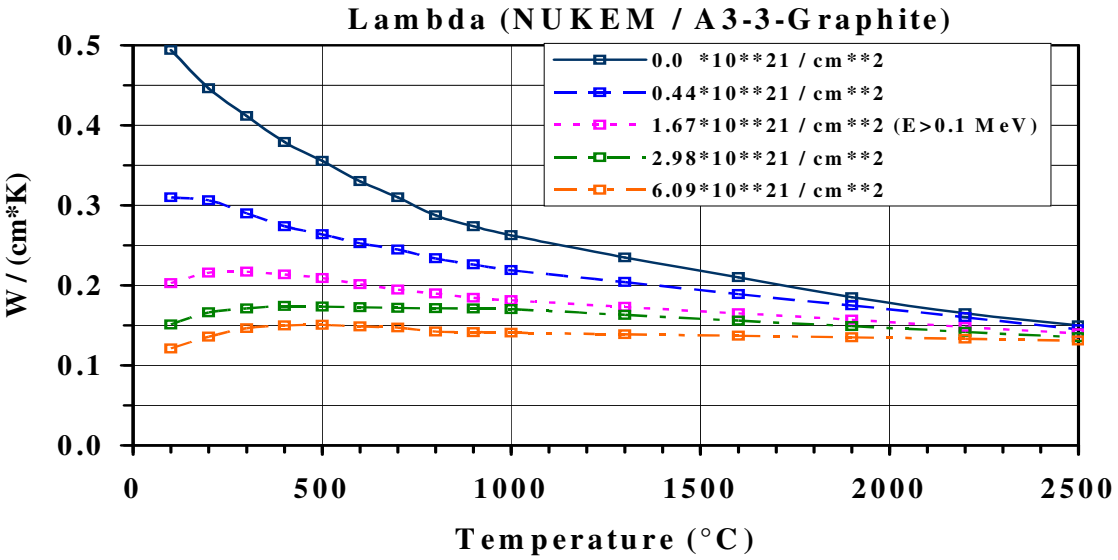

Figure 4.1: ***Thermal conductivity of the graphite as a function of temperature for various neutron fluences [37, 44].***

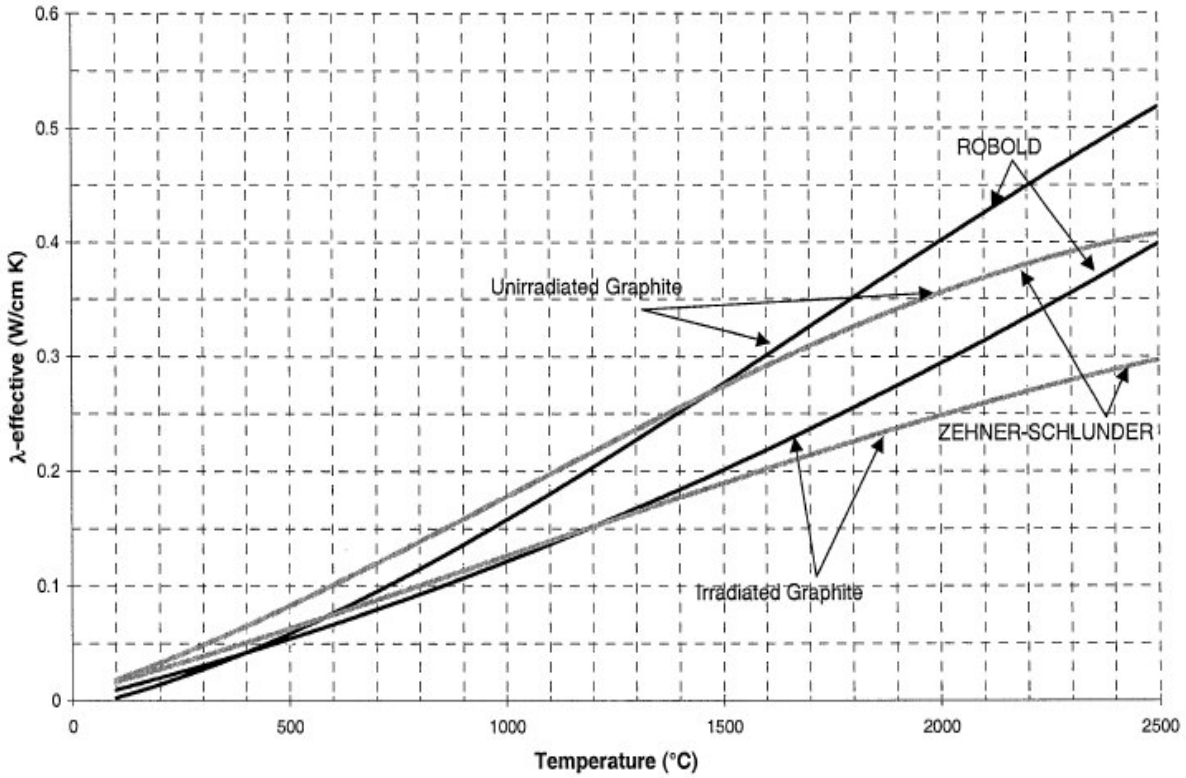

Figure 4.2: Effective thermal conductivity in a Pebble Bed (at a fluence level of about 6.09 x 10^{21} cm^{-2})[37].

The constraints imposed on the fuel especially the SiC as well as other pyrolytic carbon layers must be such that fuel spheres retain its integrity [48]. This SiC is subjected to severe stress due to fission gas pressure and fuel swelling. These phenomena depend on fuel irradiation, temperature variation, burn-up etc. Since SiC strength depends mainly on fuel manufacturing conditions [48]; that is the deposition temperature of the SiC layer during manufacturing of the coated particle. The literature [48] shows that if the SiC is deposited outside 1500-1550°C during manufacture, there is high probability that the fuel will not perform under irradiation. It should also be noted that although SiC is chemically stable at high temperatures during normal operation, i.e. in an inert atmosphere, it reacts with air and water under accident conditions (air and water ingress accidents). It is important to understand the behaviour of SiC during accident conditions and its impact on fission product releases [49].

With respect to the reactor coolant temperature limits, these are derived from the maximum fuel temperature. That is, the reactor outlet temperature should be selected such that the maximum fuel temperature achieved during normal operation and accidents is kept within the limit (~1600°C). Also the reactor core size is determined primarily by the amount of heat transfer area necessary to transfer the desired thermal power. In summary, the principal limitation on the core thermal performance include the limitations on the fuel centreline temperature, the limit on the stresses imposed on the SiC due to the

fission gas release, fuel swelling and power density.

For a given fission power distribution and reactor coolant condition, the thermal analyses will determine the temperature distribution throughout the core. However, one must ensure that the maximum fuel temperature achieved during this condition does not exceed the thermal limitations. It should be noted that the power density is not uniform and depends on the time and on the power distribution. The thermal analyses start by calculating the volumetric source of fission heat throughout the core and this fission heat is proportional to the fission rate density and requires an initial estimate of the neutron flux distribution in the core ($q(E) = \upsilon N(r)\sigma(E)\phi(E)$). During normal operation, this heat is removed by the coolant and one can use the coolant temperature as it passes through the reactor and use this information to determine the expected fuel centreline temperature and moderator temperature. It should also be noted that unlike the LWR's the coolant temperature and the core neutronic behaviour are not directly coupled because coolant phase change cannot occur and also the coolant does not provide appreciable moderation in the core due to its very low density.

Our ultimate goal is to investigate and propose the optimum in-core fuel management strategy that is economical without compromising safety (balance between the safety and economics). This can be achieved by assessing the impact of the online refuelling, enrichment and heavy metal loading variations to the safety and the economics. The safety aspect will be assessed in terms of the impact to core performance parameters and thermal constraints imposed on the fuel elements such as maximum fuel temperature, power peaking factors, control rod worths and burn-up. To achieve this, the V.S.O.P code is used to calculate the reactor core behaviour up to the steady state equilibrium condition. The results from these analyses give an indication of the reactor core burn-up, the power peaking factor, the maximum fuel temperature the fuel sphere from the first cycle (first pass) will be exposed to during normal operating condition, the flux profile, power profiles, core multiplication factor, core inventories, core leakage and fluence etc. The output of this equilibrium condition will be used as a starting condition for transient analyses (Depressurised loss of Forced cooling accident (DLOFC)) and further be used to calculate the reactor core shutdown capabilities. For the transient analyses such as DLOFC accident, the heat removal is impaired and the fuel heat-up and the negative temperature coefficient of reactivity will cause the reactor to become sub-critical. Despite the reactor core being sub-critical heat will still be generated through the decay of fission products and actinides. Shortly after the DLOFC event started this decay power amount to about 7% of the reactor power prior the event and it continues to drop exponentially. The total decay heat calculated by V.S.O.P is given by the "DIN" standard [37, 44]. The standard was established for HTR fuel and it entails the decay power from short-lived and long-lived fission products, neutron capture, precursors (Th-233, Pa-233, U-239 and Pu-239) and actinides. The heat is removed from the core through conduction, convection and radiation. The high heat capacity of the graphite limits the core heat-up rate and allows a substantial period of time for external action to be taken (such as closure of the break or restoration of cooling). To analyse this event, the following assumptions were made:

- The coolant flow through the core stops completely, and it is assumed that the

existing helium transports no decay heat out of the core

- Pressure immediately drops from 90 bars to 1bar, for DLOFC
- It is assumed that the fission power is zero immediately after the start of the DLOFC

During a DLOFC accident, the following parameters are important for the model to provide good estimates of the fuel and component temperatures and peak times. These parameters include the type of graphite used, thermal conductivity and heat capacity correlations, coefficients of emission, the decay heat standard used etc. A detailed description of the correlation is outside the scope of this dissertation and described by Muller E [37]. Only the maximum temperature during DLOFC is reported in the dissertation as it forms part of the assessment of the thermal constraints imposed on the fuel elements.

Several case studies were investigated and for each case, the neutronics and thermal hydraulics calculations were performed, followed by the control rods worth and DLOFC accident analyses. These analyses were performed to give an indication of the fuel operating conditions during normal operation and during an accident condition such as the loss of coolant accident (DLOFC). This loss of coolant accident is well known in the LWR in that it can result in core melt-down if the safety systems are not taken into consideration. The following cases were investigated and the variation of parameters in each case is reflected in table 4.4. These cases were split into three groups namely, the variation of enrichment, variation of heavy metal loadings and variations of the number of passes as follows:

Group 1:

For this group, the enrichment was varied and the number of passes and the heavy metal loadings per fuel sphere are kept constant. The enrichment was varied from 6% up to 17% wt U-235.

Group 2:

For this group, the heavy metal loading was varied and the enrichment and number of passes are kept constant. The heavy metal loading per fuel sphere was varied from 6 to 12 grams.

Group 3:

For this group, the number of fuel spheres passes is varied whilst both enrichment and heavy metal loading are fixed.

Note that the variation of enrichment, heavy metal loadings and number of passes were randomly selected (not systematic) and without any order of preference, however the results from these studies give indication in terms of the thermal constraints and the economics. The limits and the affected parameters are specified in Table 4.3.

Core Physics Parameter affected	Units	Limits
Burn-up	MWD/Ton	120 000
Maximum power per sphere	kW	4.5
Maximum fuel temperature during normal operation	°C	1200
Maximum fuel temperature during DLOFC	°C	1600
Shut down capability in hot and the most reactive conditions (cold condition)	-	$K_{eff} < 0.99$ 10%-uncertainty included

Table 4.3: Affected parameters and limit

These case studies were performed using the same online refuelling as the PBMR was fixed to 6 passes and the fuel enrichment and heavy metal loadings were varied and results are reported below. These parameters have influence on the fundamental safety functions and have been selected due to their impact to fuel economics as well.
The results of these studies will be summarised in terms of the safety implication and also in terms of the economics and discussed in chapter 5.

4.4 Results

In the determination of the optimum in-core fuel management strategy, one needs to have a thorough understanding of the core behavior and performance during normal operation and accident conditions. These involve a full understanding on the key critical core performance parameters and constraints and their impact to fuel management in terms of the economics and safety. The behavior of the core during normal operating condition and during accident condition (DLOFC) was analyzed and the results are reported later in table 4.4, 4.5 and 4.6. The main objective of the analyses was to investigate the impact of the fuel management parameters such as enrichment, heavy metal loadings and numbers of passes to plant safety and economics. And the whole safety of the PBMR fuel is based on the ability of the fuel sphere to remain intact and retain the fission products. There are three parameters that are important in determining fuel performance and failure mechanism. These parameters are fuel temperature, fluence and burn-up. Although one cannot dispute the fact that fuel manufacturing also plays a critical role in the overall performance of the fuel sphere.

4.4.1 The impact of the variations of the heavy metal loadings on reactor safety and economics

It should be noted that the fuel design specifications such as TRISO particle density and layer thickness remain unchanged, so the heavy metal loading in the fuel sphere will be increased by increasing the number of coated particles. For the equilibrium core condition, the impact of the variations or an increase in heavy metal loadings at a fixed enrichment and fixed number of passes results in higher burn-up to a certain extent. That is, results of the analyses reported in Figure 4.3 show that an increase in the heavy metal loading from 6 to 9 g results in higher burn-up and this is good in terms of the fuel

economics.

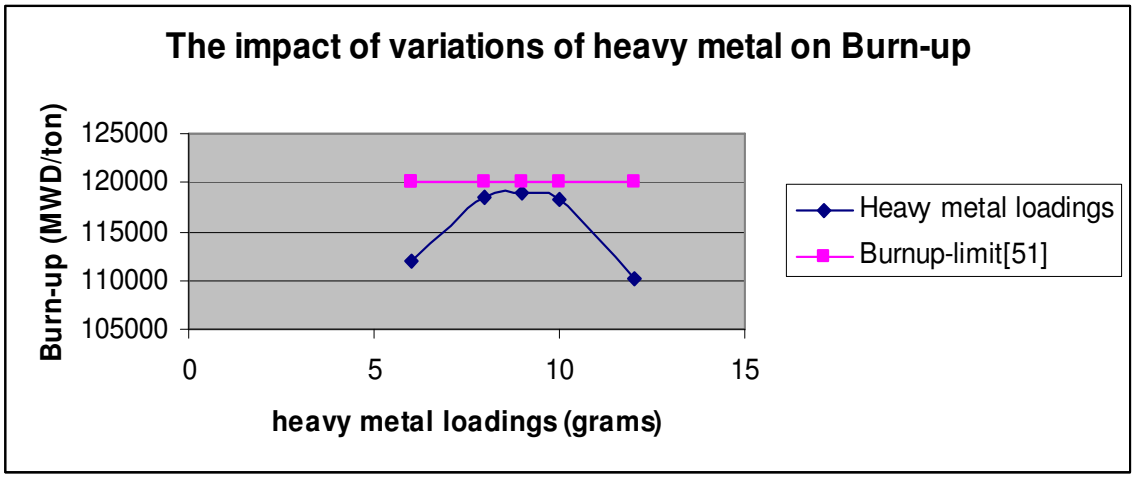

Figure 4.3: The impact of the variations of heavy metal loadings on Burn-up (for 6 passes and 12%wt enrichment).

However, the results also show that an increase in heavy metal loadings beyond 9 grams does not add any economical value and this is shown by a decrease in burn-up (see Figure 4.3). The heavy metal loadings seemed to have reached an optimal burn-up at value of about 9 g per sphere. For example, at a fixed enrichment level of about 12%wt U-235, the amount of the energy that can be extracted from a fuel sphere with a heavy metal content of about 10 and 12 gram is 118355 MWD/ton and 110066 MWD/ton respectively as compared to 118853 MWD/ton which corresponding to 9 gram (Figure 4.3). This change in burn-up is due to the moderator to fuel ratio. For example, the variation of the moderator to fuel ratio ranges from 694 to 347 for the heavy metal loadings of 6 to 12 grams respectively. This will also result in a decrease in K-eff due to increased resonance absorption in the fuel. (Note that the variation of moderator to fuel ratio affect the thermal utilization term and resonance escape probability, hence the leakage). Due to a decrease in the moderating ratio, the fuel will compete with other material for absorption of neutrons. Other parameters besides the moderating ratio that has impact on the burn-up are parameters such as the neutron-flux, capture to fission ratio, fluence, fuel moderator and control rods absorption. The increase in heavy metal loadings also has an impact on safety in terms of the core performance parameters such as power peaking factor, maximum fuel temperatures during normal operations and accident conditions and reactor core shut down capabilities. With respect to the power peaking factor and maximum power per sphere, the variations of heavy metal loadings also show a decline in the power peaking factors (defined as the ratio between the maximum power in the channel and the average power in the core) and maximum power per sphere as the heavy metal loadings increases. A graphical representation of the variation of heavy metal loadings with the burn-up and fuel sphere power can be shown in Figure 4.3 and 4.4.

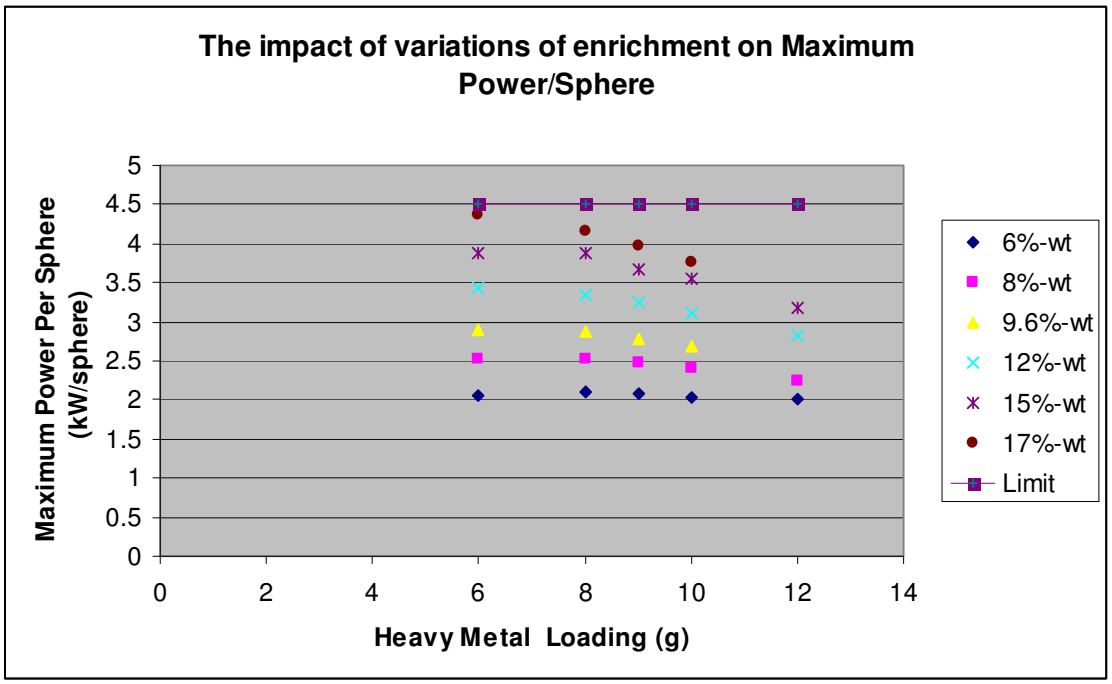

Figure 4.4: The impact of the variations of heavy-metal loadings with power in the sphere.

It should be noted that another failure mechanisms exists with fast reactivity transients such as control rod ejection where an enormous amount of energy is deposited in a sphere of coated particles within a short period of time. Experiments were performed in Nuclear Safety Research Reactor (NSRR) [48], Japan to try and verify the simulated reactivity transient. During this experiment, the energy deposited in the coated particle was in the range of 200–2300 J/g UO_2 within a time frame of about 10 to 30 ms [48]. These imply that the amount of power deposited in the coated particles ranged from 20-76 kW/g UO_2 for this very fast transient. Results from these experiments showed that 100% fuel failure was attained at 1500 J/g UO_2 and a particle failure fraction of about 1% was attained at energy deposition of about 1000 J/g UO_2. The experiment also showed that coated particles deposited with energy of about 2300 J/g UO_2 vaporized and recalling our previous discussion the vaporization (it can be implied that the coated particles were exposed to temperature above the melting temperature) of these coated particles corresponds to the UO_2 melting temperature of 2800 °C (which decreases with exposure to radiation). All these experiments were performed with un-irradiated coated particles. However, this rapid increase in energy deposition in the fuel element is not expected for the PBMR reactor during normal reactor operation and/or accident condition such as reactivity transient mainly because of the availability of reactor protection system, the design of reactor core shut system and the allowable limit for control rod withdrawal rate.

For the German fuel program, a value of about 4.5 kW/sphere was set as limit since the articles by Röllig K [50] and Nabielek H [51] have reported 4.5 kW/sphere as a limit and Röllig K has also mentioned that earlier experiments covered the ratings up to 4.8 kW/sphere and also implied that the integrity of the fuel sphere will be challenged. However for this investigation, the results show that the maximum power per sphere even

at higher enrichment such as 17%wt is 4.37 kW/sphere at heavy-metal-loadings of 6 g per sphere and still less than the limit of 4.5kW/sphere set by Rollig K [50] and Nabielek H [51] (see Figure 4.4 above). For the PBMR fuel, the fuel irradiation and test program will be extended to verify and determine this limit. It should be noted that results exclude the uncertainties. From these results, one can conclude that for normal operation, the power peaking factor for PBMR core at rated power level and enrichment level as per table 4.4 will not result in catastrophic failure of coated particles or spheres. It should also be noted that even if the maximum power in sphere is far much greater than 4.5 kW/sphere (it should be noted that a complete failure of SiC is driven by combination of high burn-up and temperature), one still needs to investigate or quantify the amount of coated particles or fuel spheres exposed to such peaking factor or power level in order to thoroughly determine the fission product release associated with such sphere. Such investigation falls outside the scope of this dissertation. The results for the key important parameters contributing to both the plant safety and economics are given in table 4.4 (using 6 passes).

Enrichment/heavy metal loadings		Limit	6%	8%	9.6%	12%	15%	17%
K-eff	6		1.0003	0.9997	1.0010	1.0006	1.0003	1.0003
	8		1.0004	1.0003	1.0005	1.0007	1.0000	0.9999
	9		1.0006	1.0004	1.0002	1.0001	1.0000	0.9998
	10		1.0008	1.0002	1.0002	0.9998	0.9999	1.0003
	12		1.0005	1.0002	-	0.9999	1.0006	-
Average Discharge Burn-up (MWd/Ton)	6	120 000	35 820	63 317	83 315	111925	145 421	166 651
	8	120 000	40 786	68 517	89 236	118 416	152 783	174 437
	9	120 000	40 944	68754	89 803	118 853	153673	174 470
	10	120 000	39 871	67 500	88 434	118 355	152 580	174 182
	12	120 000	34 791	60 694	-	110 066	143871	-
Maximum Core Power density (W/cm^3)	6		9.73	9.99	10.48	11.13	11.74	12.24
	8		9.81	10.41	10.95	11.57	12.19	12.67
	9		9.99	10.61	11.14	11.77	12.33	12.81
	10		10.14	10.78	11.31	11.94	12.48	12.92
	12		10.43	11.06	-	12.22	12.81	-
Power Peaking Factor	6		2.32	2.86	3.27	3.86	4.51	4.95
	8		2.38	2.85	3.25	3.76	4.33	4.72
	9		2.35	2.79	3.16	3.64	4.14	4.50
	10		2.31	2.71	3.04	3.49	3.95	4.26
	12		2.26	2.54	-	3.17	3.57	-
Maximum Power/sphere (kW)	6	4.5	2.05	2.53	2.89	3.44	3.89	4.37
	8	4.5	2.10	2.53	2.87	3.35	3.88	4.17
	9	4.5	2.08	2.47	2.79	3.25	3.66	3.98
	10	4.5	2.04	2.40	2.69	3.11	3.54	3.77
	12	4.5	2.00	2.25	-	2.82	3.18	-
Maximum Fuel Temperature (°C)	6	1200	1053.0	1054.8	1063.8	1071.8	1085.1	1093.3
	8	1200	1058.2	1061.8	1072.1	1080.9	1097.6	1109.0
	9	1200	1061.2	1065.9	1076.0	1087.0	1103.0	1112.9
	10	1200	1064.6	1070.5	1080.6	1094.3	1110.1	1120.8
	12	1200	1073.2	1082.3	-	1110.5	1127.7	-

Maximum coated particle Temperature (°C)	6	1200	1047	1054.8	1077	1113.8	1184	1228
	8	1200	1049	1061.8	1084		1191	1232
	9	1200	1050	1065.9	1085	1123	1187	1223
	10	1200	1052	1070.5	1083	1119	1177	1212
	12	1200	1056	1082.3	-	1108	1178	-
Maximum Fuel Temperature during DLOFC (°C)	6	1600	1467	-	1579	1636	1690	1726
	8	1600	-	-	1608	-	1710	1742
	9	1600	1508	-	1611	1665	1709	1737
	10	1600	1512	-	1607	1658	1702	1727
	12	1600	1510	-	-		1712	-

Table 4.4: V.S.O.P. Results on Fuel Management Evaluation Study for the PBMR Core.

From table 4.4, the analyses also show that an increase in heavy metal loadings has an impact on fuel temperature (that is, 1071.8-1110.5°C corresponds to an increase in heavy metal loadings from of 6 g and 12 g respectively).This increase in temperature is mainly due to the increase in the fissile material in the fuel element. This has implications on the overall source term during normal operation and experiments have shown that an increase in temperature results in increased fuel or coated particle failure [48]. For example, the fission product like Ag-110m has a melting temperature of about 961ºC and since high fuel temperature results in higher failure of coated particles; this would imply that at temperature greater than 961ºC, Ag-110m will be released (Figure 4.5). The Fickian-diffusion model is commonly used to determine the fission product release rates and is based on diffusion which depends strongly on temperature. This model is described in [48]. The results from irradiation tests with modern, high quality UO_2 TRISO particles in the German program also show that an increased temperature and burn-up results in increased release of fission products. For safe operation of the reactor, there are specific radio-nuclides (e.g. Cs-137, Cs-134, Sr-90, H-3, Xe-133, Kr-88 etc) that play a significant role during certain reactor operating conditions and these assist in the determination of the radiation exposure during normal operation and accident condition (the determination of these radio nuclides and calculation of source term and radiation exposure fall outside the scope of this dissertation). To limit the maximum fuel temperature during normal operation so that the release of fission products such as Ag-110m will stay within the limit, the reactor outlet temperature must be reduced from 900ºC to a lower temperature (that is 750ºC or even lower). This will reduce the maximum fuel temperature the fuel is exposed to during normal operation. And during the accident conditions such as DLOFC, due to this reactor outlet temperature (ROT) the maximum fuel temperature during this accident will increase due to decay heat coming from the fission products, however this increase in temperature will not be as high as compared with the starting condition of 900ºC ROT mainly due to the fact that the available heat will first need to heat-up the cooler reactor core structure such as the reflector.

An increase in heavy metal loading has an impact on the reactor core shutdown capability. For example, at a lower enrichment level such as 6 and 8%wt U-235, an increase in heavy metal loadings results in an increased reactor core reactivity. The results also show that during the most reactive core condition, the reactor can be still shutdown even though the reactor shut-down margin has decreased. The same effects can also be seen at higher enrichment.

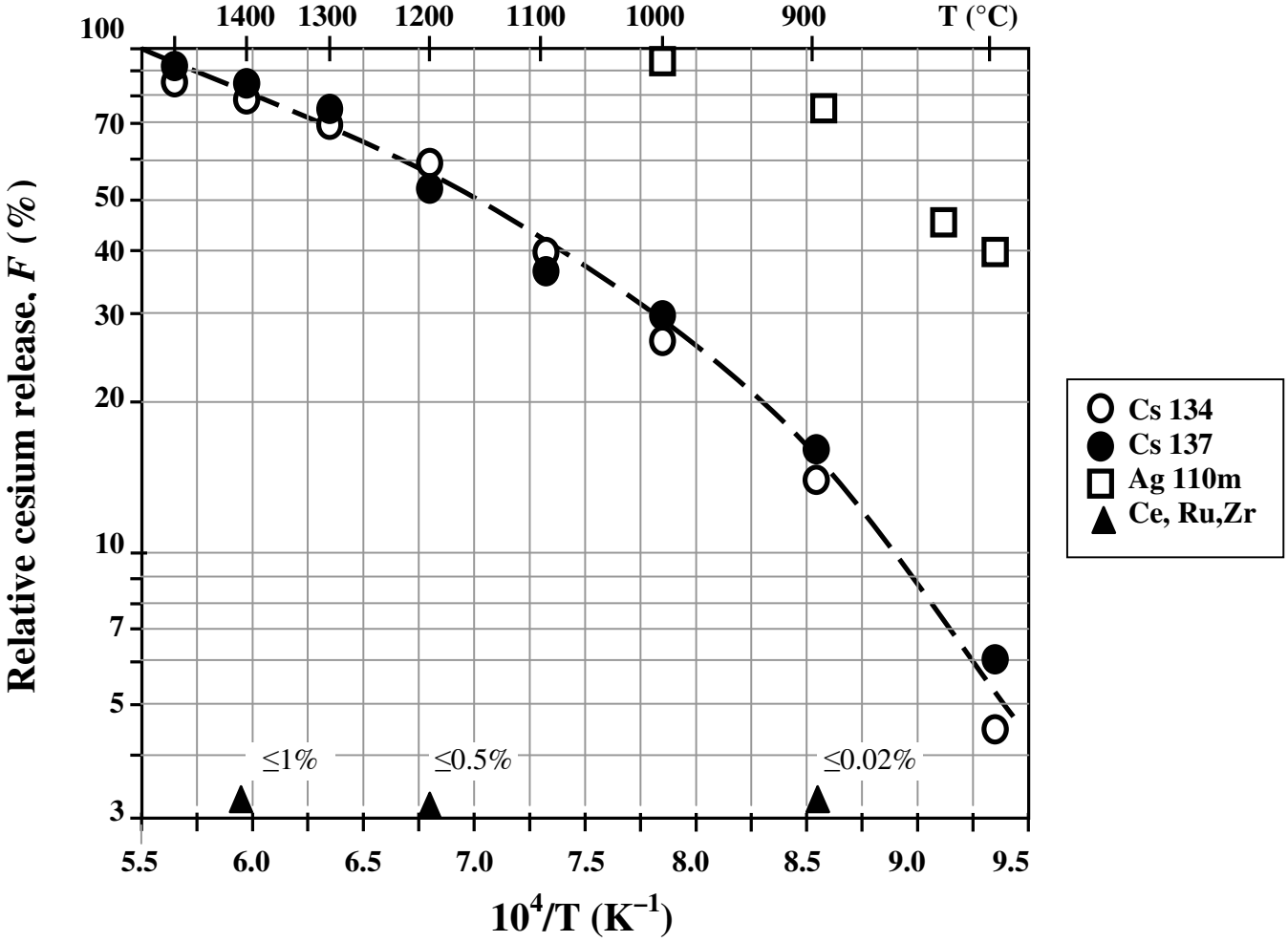

Figure 4.5: Results of the fission product release from the matrix during the heat-up experiments in Russian reactor (Koshcheyev KN).

4.4.2 The impact of the variations of the enrichment on reactor safety and economics

The results of the analyses show that the variation of enrichment has an impact on fuel burn-up. The results from table 4.4 show that a factor 2.8 increase in the enrichment can result in a burn-up increase of about factor 4.65. The variations of enrichment have shown to be more sensitive as compared to the variations of the heavy metal loadings (see figure 4.6 and 4.7 below).

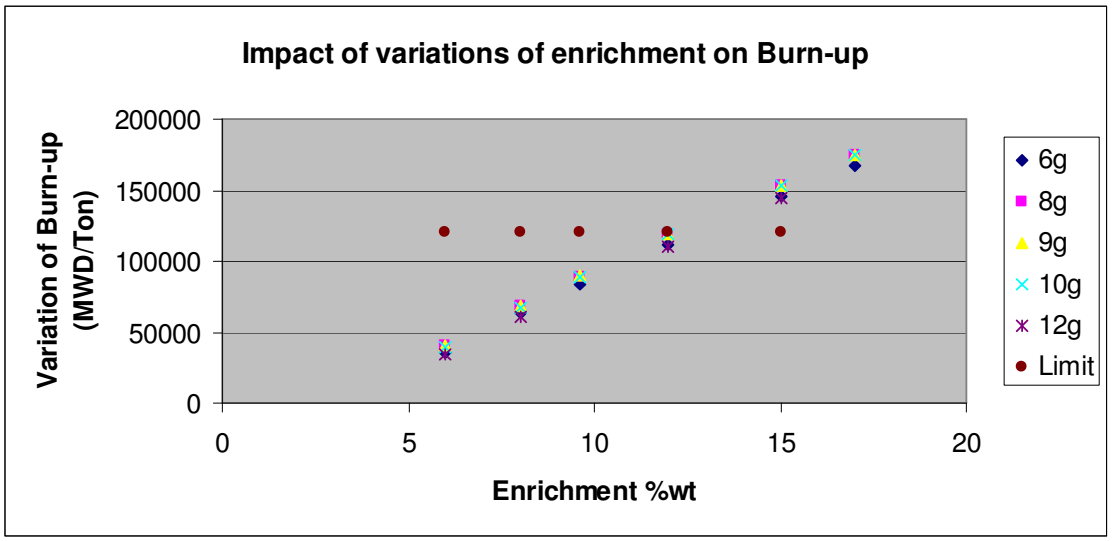

Figure 4.6: The impact of variations of enrichment on Burn-up (for 6 passes and 9 grams heavy metal loading).

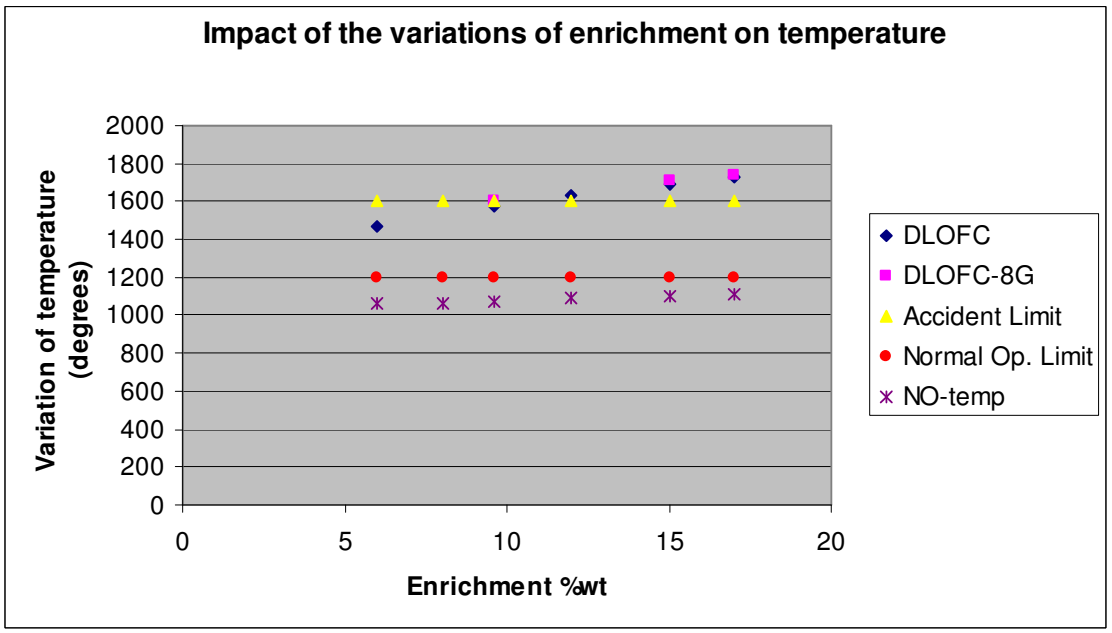

Figure 4.7: The impact of the variation of enrichment on fuel temperature (for 6 passes and 9 grams heavy metal loading).

This can be seen by an increase in burn-up and temperature during normal operation and DLOFC for any given heavy metal loading. The results show that an increase in fuel enrichment is economical as we can see that very high burn-up can be achieved (~ 174000 MWd/Ton). However, this burn-up exceeds the 120 000 MWD/Ton limit. The

results also show very high temperature and increased power peaking factors. A combination of high burn-up, temperature, power peaking and the maximum power in sphere may challenge the fuel sphere integrity. Experiments have also shown that the fuel integrity can be challenged. The increase in burn-up and temperature will result in an increase in the internal gas pressure (due to carbon monoxide and fission products) within the coated particle which can result in coated particle failure. For example, the experiments from the German tests program also show that an increase in burn-up results in fuel coated particle failure [48]. Maki [52] has also confirmed that the fission gas release during irradiation from the kernel depends on the temperature, burn-up and time. A comparison of the fission gas pressure in German coated particle at burn-up increase of about a factor 2.5 and temperature increase of about 200 degrees resulted in factor 8 increase in the gas pressure. This gas pressure is mainly driven by the excess oxygen produced during fission since fission products produced do not consume all the oxygen and this available oxygen reacts with the buffer layer to form carbon-monoxide gas (CO). The amount of CO produced is a function of temperature and burn-up. So depending on the reactor operating condition, Maki [52] has reported that the CO gas pressure can contribute up to a factor four as high as compared to the gas pressure due to the fission products. Further studies and experiments must be performed to determine the impact of this increased temperature, burn-up and power peaking to safety or fuel integrity.

Taking into consideration the findings from Maki [52] and the results in table 4.4, one can conclude that the internal gas pressure in the coated particle will be extremely sensitive to the combination of very high temperatures and high burn-ups and this can result in failure of the SiC layer and hence the release of fission products should be expected at high temperatures and burn-ups. The result from the analyses (table 4.4) show that an increase in enrichment level results in higher temperature during normal operations and during accident conditions (DLOFC), the internal gas pressure is expected to increase rapidly due to very high temperature and this will challenge the fuel integrity and plant safety. A limit of about 1600°C was set (as a result of experimental data and many other literature articles (Schenk and Nabielek [53] and figure 4.6-4.7). The results from this study show that at the higher enrichments level such as 9.6 % the maximum temperature during a DLOFC is greater than 1600°C. The impact of these high temperatures and burn-ups to fuel performance (that is fission products retention) must be determined and also be quantified as this plays a significant role in source term analyses. The experiments must be performed as part of fuel qualification programme to determine the extent of fuel failure or thermal constraints. In general, the results show that fuel is exposed to thermal (temperature) constraints and operational restriction will be required in order to reduce fission product release or fuel failures during normal operation and accident conditions (source term).

One of the fundamental safety functions besides the retention of the fission product by the SiC is the reactor core shut-down capability. Although, higher enrichment is coupled with very high burn-up and depending on the reactor operating mode and even during the most reactive core condition, the results from the analyses (table *I* in appendix A) show that adequate shut-down capability can be assured. However, the shut down margin reduced due to higher enrichment and due to an increase in fissile material. Note that for

the calculation of the shutdown margin and control rod worths, single failure criterion (or a stuck rod) was not assumed. The results does show that an increase in enrichment results in reduced shut down margin and control rod worths as shown in figure 4.8 and 4.9 and detailed results are reflected in appendix A.

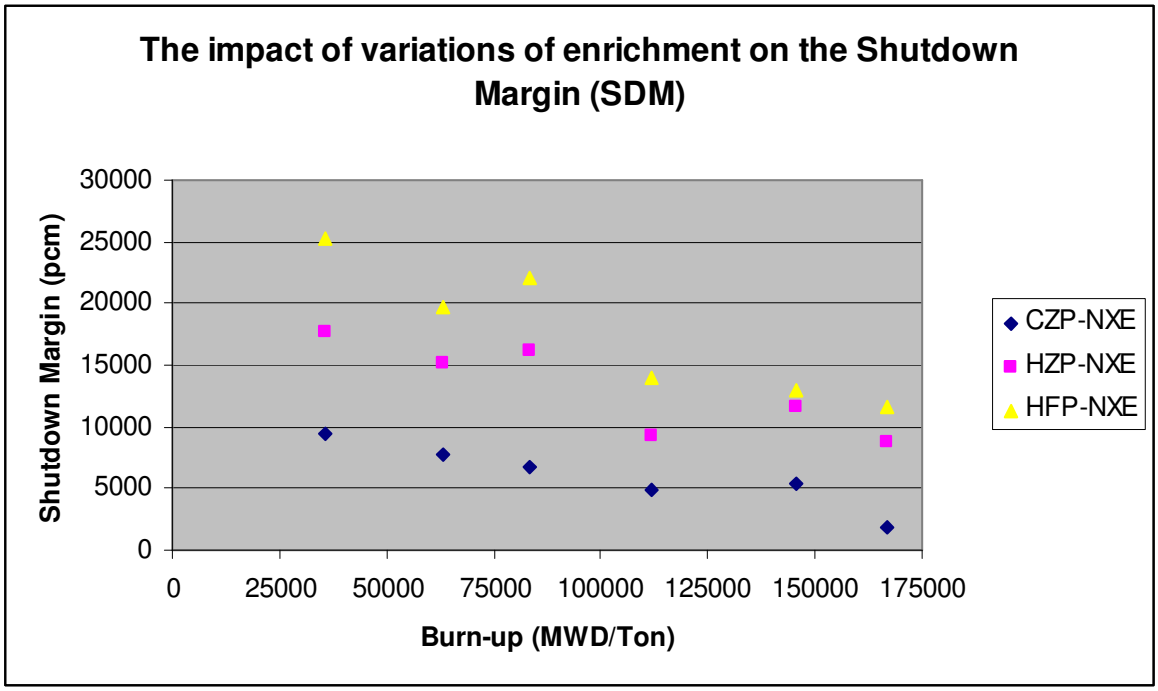

Figure 4.8: The impact of the variation of enrichments on SDM (for 6 grams heavy metal loadings).

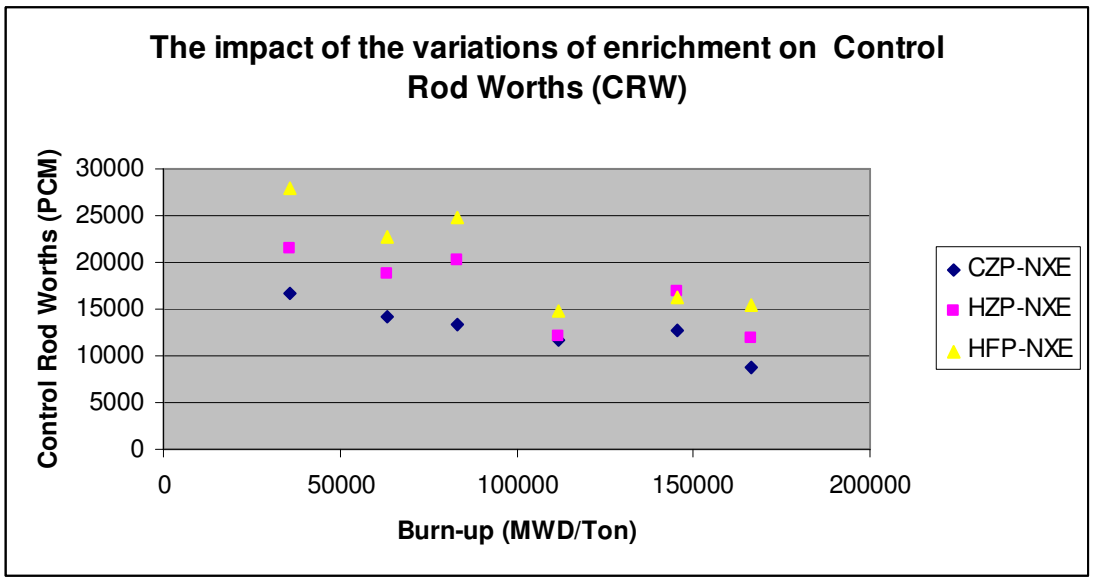

Figure 4.9: The impact of the variation of enrichments on CRW (for 6 grams heavy metal loadings).

4.4.3 The impact of the fuel sphere circulations on reactor safety and economics

Higher enriched fuel has an economic advantage as it results in more energy extracted per fuel element (that is higher burn-up) and it also implies that less new fuel elements will be loaded in the reactor per day in order to maintain the rated power level as compared to at lower enrichment level. This implies that at a fixed fuel sphere circulation value of about six (6 passes) at heavy metal loading of about 6 g per sphere, the total number of fuel spheres reloaded at 6 % enrichment level is about 11167 spheres/day as compared to 2400 spheres/day at 17% enrichment for the same heavy metal loading and the number of passes.

The results in table 4.5 also showed that at fixed enrichment and heavy loading level, the variations of number of passes does improve the economics (burn-up). For example, a 2 % increase in burn-up was observed when the number of passes was increased by factor of 2.5 (91831 versus 89660 MWd/Ton). The results also showed some improvements in the shut down margin to be specific, the margin has increased from 4568.6 to 8613.0 pcm, hence a less reactive core. The results also show a decrease in power peaking factor and maximum power per sphere and these are desirable features in terms of safety.

Parameters	**Units**	**Limits**	**Number of Passes 15**	**Number of Passes 10**	**Number of Passes 6**
K-eff	-	-	1.0003	0.9997	1.0002
Burn-up	MWD/Ton	120 000	91831	91321	89660
Maximum Fuel temperature	°C	1200	1084	1078	1076
Core power density	MW/m^3	-	10.0	10.35	11.16
Maximum Power Peaking factor	-	-	2.94	3.02	3.16
Maximum power Per sphere	kW/sphere	4.5	2.60	2.68	2.81
K-eff@ARO-CZP-NXE	-	-	1.07050	1.07227	1.07393
K-eff@ARI-CZP-NXE	-	<0.99	0.92070	0.934306	0.95631
SHUT-DOWN MARGIN	pcm	-	8613.0	7031.3	4568.6

pcm refers to percent milli-rho

Table 4.5: Variations of the number of fuel sphere passes for 9.6% enrichment and 9 grams heavy metal loading.

However, the increase in the fuel sphere passes also has some safety implication in terms of graphite dust production in the core. Depending on the type of plant (that is, direct or indirect cycle) this could challenge the plant safety (source term). This dust is expected to be highly contaminated with the radiologically relevant radionuclides such as cesium and silver isotopes. The activity level of cesium increases with an increase in burn-up. Although the amount of dust will be low, the activity level on the dust will be extremely high and safety will be challenged. Again a very high activity level on the dust will be

expected due high temperature as the silver fractional release rate increases with temperature (refer to figure 4.5 above). Note that the number of passes in the core, for example 6 passes is the average since depending on the radial location (see figure 4.10) in the core some of the fuel element will pass through the less than 6 times and others more than 6 times.

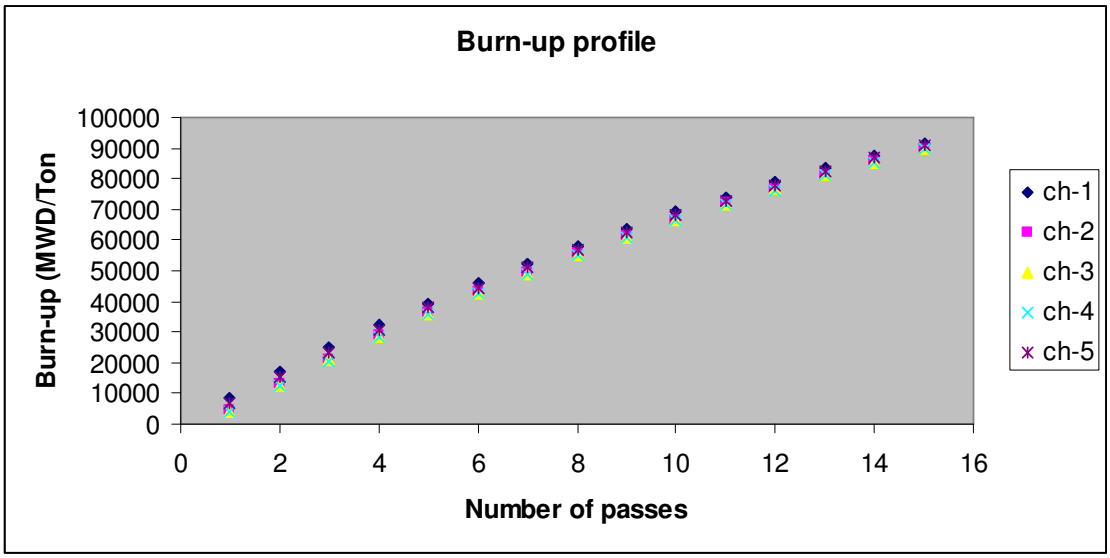

Figure 4.10: The variations of burn-up with number of passes.

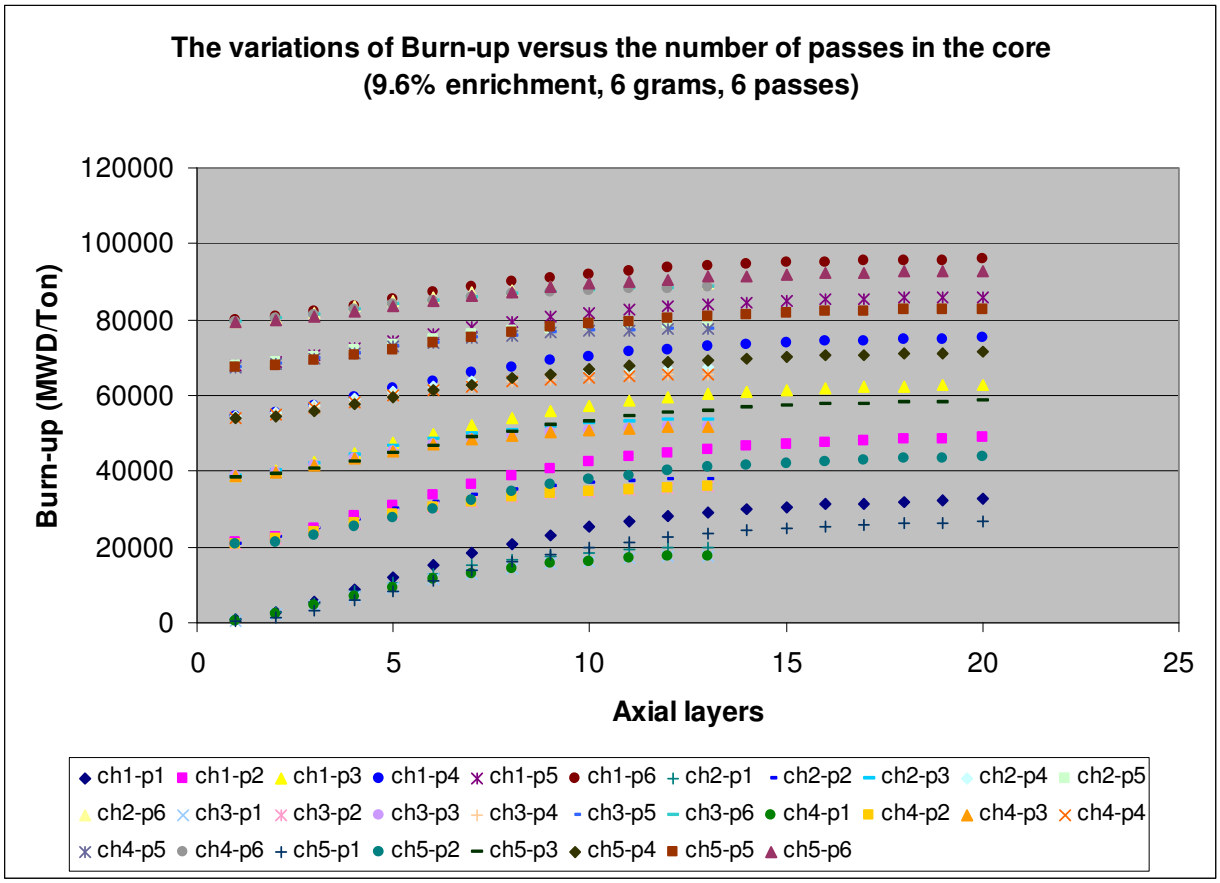

Figure 4.11: The variations of burn-up with number of passes at lower burn-up, where "ch" and "p" refers to channel and pass. For example, ch1-p1 refers to channel number one and p1 refers to the initial pass.

Figure 4.11 show the variations of fuel sphere burn-up in the core for different flow channels (flow lines) in the core. The results from this figure also show that the fuel sphere located at the periphery achieve higher burn-up as compared to fuel in the middle flow channels due to higher thermal neutron flux in the reflector as reflected by channel 1 and channel 5. However, this also implies that fuel spheres located in the middle channels will be circulated in the core more than 6 times and the fuel sphere situated at the periphery will be circulated less than 6 times in the core and on average the number of fuel sphere circulations in the core will be 6.

Chapter 5

Summary and Conclusion

The purpose of the study is to investigate an optimum fuel management scheme with special emphasis on fuel management parameters such as enrichment, heavy metal loadings and the number of passes. Several case studies were selected in order to determine the impact of these fuel management parameters to reactor safety and fuel economics. The reactor physics or reactor safety parameters that were affected by the variation of the fuel management parameters are parameters such as fuel temperature, power peaking, burn-up and shut-down margins. As already described and reported in table 4.4, the results showed that indeed the variation of fuel management parameters such as heavy metal loadings, enrichment and number of passes have an impact on safety and economics and a careful selection of a combination of these parameters can improve the fuel economy and hence reduce the energy costs for the utility. For example, these results have shown that the increase in heavy metal loadings as an example, can improve the fuel economics to a certain extent. To be specific, the increase in heavy metal loadings beyond 9 gram results in slightly lower burn-up and this does not add any value in term of the economics and may be mainly due to the reduced moderating ratio which results in a higher absorption in the fuel (the fuel will start to compete with other material for neutron absorption).The optimum burn-up is achieved at a heavy metal loading of about 9 grams per fuel element. And furthermore in terms of safety, although the increase in heavy metal loading also results in an increase in temperature and reduced shutdown margin, however due to the improvement in fuel economics the heavy metal loadings of 9 grams is recommended.

The second parameter investigated is enrichment variation, this parameter results in improved fuel economics provided the integrity of the fuel can be retained. In terms of economics, higher enrichment results in higher fuel burn–up and lesser fuel loadings since the fuel spheres stay longer in the core. This reduces the costs of power production and also improves the fuel economy (this is desirable factor in terms of the fuel economics). On the other hand, higher burn-up produces more actinides and fission products with large thermal neutron capture cross sections and hence reduces the control rods worth. That is, using the burn-up values which corresponds to 17 % enrichment with heavy metal loadings of 6 and 9 gram gives the control rods worth of about 8700 and 8300 pcm respectively. However, the increased enrichment can also result in very high temperature and power peaks. Experimental data and literature have shown that these parameters also contribute to failure of SiC which is the retention capability of fission product. Although analyses have shown that the SiC failure was not achieved for normal operation, during the accident condition such as DLOFC the release of fission products is expected since one cannot rule out the failure of SiC during these conditions. The focus should be on the impact to safety of these SiC failures during normal operation and accident conditions. It will have to be proven that failures are only limited to a small fraction of fuel spheres exposed to such temperature and it can be shown that the associated source term analyses for these conditions are within the limit, which is very difficult to demonstrate at this stage since a complete set of analyses is not yet available.

Considering the above mentioned concerns, one could recommend higher enrichment at lower heavy metal loadings of about 7-9 grams provided it can be demonstrated by the fuel qualification programme that the fuel can retain fission products and that the normal operation and accident condition source term limits are complied to. A higher enrichment level such as 15-17% can be opted for provided that the irradiation and test results ensure fuel sphere integrity (fuel qualification programme). PBMR fuel is using the 9.6% enrichment and the burn-up and the maximum power per sphere values at this enrichment level lie within the German experimental data. However, with respect to fuel temperature, the 1600°C limit is exceeded and the German statistical data for temperature above 1600°C is insufficient. And the shut down requirements are also met since it complies with the limits specified in table 4.3. The 9.6% enrichment was considered on condition that PBMR extend the fuel qualification program to cover temperature above 1600°C. Also, to reduce the normal operation fuel failure, the reactor outlet temperature can be reduced to a lower value and this will improve the fission product release during normal operation. However the impact of the reduced reactor outlet temperature as a starting condition to accident analyses may reduce the peak fuel temperature achieved during the accident due cooler reflector since the available heat dissipating from the reactor core will first heat up the core structure. This selected enrichment level will be revised only if positive results are obtained from the fuel qualification programme and taking into consideration the cost implication with respect to higher fuel level (fuel price) . The results from the investigation showed that higher enrichment fuel has an economic advantage as it results in more energy extracted per fuel element (that is higher burn-up) and it also implies that less new fuel elements will be loaded in the reactor per day in order to maintain the rated power level as compared to at lower enrichment level.

The third parameter investigated was the fuel sphere circulation, The results also showed that at a fixed enrichment and heavy metal loading level, the variations of number of passes do improve the burn-up (in directly the economics). For example, a 2 % increase in burn-up was observed when the number of passes were increased by factor of 2.5 (91831 versus 89660 MWd/T) The results also show some improvements in the shut-down margin; to be specific, the margin has increased from 4568.6 to 8613 pcm, hence a less reactive core. The results also show a decrease in power peaking factor and maximum power per sphere and these are desirable features in terms of safety.

However, the increase in the fuel sphere passes also has some safety implication in terms of dust production in the core. Depending on the type of plant (that is, direct or indirect cycle) this could challenge the plant safety (source term). This dust is expected to be highly contaminated with the radiologically relevant radionuclides such as cesium and silver isotopes. The activity level of cesium increases with an increase in burn-up. Although the amount of dust will be low, the activity level on the dust is expected to be extremely high and safety will be challenged. Again a very high activity level on the dust will be expected due high temperature as the silver fractional release rate increases with temperature (figure 4.5).

However, the above mentioned findings also require further verification of the safety aspect from the fuel qualification programme. Based on the outcome of this thesis and as

a follow up project of this thesis, it would be very interesting to perform analyses by making use of software /codes such as PANAMA, GETTER, NOBLEG,[48] etc in order to determine the impact of increased fuel temperature, power peaking and burn-up to safety and fuel performance. That is, the determination of fuel failure fractions and their impact on fission product releases and further validation of these analyses will be revealed by the fuel irradiation test programme. The outcome of this study as well as the outcome from the fuel qualification programme will then provide a basis for selecting a specific optimal fuel management scheme which is at present slightly difficult without these results.

The current experimental data and analyses from this dissertation show that a viable fuel management scheme would be the scheme that utilizes the enrichment less than 9.6%, 6 passes and heavy metal loading of about 9 grams mainly due to temperature constraints. Unless the new experimental data from the fuel qualification programme can show a reduction in fuel sphere failures at very high temperature, enrichment greater than 8% is not recommended for the 400 MW PBMR core design. Higher enrichment level such as 9.6% and 12% can only be recommended if the fuel qualification tests results show major reduction in coated particle failures at very high temperatures and if PBMR can demonstrate that the source term associated with this high temperature and fuel failure meet the regulatory requirements with sufficient margin. On condition that PBMR would demonstrate that the regulatory requirements in terms of the public and worker dose and release to the public then the fuel management scheme which utilizes the heavy metal loading of about 9 g, six passes and an enrichment level of about 12% can be considered. This is mainly due to the fact that this option complies with some of the fuel performance limits specified by Nabielek et.al [51] and Röllig K [50] except for fuel temperatures. However, PBMR has implemented the fuel qualification program will cater for temperature up to 1800°C. This option will be revisited once the operational data and experimental data become available. PBMR fuel spheres are in the process of being tested in USA (Oak Ridge and at the nuclear test reactor in Russia, Zarechney). In order to comply with all of the requirement limits specified by Nabielek et.al, the enrichment level for the PBMR fuel must be reduced to below 9.6%. Due to some of the above mentioned constraints on the design, PBMR has proposed changes to their plant design from direct to indirect (steam generation plant) and the power level was reduced from 400 to 200 MW.

Bibliography

1. **Kikstra J.F and Verkooijeu A.H.M,** "Conceptual design for energy conversion system of nuclear gas turbine cogeneration plant", 2000, Proceedings of the Institute of Mechanical Engineers part A, Journal of Power and Energy, Vol 214, page 401-411 or **Keller C**, "Forty year experience on closed cycle gas turbines"1978, Annals of Nuclear Energy, Vol.5, page 405 -422, Great Britain.

2. **IAEA Techdoc-1238,** "Development history of gas turbine modular reactor", report of a technical committee meeting held in Palo Alto, USA, 14-16 November 2000, page 1-38.

3. **IAEA Techdoc-1249 (advance electronic),"**Critical experiments and reactor physics calculation for low enriched high temperature gas cooled reactors, Vienna, 2001, page 7-13.

4. **Idaho National Engineering and Environmental laboratory,** "Idaho National Engineering and Environmental Laboratory Next Generation Nuclear Plant Research and Development Program Plan", 2005.

5. **Brinkmann, G. et al**." Important viewpoints proposed for a safety approach of the HTGR in Europe final results of the EC-funded HTR-L project", 2006, Nuclear Engineering and Design 236(2006).

6. **Nuclear Energy Advisory Committee and Generation IV International Forum**, "A Technology Roadmap for Generation IV Nuclear Energy Systems", 2002.

7. **Viljoen C.F., Van Rooyen W. J and Mtyobile V**, " The use of CFD in the design of PBMR test facilities", HTR2006 proceeding: 3rd International Topical Meeting on High Temperature Reactor Technology October 1-4 2006, Johannesburg, South Africa.
8. **IAEA Tech-doc 1163(electronic version)**, "Heat transport and afterheat removal for gas cooled reactors under accident conditions", 2000, IAEA, Vienna.

9. **Dudley T, de Villiers P, Wang Z and Luh R**," The thermal-hydraulic model for the PBMR Plant Training Simulator", HTR2006 proceeding: 3rd International Topical Meeting on High Temperature Reactor Technology October 1-4 2006, Johannesburg, South Africa.
10. **Hossain K, Buck M, Said N.B, Bernnat W and Lohnert G**. "Development of a fast 3_d thermal-hydraulic tool for design and safety studies for HTRs", HTR2006 proceedings: 3rd International Topical Meeting on High Temperature Reactor Technology , October 1-4 2006, Johannesburg, South Africa.

11. **Takamatsu K, Nakagawa S and Takeda T**, "Development of core dynamics analysis of coolant reduction tests of HTTR, HTR2006 proceeding: 3rd International

Topical Meeting on High Temperature Reactor Technology, October 1-4 2006, Johannesburg, South Africa.

12. **Kriel W, Kuhr R.W, Mckinnell R. J, Correia M and Greyvenstein R**, "The potential of PBMR for process heat applications", 2006, HTR2006 proceeding: 3rd International Topical Meeting on High Temperature Reactor Technology, October 1-4 2006, Johannesburg, South Africa.

13. **Kuijper, J. C. et al**. "HTGR reactor physics and fuel cycle studies", 2006, Nuclear Engineering and Design 236(2006)

14. **Minatsuki I, Mizokami Y, Oyama S and Ballot B**. "A study on evaluation of indirect cycle plant system of the HTGR" , 2008, Proceedings of the 4th International Topical Meeting on HTR Technology, HTR2008, September 28 to 01 October, 2008, Washington, DC, USA.

15. **Terry, W. K, Gougar H. D and Ougouag A.M**. "Direct deterministic method for neutronics analyses and computation of asymptotic burn-up distribution in a re-circulating pebble bed reactor", 2002, Ann. Nucl. Energy 29 (11), 1345-1364

16. **Kendall J.M and Bullock R.E.** "Advanced coated particle option", 2004, the 2nd International Topical meeting on High Temperature Reactor Technology, September 22-24, Beijing, CHINA.

17. **Pirson J, Ehster R, Dominguez M.T, Mansani L., Coe I, Brinkmann G, Moormann R, Van Der Mheen W.** "Important viewpoints proposed for safety approach of the HTGR reactors in Europe",12th international conference on Emerging Nuclear Energy System (ICENES'2005), Brussel, Belguim, August 21-26, 2005.

18. **Stacey W, M**."Nuclear Reactor Physics", 2001, John Wiley & Sons Inc.

19. **Slabber J**, "PBMR Safety Design Approach",Nuclear Plant Safety Course (presentation), 2008, NECSA, South Africa.

20. **Fachinger J, et al**. "Examination of dust in the AVR pipe component, Proceedings of the 4th International Topical Meeting on HTR Technology", HTR2008, September 28 to 01 October, 2008, Washington, DC, USA.

21. **Moormann R. "**Safety re-evaluation of the AVR Pebble Bed Beactor operation and its consequence for the future HTR", Proceedings of the 4th International Topical Meeting on HTR technology, HTR2008, September 28 to 01 October, 2008, Washington, DC, USA.

22. **HRB.** "The commissioning of the THTR 300, A Performance Report, 1988, Germany.

23. **Grambow B, Abdelous A, Greneche D, Mouliney M.H, Fachinger J, Bukaemskiy A, Neumann S and Titov M**, "Study of various options for final disposal of HTR coated particles", HTR2006 proceeding: 3rd International Topical meeting on High Temperature Reactor technology, October 1-4 2006, Johannesburg, South Africa.

24. **Petrunin V.V, Kodochigov N. G, Sukharev Y. P, Osipov S.L and Marova E.L**. "Analysis of the HTGR proliferation resistance, Proceedings of the 4th International Topical Meeting on HTR Technology", HTR2008 September 28 to 01 October, 2008, Washington, DC, USA.

25. **Sen S, Albernoz F and Reitsma F**, "Comparison of the V.S.O.P and MCNP results of PBMR equilibrium core model", 2006, HTR2006 proceeding: 3rd International Topical Meeting on High Temperature Reactor Technology , October 1-4 2006, Johannesburg, South Africa.

26. **Dudley T, Tsoai O and Mulder E,**"The reactor neutronic model for the PBMR Plant Training Simulator", HTR2006 proceeding: 3rd International Topical Meeting on High Temperature Reactor Technology October 1-4 2006, Johannesburg, South Africa

27. **Duderstadt J J and Hamilton LJ,** "Nuclear reactor physics", 1976, John Wiley and Sons, Inc.

28. **Leppanën J,** "Monte Carlo Burn-up Calculation", Department of Engineering Physics and mathematics, Helsinki University of Technology, 26th April 2002.

29. **Shulltis JK and Faw RE,**" Radiation and Shielding" 2000, American Nuclear Society, Inc.

30. **Reitsma F and Naidoo D**."Evaluating the control rod modelling approach used in the South African PBMR; Comparison of V.S.O.P calculations with ASTRA Experiments", 2003, Nuclear Engineering and Design 2794.

31. **McLane V,** "ENDF-102 data formats and procedures for the evaluated Nuclear data file ENDF-6", 2001, Cross Section Evaluation Working Group (CSEWG).

32. **Cullen DE**, "Point2004, a temperature dependent ENDF/B-IV, release 8 cross section library", 2004, Lawrence Livermore National Laboratory.

33. **Graves HW Jr**." Nuclear Fuel management", 1979, John Wiley and Sons Inc.

34. **Honeck H. C.** "THERMOS- A thermalization transport code for reactor lattice calculation", Brookhaven National Laboratory, USA, BNL-5826.

35. **IAEA SAFETY STANDARD SERIES,** "Safety of Nuclear Power Plants: Design Requirements No. NS-R-1", 2000, Vienna.

36. **Strydom G**, "Xenon induced spatial power oscillation in the 400MW PBMR", 2006, HTR2006 proceedings: 3rd International Topical meeting on High Temperature Reactor technology October 1-4 2006, Johannesburg, South Africa.

37. **Mulder E.** "CRP-5 Benchmark definition: PBMR 400 Neutronic and Thermal Hydraulic description, 2003, document number: 022017, Revision 1.

38. **Teuchert E, Hansen U and Haas K.A**, "V.S.O.P computer code system for reactor physics and fuel cycle simulation ", March 1980, Kernforschungsanlage Jülich, Jül-1649.

39. **Reitsma F, Rütten H. J and Scherer W.**" An overview of the FZJ-Tools for HTR core design and reactor dynamics", 2005, past present and the future.

40. **Von Lensa W., Ohlig U., Ruetten H. J, Brockmann H., Raesaet X., Damian F., Dolci F., Bernnat W., Kuijper J.C, De Haas J. B. M, Kloosterman J. L, Cerullo N., Lomonaco G., Negrini A., Brinkmann G, Feltes W, Magill J, Bonin B, Greneche D, and Abram T**. "The European programme on HTR nuclear physics, waste and fuel cycle studies", International Congress on Advances in Nuclear power Plants, ICAPP'03, May 4-7, 2003, Congress Palais, Córdoba, Spain.

41. **Viljoen C.F, Sen S, Reitsma F, Ubbink O., Pohl P and Barnet H**, "The re-evaluation of the AVR melt wire experiment using modern methods with specific focus on bounding the bypass flow effects, Proceedings of the 4th International Topical Meeting on HTR Technology", HTR2008 September 28 to 01 October, 2008, Washington, DC, USA.

42. **Sen S,** "Stochastic method to simulates the reloading of the pebble after a full core reload", HTR2006 proceedings: 3rd International Topical Meeting on High Temperature Reactor Technology, October 1-4 2006, Johannesburg, South Africa.

43. **Teuchert E, Haas K.A, Rütten, Brockmann H, Gerwin H, Ohlig U and Scherer W**. " V.S.O.P. (94) computer code for the reactor physics and fuel cycle simulation input manual", 1994, Jül-2897.

44. **Rütten H.J, Haas K.A, Brockmann H, Ohlig U and Scherer W**. "V.S.O.P (97) Computer code system for reactor physics and fuel cycle simulation; input manual and comments", 1998, Jül-3522.

45. **Nordheim L, W and Kuncir G**. "A program of research and calculations of resonance absorption", 1961, General Atomics, GA-2527.

46. **Adler F.T, Hinman G.W and Nordheim L.W.** The quantitative evaluation of

resonance integral, 1958, p155-171.

47. **Joanou G.D. and Dudek J.S**. GAM-1: A consistent P1 multi-group code for the calculation of fast neutron spectra and multi-group constants, 1961, General Atomics Division, GA1850.

48. **IAEA-TECHDOC-978."** Fuel performance and fission product behavior in gas cooled reactors, 1997.

49. **Minato K and Fukuda K,** "Thermodynamic analyses behavior of HTGR fuel and fission product under accidental air or water ingress condition", Japan Atomic Research Institute (JAERI), Tokai, Ibaraki, Japan.

50. **Röllig K and Theyman W.** "Operational requirements of the spherical HTR Fuel elements and their performance, IAEA working group on gas cooled reactors, , 18-21 October, 1983, Moscow, USSR.

51. **Nabielek H, Teuchert E and Feltes W,** "Technologische Grenzen bei der auslegung des HTR-brennstoffzyklus", 1982, KFA Julich.

52. **Maki J T, Petti D A, Knudson DL and Miller GK,** "The challenges associated with high burnup, temperature and accelerated irradiation for TRISO-coated particle fuel",2007, Journal of Nuclear Material 371(2007), page 270-280.

53. **Schenk W, Pitzer D and Nabielek H**, "Fission product release profiles from spherical HTR fuel elements at accident temperatures", 1988, KFA Julich Gmbh, Jül-2234.

APPENDICES

Appendix A

V.S.O.P Results on Fuel Management Evaluation Study for the PBMR Core.

Heavy metal Loading	**Core Condition**	**6%**	**8%**	**9.6%**	**12%**	**15%**	**17%**	**Limit**
6 g/sphere	K-eff@ CZP-NXE-ARO	1.07664	1.06967	1.07100	1.07335	1.07874	1.07311	
	K-eff@ HZP-NXE-ARO	1.03722	1.03734	1.04137	1.02790	1.03261	1.03132	
	K-eff@ HFP-NXE-ARO	1.02704	1.03004	1.02797	1.00904	1.01745	1.03883	
	K-eff@ CZP-NXE-ARI	0.913254	0.92835	0.93746	0.95337	0.94894	0.98147	K-eff < 0.99
	K-eff@ HZP-NXE-ARI	0.84914	0.86822	0.86070	0.91475	0.89522	0.91953	
	K-eff@ HFP-NXE-ARI	0.798136	0.83499	0.81895	0.87778	0.88539	0.89533	
	CRW- CZP-NXE-ARO (PCM)	16617	14231	13301	11724	12680	8701	
	CRW- HZP-NXE-ARO PCM	21354	18778	20157	12034	14862	11788	
	CRW- HFP-NXE-ARO PCM	27924	22678	24828	14820	14659	15428	
	SDM- CZP-NXE-ARI PCM	9499	7718	6671	4891	5381	1888	
	SDM- HZP-NXE-ARI PCM	17766	15178	16184	9319	11704	8751	
	SDM- HFP-NXE-ARI PCM	25292	19763	22107	13923	12946	11691	
8 g/sphere	K-eff@ CZP-NXE-ARO	1.07419	1.07162	1.07255	1.07503	1.07431	1.07801	
	K-eff@ HZP-NXE-ARO	1.03845	1.04064	1.04213	1.03259	1.03541	1.03780	
	K-eff@ HFP-NXE-ARO	1.02385	1.02688	1.01217	1.01292	1.01512	1.01807	
	K-eff@ CZP-NXE-ARI	0.93213	0.94431	0.95039	0.97212	0.98073	0.97821	K-eff < 0.99
	K-eff@ HZP-NXE-ARI	0.87461	0.89124	0.88219	0.91351	0.92564	0.93961	
	K-eff@ HFP-NXE-ARI	0.84871	0.86484	0.84498	0.88652	0.90008	0.93162	
	CRW- CZP-NXE-ARO PCM	14188	12580	11984	9847	8882	9464	
	CRW- HZP-NXE-ARO	18039	16108	17397	12624	11453	10069	
	CRW- HFP-NXE-ARO	20155	18246	19548	14076	12591	9115	
	SDB- CZP-NXE-ARI	7281	5897	5220	2867	1965	2228	
	SDB- HZP-NXE-ARI	14336	12203	13354	9468	8033	6427	
	SDB- HFP-NXE-ARI	17825	15628	18345	12800	11101	7339	

Heavy metal Loading	Core Condition	6%	8%	9.6%	12%	15%	17%	Limit
9 g/sphere	K-eff@ CZP-NXE-ARO	1.07619	1.07514	1.07393	1.07622	1.07754	1.07605	
	K-eff@ HZP-NXE-ARO	1.03949	1.04079	1.04213	1.03442	1.03691	1.03789	
	K-eff@ HFP-NXE-ARO	1.02249	1.02018	1.01214	1.01385	1.01652	1.01773	
	K-eff@ CZP-NXE-ARI	0.94156	0.95052	0.95631	0.96521	0.96148	0.98763	K-eff < 0.99
	K-eff@ HZP-NXE-ARI	0.88302	0.88004	0.88973	0.92462	0.93508	0.93619	
	K-eff@ HFP-NXE-ARI	0.85933	0.85001	0.86927	0.91652	0.91880	0.91189	
	CRW- CZP-NXE-ARO (PCM)	13286	12194	11452	10687	11202	8320	
	CRW- HZP-NXE-ARO (PCM)	17046	17550	16436	11480	10502	10647	
	CRW- HFP-NXE-ARO (PCM)	18569	19623	16238	10474	10462	11404	
	SDM- CZP-NXE-ARI (PCM)	6207	5206	4569	3604	4006	1252	
	SDM-HZP-NXE-ARI (PCM)	13247	13631	12393	8152	6943	6816	
	SDM- HFP-NXE-ARI (PCM)	16370	17645	15039	9108	8837	9662	
10 g/sphere	K-eff@ CZP-NXE-ARO	1.07655	1.07521	1.07428	1.07779	1.07846	1.07813	
	K-eff@ HZP-NXE-ARO	1.03999	1.04089	1.03814	1.03540	1.03807	1.03928	
	K-eff@ HFP-NXE-ARO	1.02362	1.02310	1.02123	1.01415	1.01709	1.01848	
	K-eff@ CZP-NXE-ARI	0.93943	0.95729	0.97500	0.97807	0.97642	0.96314	K-eff < 0.99
	K-eff@ HZP-NXE-ARI	0.90380	0.90423	0.90083	0.92273	0.93846	0.93166	
	K-eff@ HFP-NXE-ARI	0.85248	0.88186	0.88007	0.89699	0.93017	0.92774	
	CRW- CZP-NXE-ARO (PCM)	13558	11456	9478	9460	9690	11073	
	CRW- HZP-NXE-ARO (PCM)	14489	14519	14682	11793	10225	11483	
	CRW- HFP-NXE-ARO (PCM)	19612	15654	15706	12882	9188	9603	
	SDM- CZP-NXE-ARI (PCM)	6448	4462	2564	2242	2415	3827	
	SDM- HZP-NXE-ARI (PCM)	10643	10591	11008	8374	6557	7335	

Heavy metal Loading	Core Condition	6%	8%	9.6%	12%	15%	17%	Limit
	SDM- HFP-NXE-ARI (PCM)	17304	13396	13627	11484	7507	7789	
12 g/sphere	K-eff@ CZP-NXE-ARO	1.08371	1.07990	-	1.08048	1.07945	-	
	K-eff@ HZP-NXE-ARO	1.03846	1.03879	-	1.04591	1.03833	-	
	K-eff@ HFP-NXE-ARO	1.01362	1.02183	-	1.02263	1.01711	-	
	K-eff@ CZP-NXE-ARI	0.95707	0.95920	-	0.96191	0.96307	-	K-eff < 0.99
	K-eff@ HZP-NXE-ARI	0.88218	0.92208	-	0.93126	0.92864	-	
	K-eff@ HFP-NXE-ARI	0.85179	0.87856	-	0.91520	0.92485	-	
	CRW- CZP-NXE-ARO PCM	12210	11652	-	11408	11195	-	
	CRW- HZP-NXE-ARO PCM	17059	12184	-	11770	11376	-	
	CRW- HFP-NXE-ARO PCM	18743	15959	-	11478	9808	-	
	SDM- CZP-NXE-ARI PCM	4485	4253	-	3960	3834	-	
	SDM- HZP-NXE-ARI PCM	13356	8450	-	7381	7684	-	
	SDM- HFP-NXE-ARI PCM	17400	13822	-	9265	8125	-	

"-"in table 4.6 implies that the code failed to converge. ARO: All Rods Out; ARI: All Rods, SDM- Shutdown margin, CRW- Control Rods Worths.

Table I: V.S.O.P Results on Fuel Management Evaluation Study for the PBMR Core (SDM & CRW).

Appendix B

List of Abbreviations and Acronyms

AOO	: Anticipated Occupational Occurence
AVR	: Arbeitsgemeinschaft Versuchs Reaktor
CRW	: Control Rod Worths
GT-MHR	: Gas Turbine Modular Helium Reactor
HTGR	: High Temperature Gas Cooled Reactors
HTR	: High Temperature Reactors
HTTR	: High Temperature Test Reactor
INPRO	: International Project on Innovative Nuclear Reactor
KAERI	: Korean Atomic Energy Research Institute
LWR	: Light Water Reactors
NGNP	: Next Generation Nuclear Power Plant
OTTO	: Once Through Then Out
PIE	: Post Irradiation Examination
pcm	: Percent milli-rho (units for reactivity)
PWR	: Pressurized Water Reactors
RCS	: Reactivity Control System
RSS	: Reserve Shutdown System
SAS	: Small Absorber Spheres
SDM	: Shut Down Margin
SiC	: Silicon Carbide
TRISO	:Triple coated Isotropic particle
THTR	: Thorium High Temperature Reactor
VHTR	: Very High Temperature Reactor

Appendix C

This appendix will describe a list of definitions used in the thesis.

List of Definitions

Burn-up	It is the total thermal energy extracted from the fuel, expressed as megawatt-days per metric tonne of (initial) heavy metal (MWD/TU).
Control Rod Worth	It is the difference between the excess reactivity and the minimum reactivity when all control elements are fully inserted.
Excess reactivity	It is the core reactivity present when all the control elements are withdrawn from the reactor core.
Moderating Ratio	It is the ratio between the macroscopic slowing down power to the macroscopic cross section of absorption.
Power Peaking Factor:	It is the ratio between the maximum power density and the average power density in the core.
Shut down Margin:	It is the negative reactivity of the core present when all control elements have been fully inserted to achieve minimum core multiplication.

Appendix D

Typical Example of VSOP Input File:

```
vsop   0   0                                                                S  1
   PBMR 400 MW DP3 Model V1.0.1: 6X Fixed Graphite thesis                   S  2
   03001   0   1                                                            S  3
     1     0    -1     5
     0    20     6
     0    13     6
     0    13     6
     0    13     6
     1    20     6
     1    10.00000     2                                                  BI-3
     1    31.00000     2                                                  BI-3
     1    32.60000     1                                                  BI-3
     1     6.95000     1                                                  BI-3
     1    11.50000     1                                                  BI-3
     1     6.95000     1                                                  BI-3
     1     1.00000     1                                                  BI-3
     0     9.00000     2                                                  BI-3
     0    12.70000     2                                                  BI-3
     0    12.70000     2                                                  BI-3
     0    16.20000     2                                                  BI-3
     0    12.70000     2                                                  BI-3
     0    12.70000     2                                                  BI-3
     0     9.00000     2                                                  BI-3
     1     1.00000     1                                                  BI-3
     1     6.95000     1                                                  BI-3
     1    11.50000     1                                                  BI-3
     1     6.95000     1                                                  BI-3
     1    13.60000     2                                                  BI-3
     1    18.60000     1                                                  BI-3
     1    17.00000     1                                                  BI-3
     1    14.40000     1                                                  BI-3
     2    12.50000     1                                                  BI-3
     2     5.00000     1                                                  BI-3
     2    17.50000     1                                                  BI-3
     2    18.00000     2                                                  BI-3
     2   134.30000     1                                                  BI-3
     2     1.00000     2                                                  BI-3
    -1                                                                    BI-3
     2     1.00000     2                                                  BI-4
     2   330.00000     1                                                  BI-4
     2    84.00000     2                                                  BI-4
     2   258.00000     1                                                  BI-4
     2    35.00000     1                                                  BI-4
     1    15.00000     1                                                  BI-4
     1    25.00000     1                                                  BI-4
     1    10.00000     1                                                  BI-4
     1    40.80000     2                                                  BI-4
     1    40.00000     3                                                  BI-4
     1    34.50000     1                                                  BI-4
     1    78.50000    -1                                                  BI-4
     0    17.00000     1                                                  BI-4
     0    55.00000     3                                                  BI-4
     0    52.06000     3                                                  BI-4
     0    42.64000     3                                                  BI-4
     0    45.00000     3                                                  BI-4
     0    50.00000     3                                                  BI-4
     0    50.00000     3                                                  BI-4
     0    50.00000     3                                                  BI-4
     0    50.00000     3                                                  BI-4
     0    50.00000     3                                                  BI-4
     0    50.00000     3                                                  BI-4
     0    50.00000     3                                                  BI-4
     0    50.00000     3                                                  BI-4
```

```
    0    50.00000     3                                                    BI-4
    0    50.00000     3                                                    BI-4
    0    50.00000     3                                                    BI-4
    0    50.00000     3                                                    BI-4
    0    50.00000     3                                                    BI-4
    0    50.00000     3                                                    BI-4
    0    50.00000     3                                                    BI-4
    0    50.00000     3                                                    BI-4
    0    38.80000     2                                                    BI-4
    0    54.75000     2                                                    BI-4
    0    54.75000     2                                                    BI-4
    1    60.00000     2                                                    BI-4
    1    22.00000     2                                                    BI-4
    1    15.00000     2                                                    BI-4
    1    45.00000     2                                                    BI-4
    1    60.00000     1                                                    BI-4
    1    15.00000     2                                                    BI-4
    1    15.00000     2                                                    BI-4
    2    75.00000     2                                                    BI-4
    2     5.00000     1                                                    BI-4
    2   120.00000     1                                                    BI-4
    2    72.00000     1                                                    BI-4
    2    23.00000     1                                                    BI-4
    2    25.00000     1                                                    BI-4
    2    12.50000     1                                                    BI-4
    2    51.00000     1                                                    BI-4
    2   200.00000     1                                                    BI-4
    2    69.00000     2                                                    BI-4
    2   110.00000     1                                                    BI-4
    2     1.00000     2                                                    BI-4
   -1                                                                      BI-4
72 45 46 46  4 46 46 46 46 46 46 46 46 46 46 46 15 46 46 46 46 46
72 72 73 73  5 73 73 73 73 73 73 73 73 73 73 73 16 73 73 73 73 73
74 74 75 75  5 75 75 75 75 75 75 75 75 75 75 75 16 75 75 75 75 75
 2 76 77 77  5100100100100100100100100100100100 16140140157168168
 2 76 77 77  5101101118118118118118118118123123 16140140157168168
 2 76 77 77  5101101119119119119119119119123123 16140140157168168
 2 78 79 79  5102102  1  1  1  1  1  1  1124124 17141141158168168
 3 71 70 69  6 68 67  0  0  0  0  0  0  0 66 65 18 64 63 62 61169
 3 80 81 94  7103111  0  0  0  0  0  0  0125133 19142150159 60169
 3 80 81 94  7103111  0  0  0  0  0  0  0125133 20142150159 60169
 3 80 81 94  7103111  0  0  0  0  0  0  0125133 21142150159 60169
 3 80 81 94  7103111  0  0  0  0  0  0  0125133 22142150159 60169
 3 82 83 95  8104112  0  0  0  0  0  0  0126134 23143151160 60169
 3 82 83 95  8104112  0  0  0  0  0  0  0126134 24143151160 60169
 3 82 83 95  8104112  0  0  0  0  0  0  0126134 25143151160 60169
 3 82 83 95  8104112  0  0  0  0  0  0  0126134 26143151160 60169
 3 84 85 96  9105113  0  0  0  0  0  0  0127135 27144152161 60169
 3 84 85 96  9105113  0  0  0  0  0  0  0127135 28144152161 60169
 3 84 85 96  9105113  0  0  0  0  0  0  0127135 29144152161 60169
 3 84 85 96  9105113  0  0  0  0  0  0  0127135 30144152161 60169
 3 86 87 97 10106114  0  0  0  0  0  0  0128136 31145153162 60169
 3 86 87 97 10106114  0  0  0  0  0  0  0128136 32145153162 60169
 3 86 87 97 10106114  0  0  0  0  0  0  0128136 33145153162 60169
 3 86 87 97 10106114  0  0  0  0  0  0  0128136 34145153162 60169
 3 88 89 98 11107115  0  0  0  0  0  0  0129137 35146154163 60169
 3 88 89 98 11107115  0  0  0  0  0  0  0129137 36146154163 60169
 3 88 89 98 11107115  0  0  0  0  0  0  0129137 37146154163 60169
 3 88 89 98 11107115  0  0  0  0  0  0  0129137 38146154163 60169
 3 90 91 99 12108116  0  0  0  0  0  0  0130138 39147155164 60169
 3 90 91 99 12108116  0  0  0  0  0  0  0130138 40147155164 60169
 3 90 91 99 12108116  0  0  0  0  0  0  0130138 41147155164 60169
 3 90 91 99 12109117120120120120120120120131139 42148156165 60169
 3 90 91 99 12109117121121121121121121121131139 42148156165 60169
 3 47 48 48 13 49 49 50 50 50 50 50 50 50 50 51 51 43 52 52166 60169
 3 92 93 93 14110110122122122122122122122132132 44149149166 60169
 3 92 93 93 14110110122122122122122122122132132 44149149166 59169
 3 92 93 93 14110110122122122122122122122132132 44149149166167169
 3 53 54 54 13 55 55 56 56 56 56 56 56 56 57 57 43 58 58166167169
    2 20000  4000     0.00001    34.40000   148.30000
         15          0.
```

```
      .00000   400.00000   700.00000   800.00000   850.00000   875.00000
   900.00000   925.00000   950.00000  1000.00000  1025.00000  1050.00000
  1075.00000  1100.00000  1160.00000
     9.00000     9.00000     9.00000     9.00000     9.00000     9.25000
    10.00000    11.00000    12.00000    15.50000    17.50000    20.50000
    23.50000    27.00000    36.00000
          -1          0.
    35.00000    35.00000    35.00000    35.00000    35.00000    35.00000
    35.00000    35.00000    35.00000    35.50000    35.75000    36.00000
    37.00000    37.50000    40.00000
          -1          0.
    50.00000    50.00000    50.00000    50.00000    50.00000    50.00000
    50.00000    50.00000    50.00000    49.00000    48.50000    48.00000
    47.00000    46.50000    43.00000
          -1          0.
    76.00000    76.00000    76.00000    76.00000    76.00000    75.80000
    75.50000    74.80000    73.70000    70.50000    68.20000    65.60000
    62.50000    58.80000    48.00000
           0          0.
 52   0   1   0                                                          D  1
 87 160  88  35 149  52  54  57  59 151  62 143  64  67  69  75 156  84  D  2
152  89 144  99 154 101 102 103 104 107 148 147 108 109 155 110 111 175  D  2
112 113 116 117 118 120 121 122 130 164  29  26   4   5  23   1          D  2
  $   3   1  250.  170. 2550.                 4.20             2.50      D  3
        40.        400.        720.                                      D  4
 FUEL TYPE 1, FEED-I  LOW ENRICHED12.0GR/KUGEL , E=9.60W %   bum         D  5
  0 101   2   1   1                                                      D  6
     0.096          0.       0.085          1.          0.          0.  D  7
  1   4   3                                                             D  8
0.025      10.4000      0.          0.                                  D  9
0.0095      1.05          0.0040       1.90       0.0035      3.18     D 11
0.0040      1.90                                                        D 11
2.5         3.0         0.0         0.         0.137509                D 12
1.74        1.74        0.          1.                                  D 13
  4    7.270351E-08                                                     D 17
 FUEL TYPE 2,   INITIAL CORE ELEMENTS,  E=4.12W %                       D  5
  0 201   2   1   1                                                      D  6
     0.040          0.       0.085          1.          0.          0.  D  7
  1   4   3                                                             D  8
0.025     10.40000      0.          0.                                  D  9
0.0095      1.05          0.0040       1.90       0.0035      3.18     D 11
0.0040      1.90                                                        D 11
2.5         3.0         0.0         0.         0.137509                D 12
1.74        1.74        0.          1.                                  D 13
  4    7.270351E-08                                                     D 17
 FUEL TYPE 3,  DUMMY ELEMENTS                                           D  5
  0-301   2   1   0                                                     D  6
     0.007          0.       0.085          1.          0.          0.  D  7
  1   4   0                                                             D  8
0.025      10.4000      0.          0.                                  D  9
0.0095      1.05          0.0040       1.90       0.0035      3.18     D 11
0.0040      1.90                                                        D 11
0.0         3.0         0.0         0.          0.                      D 12
0.          1.72        0.0         1.                                  D 13
stop                                                                    D  5
 250   44000  30   5   3   0 100  80                                     V  1
  0   0   0   1                                                         V  2
  1   1   1   2   2   0   0   0      0.0001          0.                 V  6
  101     0     0     1     0                                 0     1 K1 V  7
  101     0     0     2                                             7    V  7
    0     7     0     3                                            13    V  7
    0     7     0     4                                            19    V  7
    0     7     0     5                                            25    V  7
    0     7     0     6                                            31    V  7
    0     7     0     7                                            37    V  7
    0     7     0     8                                            43    V  7
    0     7     0     9                                            49    V  7
    0     7     0    10                                            55    V  7
    0     7     0    11                                            61    V  7
    0     7     0    12                                            67    V  7
    0     7     0    13                                            73    V  7
```

```
     0     7     0    14                                                  79    V  7
     0     7     0    15                                                  85    V  7
     0     7     0    16                                                  91    V  7
     0     7     0    17                                                  97    V  7
     0     7     0    18                                                 103    V  7
     0     7     0    19                                                 109    V  7
     0     7     0    20                                                 115    v  7
     0     1     0    21                                                 121 K2 V  7
     0     7     0    22                                                 127    V  7
     0     7     0    23                                                 133    V  7
     0     7     0    24                                                 139    V  7
     0     7     0    25                                                 145    V  7
     0     7     0    26                                                 151    V  7
     0     7     0    27                                                 157    V  7
     0     7     0    28                                                 163    V  7
     0     7     0    29                                                 169    V  7
     0     7     0    30                                                 175    V  7
     0     7     0    31                                                 181    V  7
     0     7     0    32                                                 187    V  7
     0     7     0    33                                                 193    V  7
     0     1     0    34                                                 199 K3 V  7
     0     7     0    35                                                 205    V  7
     0     7     0    36                                                 211    V  7
     0     7     0    37                                                 217    V  7
     0     7     0    38                                                 223    V  7
     0     7     0    39                                                 229    V  7
     0     7     0    40                                                 235    V  7
     0     7     0    41                                                 241    V  7
     0     7     0    42                                                 247    V  7
     0     7     0    43                                                 253    V  7
     0     7     0    44                                                 259    V  7
     0     7     0    45                                                 265    V  7
     0     7     0    46                                                 271    V  7
     0     1     0    47                                                 277 K4 V  7
     0     7     0    48                                                 283    V  7
     0     7     0    49                                                 289    V  7
     0     7     0    50                                                 295    V  7
     0     7     0    51                                                 301    V  7
     0     7     0    52                                                 307    V  7
     0     7     0    53                                                 313    V  7
     0     7     0    54                                                 319    V  7
     0     7     0    55                                                 325    V  7
     0     7     0    56                                                 331    V  7
     0     7     0    57                                                 337    V  7
     0     7     0    58                                                 343    V  7
     0     7     0    59                                                 349    V  7
     0     1     0    60                                                 355 K5 V  7
     0     7     0    61                                                 361    V  7
     0     7     0    62                                                 367    V  7
     0     7     0    63                                                 373    V  7
     0     7     0    64                                                 379    V  7
     0     7     0    65                                                 385    V  7
     0     7     0    66                                                 391    V  7
     0     7     0    67                                                 397    V  7
     0     7     0    68                                                 403    V  7
     0     7     0    69                                                 409    V  7
     0     7     0    70                                                 415    V  7
     0     7     0    71                                                 421    V  7
     0     7     0    72                                                 427    V  7
     0     7     0    73                                                 433    V  7
     0     7     0    74                                                 439    V  7
     0     7     0    75                                                 445    V  7
     0     7     0    76                                                 451    V  7
     0     7     0    77                                                 457    V  7
     0     7     0    78                                                 463    V  7
     0     7     0    79                                                 469    V  7
     2     0     0    80                                                 475    V 7
Inner Cone
  78    7.214826E-02
  77    5.313491E-09
```

```
     2     0     0    81                                        476    V 7
Outer Cone
  78    7.214826E-02
  77    5.313491E-09
     2     0     0    82                                          1    V 7
Void above core
  78    5.014192E-08
  77    2.088370E-15
     2     0     0    83                                          2    V 7
Central Channel
  78    5.014192E-08
  77    3.692794E-15
     2     0     0    84                                          3    V 7
Central Channel
  78    1.002566E-06
  77    7.383580E-14
     2     0     0    85                                          4    V 7
RSS not in
  78    7.192475E-02
  77    2.995606E-09
     2     0     0    86                                          5    V 7
RSS not in
  78    7.065521E-02
  77    5.203532E-09
     2     0     0    87                                          6    V 7
RSS not in
  78    6.741884E-02
  77    4.965184E-09
     2     0     0    88                                          7    V 7
RSS not in
  78    6.741884E-02
  77    4.965184E-09
     2     0     0    89                                          8    V 7
RSS not in
  78    6.741884E-02
  77    4.965184E-09
     2     0     0    90                                          9    V 7
RSS not in
  78    6.741884E-02
  77    4.965184E-09
     2     0     0    91                                         10    V 7
RSS not in
  78    6.741884E-02
  77    4.965184E-09
     2     0     0    92                                         11    V 7
RSS not in
  78    6.741884E-02
  77    4.965184E-09
     2     0     0    93                                         12    V 7
RSS not in
  78    6.741884E-02
  77    4.965184E-09
     2     0     0    94                                         13    V 7
RSS not in
  78    7.327474E-02
  77    5.396452E-09
     2     0     0    95                                         14    V 7
RSS not in
  78    7.678716E-02
  77    5.655131E-09
     3     0     0    96                                         15    V 7
Control Rod - Inserted
  78    6.956451E-02
  73    6.000000E-06
  77    2.897304E-09
     3     0     0    97                                         16    V 7
Control Rod - Inserted
  78    5.830968E-02
  73    6.000000E-06
  77    4.294323E-09
```

```
     3     0     0    98                                          17    V 7
Control Rod - Inserted
  78    6.956451E-02
  73    6.000000E-06
  77    5.123206E-09
     3     0     0    99                                          18    V 7
Control Rod - Inserted + Top Inlet
  78    6.260896E-02
  73    6.000000E-06
  77    4.610951E-09
     3     0     0   100                                          19    V 7
Control Rod - Inserted
  78    6.956451E-02
  73    6.000000E-06
  77    5.123206E-09
     3     0     0   101                                          20    V 7
Control Rod - Inserted
  78    6.956451E-02
  73    6.000000E-06
  77    5.123206E-09
     2     0     0   102                                          21    V 7
Control Rod - Not in
  78    6.956451E-02
  77    5.123206E-09
     2     0     0   103                                          22    V 7
Control Rod - Not in
  78    6.956451E-02
  77    5.123206E-09
     2     0     0   104                                          23    V 7
Control Rod - Not in
  78    6.956451E-02
  77    5.123206E-09
     2     0     0   105                                          24    V 7
Control Rod - Not in
  78    6.956451E-02
  77    5.123206E-09
     2     0     0   106                                          25    V 7
Control Rod - Not in
  78    6.956451E-02
  77    5.123206E-09
     2     0     0   107                                          26    V 7
Control Rod - Not in
  78    6.956451E-02
  77    5.123206E-09
     2     0     0   108                                          27    V 7
Control Rod - Not in
  78    6.956451E-02
  77    5.123206E-09
     2     0     0   109                                          28    V 7
Control Rod - Not in
  78    6.956451E-02
  77    5.123206E-09
     2     0     0   110                                          29    V 7
Control Rod - Not in
  78    6.956451E-02
  77    5.123206E-09
     2     0     0   111                                          30    V 7
Control Rod - Not in
  78    6.956451E-02
  77    5.123206E-09
     2     0     0   112                                          31    V 7
Control Rod - Not in
  78    6.956451E-02
  77    5.123206E-09
     2     0     0   113                                          32    V 7
Control Rod - Not in
  78    6.956451E-02
  77    5.123206E-09
     2     0     0   114                                          33    V 7
Control Rod - Not in
  78    6.956451E-02
```

```
  77    5.123206E-09
     2     0     0   115                                          34    V 7
Control Rod - Not in
  78    6.956451E-02
  77    5.123206E-09
     2     0     0   116                                          35    V 7
Control Rod - Not in
  78    6.956451E-02
  77    5.123206E-09
     2     0     0   117                                          36    V 7
Control Rod - Not in
  78    6.956451E-02
  77    5.123206E-09
     2     0     0   118                                          37    V 7
Control Rod - Not in
  78    6.956451E-02
  77    5.123206E-09
     2     0     0   119                                          38    V 7
Control Rod - Not in
  78    6.956451E-02
  77    5.123206E-09
     2     0     0   120                                          39    V 7
Control Rod - Not in
  78    6.956451E-02
  77    5.123206E-09
     2     0     0   121                                          40    V 7
Control Rod - Not in
  78    6.956451E-02
  77    5.123206E-09
     2     0     0   122                                          41    V 7
Control Rod - Not in
  78    6.956451E-02
  77    5.123206E-09
     2     0     0   123                                          42    V 7
Control Rod - Not in
  78    7.426341E-02
  77    5.469264E-09
     2     0     0   124                                          43    V 7
Control Rod - Not in
  78    8.940305E-02
  77    6.584251E-09
     2     0     0   125                                          44    V 7
Control Rod - Not in
  78    8.922424E-02
  77    6.571083E-09
     2     0     0   126                                          45    V 7
Top Reflector
  78    8.940305E-02
  77    3.723563E-09
     2     0     0   127                                          46    V 7
Top Reflector
  78    8.940305E-02
  77    3.723563E-09
     2     0     0   128                                          47    V 7
Central Column - Inner Bottom
  78    8.940305E-02
  77    3.723563E-09
     2     0     0   129                                          48    V 7
Central Column - Inner Bottom
  78    8.847203E-02
  77    6.515685E-09
     2     0     0   130                                          49    V 7
Central Column - Bottom
  78    8.228657E-02
  77    6.060145E-09
     2     0     0   131                                          50    V 7
Bottom Reflector - Below core
  78    7.214826E-02
  77    3.004915E-09
     2     0     0   132                                          51    V 7
Bottom Reflector
```

```
  78    8.940305E-02
  77    6.584251E-09
     2     0     0   133                                     52    V 7
Bottom Inner Reflector
  78    8.758128E-02
  77    6.450083E-09
     2     0     0   134                                     53    V 7
Central Column - Inner Bottom
  78    8.940305E-02
  77    3.723563E-09
     2     0     0   135                                     54    V 7
Central Column - Inner Bottom
  78    8.940305E-02
  77    6.584251E-09
     2     0     0   136                                     55    V 7
Central Column - Bottom
  78    8.228657E-02
  77    6.060145E-09
     2     0     0   137                                     56    V 7
Bottom Reflector - Below core
  78    7.214826E-02
  77    3.004915E-09
     2     0     0   138                                     57    V 7
Bottom Reflector
  78    8.940305E-02
  77    6.584251E-09
     2     0     0   139                                     58    V 7
Bottom Inner Reflector
  78    8.758128E-02
  77    6.450083E-09
     2     0     0   140                                     59    V 7
Cold inlet plenum (outer reflector)
  78    8.940305E-05
  77    3.723563E-12
     2     0     0   141                                     60    V 7
Hot Gas Riser Tubes (outer reflector)
  78    6.226922E-02
  77    2.593462E-09
     2     0     0   142                                     61    V 7
Top Inlet plenum (outer reflector)
  78    5.856794E-02
  77    2.439306E-09
     2     0     0   143                                     62    V 7
Top Inlet (outer reflector)
  78    1.848855E-02
  77    7.700328E-10
     2     0     0   144                                     63    V 7
Top Inlet (inner reflector)
  78    8.296603E-02
  77    6.110185E-09
     2     0     0   145                                     64    V 7
Top Inlet (inner reflector)
  78    8.296603E-02
  77    6.110185E-09
     2     0     0   146                                     65    V 7
Top Inlet (inner reflector)
  78    8.208094E-02
  77    6.045001E-09
     2     0     0   147                                     66    V 7
Top Inlet (inner reflector)
  78    8.208094E-02
  77    6.045001E-09
     2     0     0   148                                     67    V 7
Central Column + Top Inlet
  78    4.023137E-02
  77    2.962913E-09
     2     0     0   149                                     68    V 7
Central Column - R3 + Top Inlet
  78    8.461999E-02
  77    6.231994E-09
```

```
     2     0     0   150                                          69    V 7
Central Column - R2 + Top Inlet
  78    8.940305E-02
  77    3.723563E-09
     2     0     0   151                                          70    V 7
Central Column - R1 + Top Inlet
  78    8.820505E-02
  77    3.673667E-09
     2     0     0   152                                          71    V 7
Central Column - R1 + Top Inlet
  78    8.940305E-02
  77    3.723563E-09
     2     0     0   153                                          72    V 7
Top Reflector
  78    8.940305E-02
  77    3.723563E-09
     2     0     0   154                                          73    V 7
Top Reflector
  78    8.940305E-02
  77    3.723563E-09
     2     0     0   155                                          74    V 7
Central Column - Top
  78    6.458476E-02
  77    2.689902E-09
     2     0     0   156                                          75    V 7
Central Column - Top
  78    8.653428E-02
  77    3.604081E-09
     2     0     0   157                                          76    V 7
Central Column - Top
  78    8.940305E-02
  77    3.723563E-09
     2     0     0   158                                          77    V 7
Central Column - Top
  78    8.847203E-02
  77    6.515685E-09
     2     0     0   159                                          78    V 7
Central Column - R1
  78    8.940305E-02
  77    3.723563E-09
     2     0     0   160                                          79    V 7
Central Column - R1
  78    8.847203E-02
  77    6.515685E-09
     2     0     0   161                                          80    V 7
Central Column - R1
  78    8.940305E-02
  77    3.723563E-09
     2     0     0   162                                          81    V 7
Central Column - R1
  78    8.820505E-02
  77    6.496022E-09
     2     0     0   163                                          82    V 7
Central Column - R1
  78    8.940305E-02
  77    3.723563E-09
     2     0     0   164                                          83    V 7
Central Column - R1
  78    8.820505E-02
  77    6.496022E-09
     2     0     0   165                                          84    V 7
Central Column - R1
  78    8.940305E-02
  77    3.723563E-09
     2     0     0   166                                          85    V 7
Central Column - R1
  78    8.820505E-02
  77    6.496022E-09
     2     0     0   167                                          86    V 7
Central Column - R1
  78    8.940305E-02
```

```
  77    3.723563E-09
     2     0     0   168                                          87    V 7
Central Column - R1
  78    8.820505E-02
  77    6.496022E-09
     2     0     0   169                                          88    V 7
Central Column - R1
  78    8.940305E-02
  77    3.723563E-09
     2     0     0   170                                          89    V 7
Central Column - R1
  78    8.820505E-02
  77    6.496022E-09
     2     0     0   171                                          90    V 7
Central Column - R1
  78    8.940305E-02
  77    3.723563E-09
     2     0     0   172                                          91    V 7
Central Column - R1
  78    8.820505E-02
  77    6.496022E-09
     2     0     0   173                                          92    V 7
Central Column - Inner Bottom
  78    8.940305E-02
  77    3.723563E-09
     2     0     0   174                                          93    V 7
Central Column - Inner Bottom
  78    8.913974E-02
  77    6.564860E-09
     2     0     0   175                                          94    V 7
Central Column - R2
  78    8.940305E-02
  77    6.584251E-09
     2     0     0   176                                          95    V 7
Central Column - R2
  78    8.940305E-02
  77    6.584251E-09
     2     0     0   177                                          96    V 7
Central Column - R2
  78    8.940305E-02
  77    6.584251E-09
     2     0     0   178                                          97    V 7
Central Column - R2
  78    8.940305E-02
  77    6.584251E-09
     2     0     0   179                                          98    V 7
Central Column - R2
  78    8.940305E-02
  77    6.584251E-09
     2     0     0   180                                          99    V 7
Central Column - R2
  78    8.940305E-02
  77    6.584251E-09
     2     0     0   181                                         100    V 7
Top Reflector
  78    7.641301E-02
  77    3.182538E-09
     2     0     0   182                                         101    V 7
Central Column - Top
  78    8.461999E-02
  77    6.231994E-09
     2     0     0   183                                         102    V 7
Central Column - Top
  78    8.461999E-02
  77    6.231994E-09
     2     0     0   184                                         103    V 7
Central Column - R3
  78    8.461999E-02
  77    6.231994E-09
     2     0     0   185                                         104    V 7
Central Column - R3
```

```
  78    8.461999E-02
  77    6.231994E-09
     2     0     0   186                                        105    V 7
Central Column - R3
  78    8.461999E-02
  77    6.231994E-09
     2     0     0   187                                        106    V 7
Central Column - R3
  78    8.701152E-02
  77    6.408122E-09
     2     0     0   188                                        107    V 7
Central Column - R3
  78    8.940305E-02
  77    6.584251E-09
     2     0     0   189                                        108    V 7
Central Column - R3
  78    8.228657E-02
  77    6.060145E-09
     2     0     0   190                                        109    V 7
Central Column - R3
  78    8.228657E-02
  77    6.060145E-09
     2     0     0   191                                        110    V 7
Central Column - Bottom
  78    8.225237E-02
  77    6.057626E-09
     2     0     0   192                                        111    V 7
Central Column Core Face
  78    8.457528E-02
  77    6.228702E-09
     2     0     0   193                                        112    V 7
Central Column Core Face
  78    8.457528E-02
  77    6.228702E-09
     2     0     0   194                                        113    V 7
Central Column Core Face
  78    8.457528E-02
  77    6.228702E-09
     2     0     0   195                                        114    V 7
Central Column Core Face
  78    8.698917E-02
  77    6.406476E-09
     2     0     0   196                                        115    V 7
Central Column Core Face
  78    8.940305E-02
  77    6.584251E-09
     2     0     0   197                                        116    V 7
Central Column Core Face
  78    8.227721E-02
  77    6.059456E-09
     2     0     0   198                                        117    V 7
Central Column - Bottom
  78    8.228657E-02
  77    6.060145E-09
     2     0     0   199                                        118    V 7
Top Reflector - Above core
  78    8.519608E-02
  77    3.548346E-09
     2     0     0   200                                        119    V 7
Top Reflector - Above core
  78    8.519608E-02
  77    6.274421E-09
     2     0     0   201                                        120    V 7
Bottom Reflector - Below core
  78    7.214826E-02
  77    3.004915E-09
     2     0     0   202                                        121    V 7
Bottom Reflector - Below core
  78    7.214826E-02
  77    3.004915E-09
```

```
     2     0     0   203                                          122    V 7
Bottom Reflector - Below core
  78    7.214826E-02
  77    3.004915E-09
     2     0     0   204                                          123    V 7
Top Inner Reflector
  78    8.940305E-02
  77    6.584251E-09
     2     0     0   205                                          124    V 7
Top Inner Reflector
  78    8.940305E-02
  77    6.584251E-09
     2     0     0   206                                          125    V 7
Inner Reflector Core Face
  78    8.940305E-02
  77    6.584251E-09
     2     0     0   207                                          126    V 7
Inner Reflector Core Face
  78    8.940305E-02
  77    6.584251E-09
     2     0     0   208                                          127    V 7
Inner Reflector Core Face
  78    8.940305E-02
  77    6.584251E-09
     2     0     0   209                                          128    V 7
Inner Reflector Core Face
  78    8.940305E-02
  77    6.584251E-09
     2     0     0   210                                          129    V 7
Inner Reflector Core Face
  78    8.940305E-02
  77    6.584251E-09
     2     0     0   211                                          130    V 7
Inner Reflector Core Face
  78    8.940305E-02
  77    6.584251E-09
     2     0     0   212                                          131    V 7
Bottom Reflector
  78    8.877941E-02
  77    6.538322E-09
     2     0     0   213                                          132    V 7
Bottom Reflector
  78    8.922424E-02
  77    6.571083E-09
     2     0     0   214                                          133    V 7
Inner Reflector - R1
  78    8.940305E-02
  77    6.584251E-09
     2     0     0   215                                          134    V 7
Inner Reflector - R1
  78    8.940305E-02
  77    6.584251E-09
     2     0     0   216                                          135    V 7
Inner Reflector - R1
  78    8.940305E-02
  77    6.584251E-09
     2     0     0   217                                          136    V 7
Inner Reflector - R1
  78    8.940305E-02
  77    6.584251E-09
     2     0     0   218                                          137    V 7
Inner Reflector - R1
  78    8.940305E-02
  77    6.584251E-09
     2     0     0   219                                          138    V 7
Inner Reflector - R1
  78    8.940305E-02
  77    6.584251E-09
     2     0     0   220                                          139    V 7
Bottom Reflector
  78    8.877941E-02
```

```
  77    6.538322E-09
     2     0     0   221                                    140    V 7
Top Inner Reflector
  78    5.827311E-02
  77    4.291630E-09
     2     0     0   222                                    141    V 7
Top Inner Reflector
  78    8.940305E-02
  77    6.584251E-09
     2     0     0   223                                    142    V 7
Inner Reflector - R2
  78    8.940305E-02
  77    6.584251E-09
     2     0     0   224                                    143    V 7
Inner Reflector - R2
  78    8.940305E-02
  77    6.584251E-09
     2     0     0   225                                    144    V 7
Inner Reflector - R2
  78    8.940305E-02
  77    6.584251E-09
     2     0     0   226                                    145    V 7
Inner Reflector - R2
  78    8.940305E-02
  77    6.584251E-09
     2     0     0   227                                    146    V 7
Inner Reflector - R2
  78    8.940305E-02
  77    6.584251E-09
     2     0     0   228                                    147    V 7
Inner Reflector - R2
  78    8.940305E-02
  77    6.584251E-09
     2     0     0   229                                    148    V 7
Bottom Inner Reflector
  78    8.940305E-02
  77    6.584251E-09
     2     0     0   230                                    149    V 7
Bottom Inner Reflector
  78    8.813118E-02
  77    6.490582E-09
     2     0     0   231                                    150    V 7
Inner Reflector - R3
  78    8.669414E-02
  77    6.384748E-09
     2     0     0   232                                    151    V 7
Inner Reflector - R3
  78    8.669414E-02
  77    6.384748E-09
     2     0     0   233                                    152    V 7
Inner Reflector - R3
  78    8.669414E-02
  77    6.384748E-09
     2     0     0   234                                    153    V 7
Inner Reflector - R3
  78    8.669414E-02
  77    6.384748E-09
     2     0     0   235                                    154    V 7
Inner Reflector - R3
  78    8.669414E-02
  77    6.384748E-09
     2     0     0   236                                    155    V 7
Inner Reflector - R3
  78    8.669414E-02
  77    6.384748E-09
     2     0     0   237                                    156    V 7
Bottom Inner Reflector
  78    8.669414E-02
  77    6.384748E-09
     2     0     0   238                                    157    V 7
Top Outer Reflector
```

```
  78    5.827311E-02
  77    2.427027E-09
     2     0     0   239                                          158    V 7
Top Outer Reflector
  78    8.940305E-02
  77    3.723563E-09
     2     0     0   240                                          159    V 7
Outer Reflector
  78    8.940305E-02
  77    3.723563E-09
     2     0     0   241                                          160    V 7
Outer Reflector
  78    8.940305E-02
  77    3.723563E-09
     2     0     0   242                                          161    V 7
Outer Reflector
  78    8.940305E-02
  77    3.723563E-09
     2     0     0   243                                          162    V 7
Outer Reflector
  78    8.940305E-02
  77    3.723563E-09
     2     0     0   244                                          163    V 7
Outer Reflector
  78    8.940305E-02
  77    3.723563E-09
     2     0     0   245                                          164    V 7
Outer Reflector
  78    8.940305E-02
  77    3.723563E-09
     2     0     0   246                                          165    V 7
Bottom Outer Reflector
  78    8.940305E-02
  77    3.723563E-09
     2     0     0   247                                          166    V 7
Bottom Outer Reflector
  78    8.924757E-02
  77    3.717087E-09
     2     0     0   248                                          167    V 7
Bottom Outer Reflector
  78    8.852202E-02
  77    3.686869E-09
     2     0     0   249                                          168    V 7
Top Outer Reflector
  78    7.088250E-02
  77    2.952197E-09
     2     0     0   250                                         -169    V 7
Outer Outer Reflector
  78    8.897492E-02
  77    3.705732E-09
         1.    1.000+02          0.       0.1                           V 10
   1   1                                                               V 11
   0   1  -1   1   0                                                   V 15
   1                                                                   V 16
   1                                                                   V 17
gam5115        180     3     5     0     0     0                       G  1
         20.          20.          20.          20.          20.          20.    G  2
         20.          20.          20.          20.          20.          20.    G  2
         20.          20.          20.          20.          20.          20.    G  2
         20.          20.          20.          20.          20.          20.    G  2
         20.          20.          20.          20.          20.          20.    G  2
         20.          20.          20.          20.          20.          20.    G  2
         20.          20.          20.          20.          20.          20.    G  2
         20.          20.          20.          20.          20.          20.    G  2
         20.          20.          20.          20.          20.          20.    G  2
         20.          20.          20.          20.          20.          20.    G  2
         20.          20.          20.          20.          20.          20.    G  2
         20.          20.          20.          20.          20.          20.    G  2
         20.          20.          20.          20.          20.          20.    G  2
         20.           0.           0.           0.           0.           0.    G  2
          0.           0.           0.           0.           0.           0.    G  2
```

```
          0.          0.          0.          0.          0.          0.    G  2
          0.          0.          0.          0.          0.          0.    G  2
          0.          0.          0.          0.          0.          0.    G  2
          0.          0.          0.          0.          0.          0.    G  2
          0.          0.          0.          0.          0.          0.    G  2
          0.          0.          0.          0.          0.          0.    G  2
          0.          0.          0.          0.          0.          0.    G  2
          0.          0.          0.          0.          0.          0.    G  2
          0.          0.          0.          0.          0.          0.    G  2
          0.          0.          0.          0.          0.          0.    G  2
          0.          0.          0.          0.          0.          0.    G  2
          0.          0.          0.          0.          0.          0.    G  2
          0.          0.          0.          0.          0.          0.    G  2
          0.          0.          0.          0.          0.          0.    G  2
          0.          0.          0.          0.          0.          0.    G  2
          0.          0.          0.          0.          0.          0.    G  2
          0.          0.          0.          0.          0.          0.    G  2
          0.          0.          0.          0.          0.          0.    G  2
          0.          0.          0.          0.          0.          0.    G  2
          0.          0.          0.          0.          0.          0.    G  2
          0.          0.          0.          0.          0.          0.    G  2
          0.          0.          0.          0.          0.          0.    G  2
          0.          0.          0.          0.          0.          0.    G  2
          0.          0.          0.          0.          0.          0.    G  2
          0.          0.          0.          0.          0.          0.    G  2
          0.          0.          0.          0.          0.          0.    G  2
          0.          0.          0.          0.                            G  2
     1     1     1     1     1     1     1     1     1     1     1     1    G  3
     1     1     1     1     1     1     1     1     1     1     1     1    G  3
     1     1     1     1     1     1     1     1     1     1     1     1    G  3
     1     1     1     1     1     1     1     1     1     1     1     1    G  3
     1     1     1     1     1     1     1     1     1     1     1     1    G  3
     1     1     1     1     1     1     1     1     1     1     1     1    G  3
     1     1     1     1     1     1     1     2     2     2     2     2    G  3
     3     2     2     2     2     2     2     2     2     3     2     3    G  3
     2     2     2     2     2     2     2     2     2     2     2     2    G  3
     2     2     2     2     2     2     2     2     2     2     2     2    G  3
     2     2     2     3     2     3     3     3     3     3     3     3    G  3
     3     3     3     3     2     2     2     2     2     2     2     2    G  3
     2     2     2     2     2     2     2     2     2     2     2     2    G  3
     2     2     2     2     2     2     2     2     2     2     2     2    G  3
     2     2     2     2     2     2     2     2     2     2     2     2    G  3
     2     2     2     2     2     2     2     2     2     2     2     2    G  3
     2     2     2     2     2     2     2     2     2     2     2     2    G  3
     2     2     2     2     2     2     2     2     2     2     2     2    G  3
     2     2     2     2     2     2     2     2     2     2     2     2    G  3
     2     2     2     2     2     2     2     2     2     2     2     2    G  3
     2     2     2     2     2     2     2     2     2     2                G  3
     0.        0.            1                                              G  4
   232                                                                      G  5
   232                                                                      G  5
     0.               0.     6                                              G  4
120020120400120700121000121300121600                                        G  5
120021120401120701121001121301121601                                        G  5
     0.               0.     3                                              G  4
170020171000171600                                                          G  5
170021171001171601                                                          G  5
     0.        0.            1                                              G  4
   232                                                                      G  5
   232                                                                      G  5
    -1.       -1.            1                                              G  4
   238                                                                      G  5
   238                                                                      G  5
    -1.       -1.            1                                              G  4
   242                                                                      G  5
   242                                                                      G  5
     0.        0.            1                                              G  4
   232                                                                      G  5
   232                                                                      G  5
    -1.       -1.            1                                              G  4
   238                                                                      G  5
```

```
   238                                                                      G  5
    -1.       -1.          1                                                G  4
   242                                                                      G  5
   242                                                                      G  5
     100000.        29.        1.86                                         G  6
therm1515       3     1     1    17     0     0                             T  1
  1600  1601  1602  1603  1604  1605  1606  1607  1608  1609  1610  1611    T  3
  1612  1613  1614  1615  1616                                              Ts 3
         20.         20.         20.         20.         20.         20.    T  4
         20.         20.         20.         20.         20.         20.    T  4
         20.         20.         20.         20.         20.         20.    T  4
         20.         20.         20.         20.         20.         20.    T  4
         20.         20.         20.         20.         20.         20.    T  4
         20.         20.         20.         20.         20.         20.    T  4
         20.         20.         20.         20.         20.         20.    T  4
         20.         20.         20.         20.         20.         20.    T  4
         20.         20.         20.         20.         20.         20.    T  4
         20.         20.         20.         20.         20.         20.    T  4
         20.         20.         20.         20.         20.         20.    T  4
         20.         20.         20.         20.         20.         20.    T  4
         20.         20.         20.         20.         20.         20.    T  4
         20.         20.         20.         20.         20.         20.    T  4
         20.         20.         20.         20.         20.         20.    T  4
         20.         20.         20.         20.         20.         20.    T  4
         20.         20.         20.         20.         20.         20.    T  4
         20.         20.         20.         20.         20.         20.    T  4
         20.         20.         20.         20.         20.         20.    T  4
         20.         20.         20.         20.         20.         20.    T  4
         20.         20.         20.         20.         20.         20.    T  4
         20.         20.         20.         20.         20.         20.    T  4
         20.         20.         20.         20.         20.         20.    T  4
         20.         20.         20.         20.         20.         20.    T  4
         20.         20.         20.         20.         20.         20.    T  4
         20.         20.         20.         20.         20.         20.    T  4
         20.         20.         20.         20.         20.         20.    T  4
         20.         20.         20.         20.         20.         20.    T  4
         20.         20.         20.         20.         20.         20.    T  4
         20.         20.         20.         20.         20.         20.    T  4
         20.         20.         20.         20.         20.         20.    T  4
         20.         20.         20.         20.         20.         20.    T  4
         20.         20.         20.         20.         20.         20.    T  4
         20.         20.         20.         20.         20.         20.    T  4
         20.         20.         20.         20.         20.         20.    T  4
         20.         20.         20.         20.         20.         20.    T  4
         20.         20.         20.         20.         20.         20.    T  4
         20.         20.         20.         20.         20.         20.    T  4
         20.         20.         20.         20.         20.         20.    T  4
         20.         20.         20.         20.         20.         20.    T  4
         20.         20.         20.         20.         20.         20.    T  4
         20.         20.         20.         20.                            T  4
  1121  1122  1123  1124  1125  1126  1127  1128                            T  3

         20.         20.         20.         20.         20.         20.    T  4
         20.         20.         20.         20.         20.         20.    T  4
         20.         20.         20.         20.         20.         20.    T  4
         20.         20.         20.         20.         20.         20.    T  4
         20.         20.         20.         20.         20.         20.    T  4
         20.         20.         20.         20.         20.         20.    T  4
         20.         20.         20.         20.         20.         20.    T  4
         20.         20.         20.         20.         20.         20.    T  4
         20.         20.         20.         20.         20.         20.    T  4
         20.         20.         20.         20.         20.         20.    T  4
         20.         20.         20.         20.         20.         20.    T  4
         20.         20.         20.         20.         20.         20.    T  4
         20.         20.         20.         20.         20.         20.    T  4
         20.          0.          0.          0.          0.          0.    T  4
          0.          0.          0.          0.          0.          0.    T  4
          0.          0.          0.          0.          0.          0.    T  4
          0.          0.          0.          0.          0.          0.    T  4
          0.          0.          0.          0.          0.          0.    T  4
          0.          0.          0.          0.          0.          0.    T  4
```

```
         0.        0.        0.        0.        0.        0.   T  4
         0.        0.        0.        0.        0.        0.   T  4
         0.        0.        0.        0.        0.        0.   T  4
         0.        0.        0.        0.        0.        0.   T  4
         0.        0.        0.        0.        0.        0.   T  4
         0.        0.        0.        0.        0.        0.   T  4
         0.        0.        0.        0.        0.        0.   T  4
         0.        0.        0.        0.        0.        0.   T  4
         0.        0.        0.        0.        0.        0.   T  4
         0.        0.        0.        0.        0.        0.   T  4
         0.        0.        0.        0.        0.        0.   T  4
         0.        0.        0.        0.        0.        0.   T  4
         0.        0.        0.        0.        0.        0.   T  4
         0.        0.        0.        0.        0.        0.   T  4
         0.        0.        0.        0.        0.        0.   T  4
         0.        0.        0.        0.        0.        0.   T  4
         0.        0.        0.        0.        0.        0.   T  4
         0.        0.        0.        0.        0.        0.   T  4
         0.        0.        0.        0.        0.        0.   T  4
         0.        0.        0.        0.        0.        0.   T  4
         0.        0.        0.        0.        0.        0.   T  4
         0.        0.        0.        0.        0.        0.   T  4
         0.        0.        0.        0.                       T  4
 1101 1102 1103 1104 1105                                       T  3
                                                                T  3
        20.       20.       20.       20.       20.       20.   T  4
        20.       20.       20.       20.       20.       20.   T  4
        20.       20.       20.       20.       20.       20.   T  4
        20.       20.       20.       20.       20.       20.   T  4
        20.       20.       20.       20.       20.       20.   T  4
        20.       20.       20.       20.       20.       20.   T  4
        20.       20.       20.       20.       20.       20.   T  4
        20.       20.       20.       20.       20.       20.   T  4
        20.       20.       20.       20.       20.       20.   T  4
        20.       20.       20.       20.       20.       20.   T  4
        20.       20.       20.       20.       20.       20.   T  4
        20.       20.       20.       20.       20.       20.   T  4
        20.       20.       20.       20.       20.       20.   T  4
        20.       20.       20.       20.       20.       20.   T  4
        20.       20.       20.       20.       20.       20.   T  4
        20.       20.       20.       20.       20.       20.   T  4
        20.       20.       20.       20.       20.       20.   T  4
        20.       20.       20.       20.       20.       20.   T  4
        20.       20.       20.       20.       20.       20.   T  4
        20.       20.       20.       20.       20.       20.   T  4
        20.       20.       20.       20.       20.       20.   T  4
        20.       20.       20.       20.       20.       20.   T  4
        20.       20.       20.       20.       20.       20.   T  4
        20.       20.       20.       20.       20.       20.   T  4
        20.       20.       20.       20.       20.       20.   T  4
        20.       20.       20.       20.       20.       20.   T  4
        20.       20.       20.       20.       20.       20.   T  4
        20.       20.       20.       20.       20.       20.   T  4
        20.       20.       20.       20.       20.       20.   T  4
        20.       20.       20.       20.       20.       20.   T  4
        20.       20.       20.       20.       20.       20.   T  4
        20.       20.       20.       20.       20.       20.   T  4
        20.       20.       20.       20.       20.       20.   T  4
        20.       20.       20.       20.       20.       20.   T  4
        20.       20.       20.       20.       20.       20.   T  4
        20.       20.       20.       20.       20.       20.   T  4
        20.       20.       20.       20.       20.       20.   T  4
        20.       20.       20.       20.       20.       20.   T  4
        20.       20.       20.       20.       20.       20.   T  4
        20.       20.       20.       20.       20.       20.   T  4
        20.       20.       20.       20.                       T  4
        4.0  26                                                 T  5
    3    1    1    1    1    1    1    1    1    1    1    1
    1    1    1    1    1    1    1    1    1    1    1    1
    1    1    1    1    1    1    1    1    1    1    1    1
```

```
     1     1     1     1     1     1     1     1     1     1     1     1
     1     1     1     1     1     1     1     1     1     1     1     1
     1     1     1     1     1     1     1     1     1     1     1     1
     1     1     1     1     1     1     1     1     2     2     2     2
     2     3     2     2     2     2     2     2     2     2     3     2
     3     2     2     2     2     2     2     2     2     2     2     2
     2     2     2     2     2     2     2     2     2     2     2     2
     2     2     2     2     3     2     3     3     3     3     3     3
     3     3     3     3     3     3     3     3     2     2     2     2
     2     2     2     2     2     2     2     2     2     2     2     2
     2     2     2     2     2     2     2     2     2     2     2     2
     2     2     2     2     2     2     2     2     2     2     2     2
     2     2     2     2     2     2     2     2     2     2     2     2
     2     2     2     2     2     2     2     2     2     2     2     2
     2     2     2     2     2     2     2     2     2     2     2     2
     2     2     2     2     2     2     2     2     2     2     2     2
     2     2     2     2     2     2     2     2     2     2     2     2
     2     2     2     2     2     2     2     2     2     2     2     2
     2     2     2     2     2     2     2     2     2     2     2     2
     2     2     2     2     2     2     2     2     2     2     2     2
     2     2     2     2     2     2     2     2     2     2     2     2
     2     2     2     2     2     2     2     2     2     2     2          T  6
     1   1.5  0.61   1.0    1.   -1.    1.                                 T  7
11111111122222220000                                                      T  8
    4   01  -2.0   0.0    0.                                              T 10
    6   00  -1.0   0.     1.                                              T 10
   26   01   1.0   0.0    0.                                              T 10
  130   01  -2.0   0.0    0.                                              T 10
 1001   01  -2.0   0.0    0.                                              T 10
-1003   01   0.0   1.     0.                                              T 10
    1    2.0   1.0   0.0    1.    0.    0.                                T  7
11110000000000000000                                                      T  8
         5.0                                                              T  9
   -4   00   1.                                                          T 10
    1    2.0   1.0   0.0    1.    0.    0.                                T  7
11110000000000000000                                                      T  8
         5.0                                                              T  9
   -4   00   1.                                                          T 10
CITATION-SECTION, CARDS "C"                                               C  1
001                                                                       C  2
  0  0 -1                                                                 C  3
  0  0  0  0  0  2  0  0                                                  C  4
999 60 30                                                                 C  5
         2.5         0.5                                                  C  6
003                                                                       C  7
     1     0     0     0     0     0     0     1     0    -1     1          C  8
      1.0099       0.099                                                  C  9
          0.          0.          0.                                      C 10
     3     3                                                              C 11
   1 169 169   2 170 171   3 227 227                                      C 12
        42.5          0.          0.          0.                         C 13
                                                                          C 14
                                                                          C 15
                                                                          C 15
                                                                          C 15
                                                                          C 15
    0.100677    0.536656          0.  0                                   C 16
         5.0          0.          0.          0.                         C 13
                                                                          C 14
                                                                          C 15
                                                                          C 15
                                                                          C 15
                                                                          C 15
    0.017147    0.665097          0.  0                                   C 16
         8.5          0.          0.          0.                         C 13
                                                                          C 14
                                                                          C 15
                                                                          C 15
                                                                          C 15
                                                                          C 15
    0.057687    0.608499          0.  0                                   C 16
2006   0 240   3   0   0   0   0   0   $1000MILL                          K  1
        0.80        0.40         30.          1.                         K  2
        0.04        0.04        0.04        0.04        0.04        0.04  K  3
        0.02        1.00        1.00         0.0        0.00              K  4
```

```
     30.00        6.2         140.      0.0025        0.00        0.00    K  5
     30.00       -1.25        -0.5                                       K  6
        6.        0.10          0.         -1.         -1.           TP1 K  7
       0.0         1.0         1.0       1.000                          K  8
      360.        360.        360.        360.        360.              K  9
      360.        360.        360.                                       K 10
        6.        0.10          0.         -1.         -1.           TP2 K  7
       0.0         1.0         1.0       1.000                          K  8
      360.        360.        360.        360.        360.              K  9
      360.        360.        360.                                       K 10
        6.        0.10          0.         -1.         -1.           TP3 K  7
       0.0         1.0         1.0       1.000                          K  8
      360.        360.        360.        360.        360.              K  9
      360.        360.        360.                                       K 10
      1.        0.        0.      365.       0.8        0.        0.      R  2
   1    1.  E+00  -101                 EQUILIBR.- ELEMENT                 R  3
   2    1.  E+00  -201                 INITIAL- ELEMENTS                  R  3
   3    1.  E+00  -301                 DUMMY ELEMENTS                     R  3
0 -1  0 -1  0  0  0  0  1  1 0 3 0 0 0 0 0 0 0 0 0 0 0 0 0 0          0    R  7
  1    0 0   0   0   0   0   1   0             5.98000E+04                R 21
  2                          1                 5.98000E+04                R 21
  3                          1                 5.98000E+04                R 21
  4                          1                 5.98000E+04                R 21
  5                          1                 5.98000E+04                R 21
  6                          1                 5.98000E+04                R 21
115  109 1                                                                R 21
116  110 2                                                                R 21
117  111 3                                                                R 21
118  112 4                                                                R 21
119  113 5                                                                R 21
120  114                                                                  R 21
121                        1                 2.731667+05                R 21
122                        1                 2.731667+05                R 21
123                        1                 2.731667+05                R 21
124                        1                 2.731667+05                R 21
125                        1                 2.731667+05                R 21
126                        1                 2.731667+05                R 21
193  187 1                                                                R 21
194  188 2                                                                R 21
195  189 3                                                                R 21
196  190 4                                                                R 21
197  191 5                                                                R 21
198  192                                                                  R 21
199                        1                 1.89683E+05                R 21
200                        1                 1.89683E+05                R 21
201                        1                 1.89683E+05                R 21
202                        1                 1.89683E+05                R 21
203                        1                 1.89683E+05                R 21
204                        1                 1.89683E+05                R 21
271  265 1                                                                R 21
272  266 2                                                                R 21
273  267 3                                                                R 21
274  268 4                                                                R 21
275  269 5                                                                R 21
276  270                                                                  R 21
277                        1                 3.66083E+05                R 21
278                        1                 3.66083E+05                R 21
279                        1                 3.66083E+05                R 21
280                        1                 3.66083E+05                R 21
281                        1                 3.66083E+05                R 21
282                        1                 3.66083E+05                R 21
349  343 1                                                                R 21
350  344 2                                                                R 21
351  345 3                                                                R 21
352  346 4                                                                R 21
353  347 5                                                                R 21
354  348                                                                  R 21
355                        1                 9.90067E+04                R 21
356                        1                 9.90067E+04                R 21
357                        1                 9.90067E+04                R 21
358                        1                 9.90067E+04                R 21
```

```
 359                          1                 9.90067E+04                 R 21
 360                          1                 9.90067E+04                 R 21
 469  463 1                                                                 R 21
 470  464 2                                                                 R 21
 471  465 3                                                                 R 21
 472  466 4                                                                 R 21
 473  467 5                                                                 R 21
-474  468                                                                   R 21
 1 -1  0 -1  0  0  0  0  1  1 0 0 0 0 0 0 0 0 0 0 0 0 0 0 0            0    R  7
 1 -1  0 -1  0  0  0  0  1  1 0 0 0 0 0 0 0 0 0 0 0 0 0 0 0            0    R  7
 1 -1  0 -1  0  0  0  0  1  1 0 0 0 0 0 0 0 0 0 0 0 0 0 0 0            0    R  7
 1 -1  0 -1  0  0  0  0  1  1 0 0 0 0 0 0 0 0 0 0 0 0 0 0 0            0    R  7
 1 -1  0 -1  0  0  0  0  1  1 0 0 0 0 0 0 0 0 0 0 0 0 0 0 0            0    R  7
 1 -1  0 -1  0  0  0  0  1  1 0 0 0 0 0 0 0 0 0 0 0 0 0 0 0            0    R  7
 1 -1  0 -1  0  0  0  0  1  1 0 0 0 0 0 0 0 0 0 0 0 0 0 0 0            0    R  7
 1 -1  0 -1  0  0  0  0  1  1 0 0 0 0 0 0 0 0 0 0 0 0 0 0 0            0    R  7
 1 -1  0 -1  0  0  0  0  1  1 0 0 0 0 0 0 0 0 0 0 0 0 0 0 0            0    R  7
 1 -1  0 -1  0  0  0  0  1  1 0 0 0 0 0 0 0 0 0 0 0 0 0 0 0            0    R  7
 1 -1  0 -1  0  0  0  0  1  1 0 0 0 0 0 0 0 0 0 0 0 0 0 0 0            0    R  7
 1 -1  0 -1  0  0  0  0  1  1 0 0 0 0 0 0 0 0 0 0 0 0 0 0 0            0    R  7
 1 -1  0 -1  0  0  0  0  1  1 0 0 0 0 0 0 0 0 0 0 0 0 0 0 0            0    R  7
 1 -1  0 -1  0  0  0  0  1  1 0 0 0 0 0 0 0 0 0 0 0 0 0 0 0            0    R  7
 1 -1  0 -1  0  0  0  0  1  1 0 0 0 0 0 0 0 0 0 0 0 0 0 0 0            0    R  7
 1 -1  0 -1  0  0  0  0  1  1 0 0 0 0 0 0 0 0 0 0 0 0 0 0 0            0    R  7
 1 -1  0 -1  0  0  0  0  1  1 0 0 0 0 0 0 0 0 0 0 0 0 0 0 0            0    R  7
 1 -1  0 -1  0  0  0  0  1  1 0 0 0 0 0 0 0 0 0 0 0 0 0 0 0            0    R  7
 1 -1  0 -1  0  0  0  0  1  1 0 0 0 0 0 0 0 0 0 0 0 0 0 0 0            0    R  7
 0 -1  0 -1  0  0  0  0  1  1 0 0 0 0 0 0 0 0 0 0 0 0 0 0 0            1    R  7

 1 -1  0 -1  0  0  0  0  1  1 0 0 0 0 0 0 0 0 0 0 0 0 0 0 0            0    R  7
 1 -1  0 -1  0  0  0  0  1  1 0 0 0 0 0 0 0 0 0 0 0 0 0 0 0            0    R  7
 1 -1  0 -1  0  0  0  0  1  1 0 0 0 0 0 0 0 0 0 0 0 0 0 0 0            0    R  7
 1 -1  0 -1  0  0  0  0  1  1 0 0 0 0 0 0 0 0 0 0 0 0 0 0 0            0    R  7
 1 -1  0 -1  0  0  0  0  1  1 0 0 0 0 0 0 0 0 0 0 0 0 0 0 0            0    R  7
 1 -1  0 -1  0  0  0  0  1  1 0 0 0 0 0 0 0 0 0 0 0 0 0 0 0            0    R  7
 1 -1  0 -1  0  0  0  0  1  1 0 0 0 0 0 0 0 0 0 0 0 0 0 0 0            0    R  7
 1 -1  0 -1  0  0  0  0  1  1 0 0 0 0 0 0 0 0 0 0 0 0 0 0 0            0    R  7
 1 -1  0 -1  0  0  0  0  1  1 0 0 0 0 0 0 0 0 0 0 0 0 0 0 0            0    R  7
 1 -1  0 -1  0  0  0  0  1  1 0 0 0 0 0 0 0 0 0 0 0 0 0 0 0            0    R  7
 1 -1  0 -1  0  0  0  0  1  1 0 0 0 0 0 0 0 0 0 0 0 0 0 0 0            0    R  7
 1 -1  0 -1  0  0  0  0  1  1 0 0 0 0 0 0 0 0 0 0 0 0 0 0 0            0    R  7
 1 -1  0 -1  0  0  0  0  1  1 0 0 0 0 0 0 0 0 0 0 0 0 0 0 0            0    R  7
 1 -1  0 -1  0  0  0  0  1  1 0 0 0 0 0 0 0 0 0 0 0 0 0 0 0            0    R  7
 1 -1  0 -1  0  0  0  0  1  1 0 0 0 0 0 0 0 0 0 0 0 0 0 0 0            0    R  7
 1 -1  0 -1  0  0  0  0  1  1 0 0 0 0 0 0 0 0 0 0 0 0 0 0 0            0    R  7
 1 -1  0 -1  0  0  0  0  1  1 0 0 0 0 0 0 0 0 0 0 0 0 0 0 0            0    R  7
 1 -1  0 -1  0  0  0  0  1  1 0 0 0 0 0 0 0 0 0 0 0 0 0 0 0            0    R  7
 1 -1  0 -1  0  0  0  0  1  1 0 0 0 0 0 0 0 0 0 0 0 0 0 0 0            0    R  7
 1 -1  0 -1  0  0  0  0  1  1 0 0 0 0 0 0 0 0 0 0 0 0 0 0 0            0    R  7
 1 -1  0 -1  0  0  0  0  1  1 0 0 0 0 0 0 0 0 0 0 0 0 0 0 0            0    R  7
```